Title
Cation-Chloride Cotransporters and Seizure State Transitions in Drosophila

Author
Rusan, Zeid Marwan

Publication Date
2013

Peer reviewed|Thesis/dissertation

Cation-Chloride Cotransporters and Seizure State Transitions in *Drosophila*

by

Zeid Marwan Rusan

A dissertation submitted in partial satisfaction of the

requirements for the degree of

Doctor of Philosophy

in

Molecular and Cell Biology

in the

Graduate Division

of the

University of California, Berkeley

Committee in charge:

Professor Mark A. Tanouye, Chair
Professor Diana M. Bautista
Professor Damian O. Elias
Professor Mu-ming Poo
Professor Kristin Scott

Spring 2013

Cation-Chloride Cotransporters and Seizure State Transitions in *Drosophila*

By Zeid Marwan Rusan

Abstract

Cation-Chloride Cotransporters and Seizure State Transitions in *Drosophila*

by

Zeid Marwan Rusan

Doctor of Philosophy in Molecular and Cell Biology

University of California, Berkeley

Professor Mark A. Tanouye, Chair

Seizure disorders, including the epilepsies, are debilitating misfortunes suffered by over 1% of the world's human population. Spontaneous recurrent seizures—paroxysmal events characterized by large groups of hyperexcited and hypersynchronized neurons—are hallmarks of epilepsy and destructive to the quality of life of many individuals. Although antiepileptic drug (AED) development is continuingly improving, available cures for attenuating and reducing the frequency of seizures are completely ineffective for a third of epileptics. Basic research concerning properties of seizures and their causes will yield critical insight required for the design of novel therapeutics. Such scientific advances may arise from experimentation using model organisms, with one such promising animal model being the fruit fly, *Drosophila melanogaster*.

Flies, like most other organisms with complex nervous systems given a sufficient stimulus, exhibit transitions between behavioral seizure states with a detectable underlying neural correlate. Conservation of nervous system genes and functions throughout evolution has made the fly a relevant model for human seizure disorders. In addition to such relevance, the advantages of the *Drosophila* system techniques enable finer dissection and identification of members in molecular pathways related to seizure-genesis, seizure-propagation, seizure-termination and recovery. For my thesis work I capitalized on the powerful tools available in *Drosophila* to attempt to tease apart the pleiotropic functions of cation-chloride cotransporters (CCCs) throughout the nervous system that are important for seizure manifestation. I also screened a collection of chromosomal deletions for their effect on behavioral paralysis after a seizure in hope of eventually identifying endogenous seizure-suppression and recovery mechanisms.

kcc mutants are more seizure-susceptible than wild-type flies. *kcc* is the highly conserved *Drosophila* ortholog of K^+/Cl^- cotransporter genes (*KCC*s) thought to be expressed in all animal cell types. I examined the spatial and temporal requirements for *kcc* loss-of-function to modify seizure-

susceptibility in flies. Targeted RNAi of *kcc* in various sets of neurons is sufficient to induce severe seizure-sensitivity. Interestingly, *kcc* RNAi in glia was found to be particularly effective in causing seizure-sensitivity. *kcc* knockdown during development causes reduction in seizure induction threshold, lengthening of seizure refractory period, cell swelling and blood-brain barrier (BBB) degradation in adult flies. Results suggest that a threshold of K^+/Cl^- cotransport dysfunction in the nervous system during development, and concomitant malformation of the BBB, are major determinants of seizure-susceptibility in *Drosophila*.

Although many genes and synaptic/non-synaptic mechanisms linked with seizure-susceptibility have been described, relatively much less is known about how seizures stop, regardless of etiology. Theoretically, given the significant chance of seizure occurrence, there exist mechanisms for terminating, and recovering from, seizures. I hypothesized that defects in such mechanisms would affect post-seizure states such as the postictal or refractory state of flies. To identify such possible mechanisms, I screened over 150 chromosomal deletions for their affect on the duration of paralysis of the seizure-susceptible bang-sensitive (BS) mutant, $para^{bss1}$. 5 deletions gave rise to significant lengthening of $para^{bss1}$ mean recovery time (MRT). *charlatan*, *chn*, a gene encoding a NRSF/REST transcriptional repressor, was identified as the causative gene for one of these deletions. *chn* RNAi caused an increase in paralysis times and synaptic failure duration after a $para^{bss1}$ seizure, but seizure induction threshold was not significantly altered. RNAi of *chn* lengthened MRT of another BS mutant, *eas*, suggesting that *chn* is a general seizure-enhancer. Although identification of *chn* as a general seizure-enhancer did not expose specific molecular mechanisms, the screen was a proof of principle for the postulate that genetic factors may impact different aspects of seizures, some of which have been overlooked during the history of seizure disorder research.

My thesis lays a foundation for better understanding the role of CCCs in nervous system disease and draws needed attention to the relatively neglected postictal state. Specific manipulation and marking of glia in *Drosophila* has implicated CCC functions in these cells as important factors in seizure-susceptibility before and after seizures. Seizure-sensitivity arising from CCC loss can be further examined with precision using manipulations and rescue experiments already possible with today's techniques. Extracellular ion regulations are critical factors affecting seizure-onset, and perhaps also, seizure-recovery and refractory states. Nervous system parameters unique to seizures might trigger specialized mechanisms involved in restoring normal conditions after seizures and rendering the reoccurrence of seizures less-likely for some time. Examining effects of well-controlled perturbations on all aspects of seizures is critical for solving problems presented by seizure disorders.

Dedication

To my uncle, Thomas Anthony Russo

Table of Contents

List of Figures

List of Tables

List of Abbreviations

AED	antiepileptic drug
ASIC	acid-sensing ion channel
AL	antennal lobe
BBB	blood-brain barrier
BNB	blood-nerve barrier
BS	bang-sensitive
CCAP	crustacean cardioactive peptide
CCC	cation-chloride cotransporter
CNS	central nervous system
Cyx	MB calyx
DIC	differential interference contrast
DLM	dorsal longitudinal flight muscle
DNA	deoxyribonucleic acid
ECS	extracellular space
EEG	electroencephalography
GABA	gamma-aminobutyric acid
GF	giant fiber
GFP	green fluorescent protein
HFS	high-frequency stimulus
HRP	horseradish peroxidase
KCC	potassium-chloride cotransporter
Lam	optic lamina
LN	lateral neurons
MARCM	mosaic analysis using a recombinant cell marker
MB	mushroom body
Med	optic medulla
MRT	mean recovery time
NKCC	sodium-potassium-chloride cotransporter
NMJ	neuromuscular junction
nMRT	normalized mean recovery time
PG	perineurial glia
PN	peripheral nerve
PNS	peripheral nervous system
RNA	ribonucleic acid
RNAi	RNA interference
SJ	septate junction
SPG	subperineurial glia
SUDEP	sudden unexpected death in epilepsy
TARGET	temporal and regional gene expression targeting
VNC	ventral nerve cord

Acknowledgments

After five years of undergraduate studies at the University of Massachusetts and six years of graduate work at UC Berkeley, it is time for me to thank the many friends, family, colleagues and professors who helped me reach this day.

The University of Massachusetts Amherst with its diverse student body and infinite curriculum choices as well as excellent professors gave me the opportunity to explore many fields of study. Having been accepted into the Graduate Program at UC Berkeley was a challenge I was ready to accept.

I am fortunate to have parents who believe in higher education and that the more knowledge you have, the more choices you will have in life. My Mother always said to treat others the way you would like to be treated and always made the biggest problems into a lot of little problems that could be handled easily. My father has always been a man of great and simple integrity. His dedication to his profession, his respect for all people and his unwavering ethics have given me values to live by.

How could a dissertation acknowledgements section be complete without mention of my brother, Nasser. He has paved the way for me from my freshman orientation up until today as I put the final touches on my thesis. Going from annoying "little brother" to respected equal has been a long and exciting journey.

I have learned from my sister, Nada to forever find good in any situation and always follow your heart. She has encouraged me every step of the way and I am as proud of her as she is of me.

I thank all of my extended family in both Massachusetts and Jordan. Their interest and contact throughout the years has been invaluable, seeming to always be there when I needed it the most. God bless you all.

To all my friends who have touched my life, now all scattered in different places in the world yet always close to heart, thank you all for the memories and kindnesses you gave so generously. Especially I would like to thank Meh, Mo, Mary, Wael, Emi, Shivan, Joey, Ryan, Aaron, Joel, Sean, Guillo and Anjali for all the many long talks and for enriching my life.

Life in Dr. Mark Tanouye's Lab/Institution/Family has had its ups and downs but, over the last six years has been as close to a perfect working and learning environment as one could hope for. I would like to thank Dr. John Nambu, my undergraduate mentor at UMass, for reinventing my view of science and for helping me make it to UC Berkeley. I thank Dr. Mark Tanouye for giving me the freedom to study what my heart desired and making sure I had solid findings in the end.

I honestly believe that I could not have gotten through the day-to-day life of graduate school without my co-Tanouye Lab compatriot, Iris Howlett. Without Iris I probably would not be sitting here today writing this. Although, we did not see much of each other outside work, we sure were a

great team making the Lab our own hangout. Much love to you Iris and best of luck in your career. Many thanks to our former, but not forgotten, Post-Doc Louise Parker who gave us hope in the Lab with her wisdom and work ethic.

Finally, I save the last thank you for my wonderful girlfriend, Angelica Anguiano. This final year was made much less difficult having you in my life. Your calm and compassionate way of looking at life always helped me to see things in a more positive perspective. Thank you so much for being you, and for having faith in me and for letting me be me.

Chapter 1
Introduction to Epilepsy - The Sacred Disease and Prospects for Catholicons

Seizure disorders and the epilepsies

Seizures have been documented since the days of ancient civilizations. Seizure, from the Latin *sacire*, means to take possession of. As with many other natural phenomena observed throughout history, seizures were attributed to supernatural causes. The dramatic and rapid change in behavior of individuals undergoing a seizure played a part in the demonic-possession diagnosis and coining of epilepsy as The Sacred Disease. Epilepsy, from the Greek *epilepsia* meaning seizure, is a disease marked by spontaneous, unprovoked, and recurrent seizures. Modern neurobiology informs us that seizures, like other behaviors, are outputs of the nervous system. An all-or-none electrical event that has a sudden onset and is characterized by overexcited populations of neurons firing nearly synchronously defines a seizure. Ectopic nervous system discharges such as seizures are detrimental to the health and well-being of individuals experiencing them. Seizures continue to plague humanity with their still largely mysterious causes and tendency to resist treatment.

Epilepsy is a blanket term for a collection of diseases with different classifications that comprise most of seizure disorders (Berg & Scheffer, 2011). Classification is based on criteria such as age of onset, whether or not consciousness is impaired, location of the seizure and the observed behavioral output. An estimated 1-2% of people are believed to suffer from seizure disorders reflecting the size of the seizure etiology set (Jackson, 2011). To explain the common presentation of seizures, physicians have sought after commonalities in epileptic patients. As late as the mid 1800s, seizures were attributed to factors such as fear, masturbation, drunkenness and heredity (35, 12, 6 and 1% of seizure etiologies, respectively) (Lauret 1843). With the invention of the electroencephalogram (EEG) by Hans Berger in the 1920's, suspicions of an electrical foundation for seizures were confirmed. Neuronal hypersynchronization primarily relies on electrical hyperexcitability of neurons in endogenously-rhythmic networks (Margineanu, 2010; Timofeev, Bazhenov, Seigneur, & Sejnowski, 2012).

Today, a more precise understanding of seizure disorders has mostly pointed to the imbalance of synaptic transmission favoring excitation as the main culprit behind seizures. Several antiepileptic drugs (AEDs), and genetic lesions, affect the excitatory and inhibitory mechanisms of neuronal communication thus suggesting defects in these mechanisms as the causes of seizures. Non-synaptic mechanisms have more recently been implicated in seizure etiology as well. Some AEDs, such as the loop-diuretics, are now believed to primarily suppress seizures by acting on extracellular volume regulation systems (Hochman, 2012). Thus, accumulating evidence continues to bolster the idea of a complex combinatorial basis for seizures.

Seizure disorders are associated with a myriad of factors including stroke, fever, trauma, tumors, drug-use, infection and heritable factors.

Genetic epilepsies—formally known as idiopathic epilepsies with a genetic or presumed genetic basis—often exhibit complex, non-Mendalian, inheritance (Gallentine & Mikati, 2012). Mutations in voltage-gated sodium channels are known to underlay many intractable epilepsies; epilepsies that are resistant to available treatments (Oliva, Berkovic, & Petrou, 2012). These are believed to be gain-of-function mutations which enhance impulse propagation and cause hyperexcitability through persistent sodium currents (Parker, Padilla, Du, Dong, & Tanouye, 2011). Lesions in genes involved in excitatory glutamatergic and inhibitory GABAergic signaling pathways (loss-of-function and gain-of-function mutations, respectively) have also been linked to epilepsy (Galanopoulou, 2010; Russo, Gitto, Citraro, Chimirri, & De Sarro, 2012). However, treatment efficacies are considerably variable in patients with the same primary principal genetic component. Secondary genetic components presumed to account for such variability remain mostly illusive and are the focus of much genetic epilepsy research.

Clearly, simplistic models of increased excitatory neurotransmission, decreased inhibitory neurotransmission and enhanced impulse propagation fail to account for all observed seizure-related phenomena; when applied to inhibitory neurons, such dysfunctions are in fact contradictory to the current understanding of seizures. Moreover, AEDs sometimes exacerbate seizures in some patients. The path from excitability of individual neurons to seizures is ill-defined, and a full understanding of seizure phenomena must include precise knowledge of relevant genetic predispositions and temporal dynamics of neural circuits. In summary, progress towards potent treatments for epilepsy is predicated on the advancement of the understanding of the causative mechanisms revealed through biomedical research, or else, treatments will continue to mostly rely on avoiding precipitants, trial and error using AEDs with multiple unwanted side effects and dangerous surgical intervention.

Seizures are radical, yet somewhat predictable, transitions through neural state space

Spontaneity is a human construct regarding a chronological event with an incomplete set of pertinent information leading up to the event. Although seizures are immensely complicated patterns of nervous system activity, their overall progression is not entirely unpredictable; the emergence of the preictal state, seizure onset, seizure propagation and seizure termination time courses are not entirely random (Navarro et al., 2011). Exact temporal sequences of neuronal firing patterns (neuronal state space transitions) may not be known, but distinct phases or states of cumulative neural activity for a particular epilepsy often have structure (Figure 1.1). Indeed, many patients can even predict their own seizures from sensations called auras. Auras arise from neuronal activity during the preictal (before seizure) state and, depending on the neurons participating in the activity, result in

sensations that are often indescribable in words. The neural activity associated with seizure states is mostly ectopic, thus feelings and sensations experienced during such events are often odd and surreal. Some animals such as dogs are known to be able to sense oncoming seizures and alert patients to prepare for them. EEG recordings during preictal states have revealed certain signatures of neuronal activity that increase the probability of seizure occurrence following their detection (Le Van Quyen et al., 2005; Stamoulis & Chang, 2012). This means that the preictal state is different than other states; it is a distinguishable period that is more likely to precede seizures (Figure 1.1*A*).

The all-or-none property of seizures implies the existence of a seizure threshold. Indeed, it is believed that any nervous system can display paroxysmal activity given a sufficient amount of excitatory drive (Figure 1.1*B*). Seizure thresholds are dynamic in a single individual and influenced by components such as sleep-deprivation, alcohol-withdrawal, stress, diet and distinct rhythmic stimuli. These so called precipitants are personalized, and epileptics benefit from recognizing and avoiding them to keep their thresholds as high as possible. Focal, or partial, seizures are restricted to a subset of neurons residing in the seizure focus. Generalized seizures involve the entire cerebral cortex. A seizure focus sometimes recruits the rest of the brain in what is called secondary-generalization (Figure 1.1*C*).

Most seizures terminate in less than 30 s without external intervention, although some may persist for extended periods i.e. *status epilepticus* (Trinka, Hofler, & Zerbs, 2012). Sudden unexpected death in epilepsy (SUDEP) can follow seizures, but most seizures are self-limited and the hyperinhibited postictal state ensues (Figure 1.1*D*; Surges & Sander, 2012; Widdess-Walsh & Devinsky, 2010). Regaining consciousness, fatigue, paralysis, confusion, fear and psychosis are telltale signs of this post-seizure state. There is a dearth of information concerning the postictal state; how seizures stop and how normal behavior is restored are poorly understood seizure state transitions. This is unfortunate since the postictal state has negative effects on an epileptic's quality of life. Fortunately, research pertaining to treatments related to the postictal state has been recently increasing (Schmidt, 2010). *in silico* modeling of seizure state transitions has yielded insight into the neural correlate at the core of these states; fitting models to the data can reveal dynamics of neural activity state space transitions (Chiu & Bardakjian, 2004). Having such an accurate measure allows for the detection of affecters influencing many aspects of seizures. Detection of affecters which expedite the postictal state, and therefore shorten the ictal period, could expose novel and invaluable targets for therapy (Schmidt & Noachtar, 2010).

Computational complexity via neuronal inhibition comes at a price

An animal's success in its environment hinges on its behavioral capabilities. Neural circuit computation is possible only by inhibition of neurons by stimuli and other neurons, in addition to excitation by them. Inhibition greatly increases the possible permutations of neuronal activation which scales up to more intricate outputs based on external and internal stimuli, or inputs. Transitions through neural state space—circuit computations—which achieve desirable outputs are tightly controlled through the balance of excitation and inhibition whilst maintaining circuit logic. However, inhibition may be compromised leading to overrun excitation that in turn leads to seizures.

Loss of inhibition is not the only path to seizures. Excess excitation may be sufficient to cause pathological neural state transitions. Similarly, seizure termination may be a consequence of increased inhibition and/or reduced excitation. For these reasons it has been difficult to determine the most vital mechanisms leading to seizure-susceptibility from a particular causative source; simultaneous effects on excitation and inhibition usually coexist. gamma-aminobutyric acid (GABA), the chief inhibitory neurotransmitter of the mammalian central nervous system (CNS), and its relationship to seizures exemplifies this difficulty (Ben-Ari, Gaiarsa, Tyzio, & Khazipov, 2007). Dampening of fast and slow GABAergic inhibition as the primary source of neuronal hyperexcitability is supported by a large body of evidence (Ben-Ari, Khalilov, Kahle, & Cherubini, 2012). However, disruption of a protein important for GABAergic signaling has been reported to have effects on the chief excitatory transmitter of the CNS, glutamate (Fiumelli et al., 2013; Gauvain et al., 2011). Chapter 2 explores the complicated contributions of the GABA system to seizure-sensitivity in thorough detail, while Chapter 3 deals with searching for insight into the crucial mechanisms of seizure-termination, whether involving increased inhibition or decreased excitation.

Glia and seizures

Even though glial cell abnormalities have long been correlated with seizures, almost nothing is known about causative links between these abnormalities and neuropathology. Glial cells constitute 90% of human brain cells, but have received considerably less attention than their neuronal brethren. This is intriguing since glia express many of the same genes as neurons do. The one trillion brain glia, named for the Latin word for glue, have historically been considered mainly "support" cells for the main excitable unit of the nervous system; the neuron. Research over the last 20 years has shown that contrary to this view, glia are critical for nervous system development and function. For example, a tripartite synaptic model—presynaptic neuron, postsynaptic neuron and associated glia—has increasingly replaced the binary model of synaptic transmission (Danjo, Kawasaki, & Ordway, 2011; Halassa, Fellin, & Haydon, 2007). Proliferation, differentiation, migration, maturation and activity of neurons during development are all dependent on

glia. Thus, it was only a matter of time before a causative link between some aspect of glia and seizures was discovered, as was the case in the 2013 report on loss of the glial-specific Na^+/Ca^{2+}, K^+ exchanger, Zydeco, and advent of seizure-genesis (Melom & Littleton, 2013).

Glial cell subtypes play specialized parts in development and activity of nervous systems, therefore different cell types could play different roles in seizure-susceptibility. At the synapse, closely-associated astrocyte glial processes uptake released neurotransmitters from the extra cellular space (ECS) (Coulter & Eid, 2012). They also directly affect neuronal excitability by exocytosis of gliotransmitters (Carmignoto & Haydon, 2012). Astrocytes are a significant fraction of the cells comprising the blood-brain barrier (BBB); the collection of mechanisms which create the unique environment of the brain. The BBB insures appropriate levels of ions are in contact with neurons and protects the brain from harmful molecules; its integrity is essential for preventing seizures (Kovacs, Heinemann, & Steinhauser, 2012; Marchi et al., 2007; Seiffert et al., 2004; Steinhauser, Seifert, & Bedner, 2012). Not only do astrocytes regulate ion concentrations of the ECS with flux across their membranes, they are believed to buffer K^+ via pericellular flux to and from other astrocytes with which they are electrically coupled. Astrocytes also supply energy to neurons necessary for their physiological performance. Microglia are the immune cells of the brain that seek out and eliminate pathogens invading the CNS. Lastly, many glial cell types can form gliomas, the most abundant type of brain tumor (Thom, Blumcke, & Aronica, 2012). Thus, ion-homeostasis and synaptic transmission, neural network development, energy requirements, infections and tumors—all elements affiliated with seizures—involve glial cells to an enormous degree. There is no doubt that continual basic research on glial cells will pave the way towards better cures for epilepsy.

Drosophila melanogaster **is a versatile model for studying seizure disorders**

The main conclusion drawn from the information introduced so far is that finding cures for epilepsy is one of the most challenging problems facing biologists and physicians (Lowenstein, 2008). Seizures are phenomena which involve almost all pieces of the brain; the most complex entity in the known universe. The only path towards successful treatment of seizure diseases is through scientific research. Epilepsy catholicons of the future will likely be a mixture of drugs tailored to precisely diagnosed seizure disorders. Results from several different disciplines must eventually be incorporated into one synthesized and consistent model of brain functionality to achieve this. Disciplines include research using model organisms and *in vitro* systems, each with its particular set of advantages and disadvantages (Raol & Brooks-Kayal, 2012). One important *in vivo* model of epilepsy is the fruit fly, *Drosophila melanogaster* (Parker, Howlett, Rusan, & Tanouye, 2011).

Unique advantages to the *Drosophila* system promise to reveal essential knowledge needed for generation of novel and potent anti-epileptic therapies.

Fruit flies have about a quarter of a million neurons and a tenth as many glia. Flies sing and dance for their mates, learn and remember, fight for territory and sleep. Most importantly, 70% of fly nervous system genes are conserved with those of mammals. Many fundamental mechanisms are in turn conserved, especially those of the developing nervous system and functionality of individual neurons and glia (Oland & Tolbert, 2011; Stork, Bernardos, & Freeman, 2012). It is true that the fly nervous system has drastically different neural network architecture, but how individual neurons and glia function and communicate are believed to be quite similar to those of larger multi-cellular organisms. Proof of this comes from recapitulation of mammalian phenotypes in flies in the event the same genes are manipulated in both cases. Seizure-sensitive mutant flies have been isolated since the 1970s, and genetic mapping has revealed that these mutants share common lesions with many seizure-sensitive mammalian models and humans (Ganetzky & Wu, 1982). Flies have behavioral seizure state transitions similar to those of epileptic humans (Figure 1.2). Moreover, electrophysiologically-recorded seizures and high-frequency stimulus (HFS) threshold estimations can be performed *in vivo*, with distinct phases of activity matching the behavioral states (Figure 1.3). A list of *Drosophila* seizure-susceptible mutants, their degree of seizure-susceptibility and their corresponding affected proteins is found in Table 1.1. For these and many other reasons, it is believed that the fly is a highly-relevant and indispensible model for the struggle against epilepsy that calls for more attention.

Cell-type specific and temporal manipulation of many fly gene dosages allows for fine dissection of the roles of genes in a particular process. Especially important is the ability to target a rich variety of conserved glial subtypes; a much needed capability given the state of glial cell knowledge. In addition, flies have long been critical research tools for large-scale screening for mutations modifying phenotypes (Nusslein-Volhard & Wieschaus, 1980). So, for my thesis, I utilized a multitude of resources exclusive to the fly to address questions concerning seizure-susceptibility. In Chapter 2 I investigated the role that the cation-chloride cotransporter (CCC) integral membrane proteins play in setting fly seizure-susceptibility. These pleiotropic ion transporters—famous for regulating internal chloride and thus GABAergic signaling—have many proposed mechanisms of action for determining seizure-sensitivity including developmental, acute, neuronal and glial processes. The most important finding was that targeted reduction of CCCs only in glia during development causes severe seizure-sensitivity; which, to my knowledge, is only the second report of a causative link between glial cell dysfunction and seizures. Particularly important were the subperineurial glia (SPG) which make up the major BBB glia of the fly. In

Chapter 3 I make use of the powerful genetic screening capability of *Drosophila* to locate genes which affect the post-seizure refractory period of the most seizure-sensitive BS mutant, *para*^{bss1}. Five chromosomal deficiencies which delete ~10-30 genes lengthened paralysis time of *para*^{bss1}. Following up on one deficiency, I discovered that a reduction in the transcription factor *charlatan*, *chn*, induced a near doubling of the duration of seizure-induced paralysis for *para*^{bss1}, without altering seizure threshold. My dissertation lays the foundation for intricate exploration of CCCs in seizure-susceptibility, especially in glia, and provides a proof of principle for the genetic modification of seizure-susceptibility beyond the seizure threshold.

REFERENCES

Ben-Ari, Y., Gaiarsa, J. L., Tyzio, R., & Khazipov, R. (2007). GABA: a pioneer transmitter that excites immature neurons and generates primitive oscillations. *Physiol Rev, 87*(4), 1215-1284. doi: 10.1152/physrev.00017.2006

Ben-Ari, Y., Khalilov, I., Kahle, K. T., & Cherubini, E. (2012). The GABA excitatory/inhibitory shift in brain maturation and neurological disorders. *Neuroscientist, 18*(5), 467-486. doi: 10.1177/1073858412438697

Berg, A. T., & Scheffer, I. E. (2011). New concepts in classification of the epilepsies: entering the 21st century. *Epilepsia, 52*(6), 1058-1062. doi: 10.1111/j.1528-1167.2011.03101.x

Carmignoto, G., & Haydon, P. G. (2012). Astrocyte calcium signaling and epilepsy. *Glia, 60*(8), 1227-1233. doi: 10.1002/glia.22318

Chiu, A. W., & Bardakjian, B. L. (2004). Control of state transitions in an in silico model of epilepsy using small perturbations. *IEEE Trans Biomed Eng, 51*(10), 1856-1859. doi: 10.1109/tbme.2004.831520

Coulter, D. A., & Eid, T. (2012). Astrocytic regulation of glutamate homeostasis in epilepsy. *Glia, 60*(8), 1215-1226. doi: 10.1002/glia.22341

Danjo, R., Kawasaki, F., & Ordway, R. W. (2011). A tripartite synapse model in Drosophila. *PLoS One, 6*(2), e17131. doi: 10.1371/journal.pone.0017131

Fiumelli, H., Briner, A., Puskarjov, M., Blaesse, P., Belem, B. J., Dayer, A. G., . . . Vutskits, L. (2013). An ion transport-independent role for the cation-chloride cotransporter KCC2 in dendritic spinogenesis in vivo. *Cereb Cortex, 23*(2), 378-388. doi: 10.1093/cercor/bhs027

Galanopoulou, A. S. (2010). Mutations affecting GABAergic signaling in seizures and epilepsy. *Pflugers Arch, 460*(2), 505-523. doi: 10.1007/s00424-010-0816-2

Gallentine, W. B., & Mikati, M. A. (2012). Genetic generalized epilepsies. *J Clin Neurophysiol, 29*(5), 408-419. doi: 10.1097/WNP.0b013e31826bd92a

Ganetzky, B., & Wu, C. F. (1982). Drosophila mutants with opposing effects on nerve excitability: genetic and spatial interactions in repetitive firing. *J Neurophysiol, 47*(3), 501-514.

Gauvain, G., Chamma, I., Chevy, Q., Cabezas, C., Irinopoulou, T., Bodrug, N., . . . Poncer, J. C. (2011). The neuronal K-Cl cotransporter KCC2 influences postsynaptic AMPA receptor content and lateral diffusion in dendritic spines. *Proc Natl Acad Sci U S A, 108*(37), 15474-15479. doi: 10.1073/pnas.1107893108

Halassa, M. M., Fellin, T., & Haydon, P. G. (2007). The tripartite synapse: roles for gliotransmission in health and disease. *Trends Mol Med, 13*(2), 54-63. doi: 10.1016/j.molmed.2006.12.005

Hochman, D. W. (2012). The extracellular space and epileptic activity in the adult brain: explaining the antiepileptic effects of furosemide and bumetanide. *Epilepsia, 53 Suppl 1*, 18-25. doi: 10.1111/j.1528-1167.2012.03471.x

Jackson, G. (2011). Classification of the epilepsies 2011. *Epilepsia, 52*(6), 1203-1204; discussion 1205-1209. doi: 10.1111/j.1528-1167.2011.03093.x

Kovacs, R., Heinemann, U., & Steinhauser, C. (2012). Mechanisms underlying blood-brain barrier dysfunction in brain pathology and epileptogenesis: role of astroglia. *Epilepsia, 53 Suppl 6*, 53-59. doi: 10.1111/j.1528-1167.2012.03703.x

Le Van Quyen, M., Soss, J., Navarro, V., Robertson, R., Chavez, M., Baulac, M., & Martinerie, J. (2005). Preictal state identification by synchronization changes in long-term intracranial EEG recordings. *Clin Neurophysiol, 116*(3), 559-568. doi: 10.1016/j.clinph.2004.10.014

Lowenstein, D. H. (2008). Pathways to discovery in epilepsy research: rethinking the quest for cures. *Epilepsia, 49*(1), 1-7. doi: 10.1111/j.1528-1167.2007.01309.x

Marchi, N., Angelov, L., Masaryk, T., Fazio, V., Granata, T., Hernandez, N., . . . Janigro, D. (2007). Seizure-promoting effect of blood-brain barrier disruption. *Epilepsia, 48*(4), 732-742. doi: 10.1111/j.1528-1167.2007.00988.x

Margineanu, D. G. (2010). Epileptic hypersynchrony revisited. *Neuroreport, 21*(15), 963-967. doi: 10.1097/WNR.0b013e32833ed111

Melom, J. E., & Littleton, J. T. (2013). Mutation of a NCKX eliminates glial microdomain calcium oscillations and enhances seizure susceptibility. *J Neurosci, 33*(3), 1169-1178. doi: 10.1523/JNEUROSCI.3920-12.2013

Navarro, V., Le Van Quyen, M., Clemenceau, S., Adam, C., Petitmengin, C., Dubeau, F., . . . Baulac, M. (2011). [Seizure prediction: from myth to reality]. *Rev Neurol (Paris), 167*(3), 205-215. doi: 10.1016/j.neurol.2010.07.027

Nusslein-Volhard, C., & Wieschaus, E. (1980). Mutations affecting segment number and polarity in Drosophila. *Nature, 287*(5785), 795-801.

Oland, L. A., & Tolbert, L. P. (2011). Roles of glial cells in neural circuit formation: insights from research in insects. *Glia, 59*(9), 1273-1295. doi: 10.1002/glia.21096

Oliva, M., Berkovic, S. F., & Petrou, S. (2012). Sodium channels and the neurobiology of epilepsy. *Epilepsia, 53*(11), 1849-1859. doi: 10.1111/j.1528-1167.2012.03631.x

Parker, L., Howlett, I. C., Rusan, Z. M., & Tanouye, M. A. (2011). Seizure and epilepsy: studies of seizure disorders in Drosophila. *Int Rev Neurobiol, 99*, 1-21. doi: 10.1016/b978-0-12-387003-2.00001-x

Parker, L., Padilla, M., Du, Y., Dong, K., & Tanouye, M. A. (2011). Drosophila as a model for epilepsy: bss is a gain-of-function mutation in the para sodium channel gene that leads to seizures. *Genetics, 187*(2), 523-534. doi: 10.1534/genetics.110.123299

Raol, Y. H., & Brooks-Kayal, A. R. (2012). Experimental models of seizures and epilepsies. *Prog Mol Biol Transl Sci, 105*, 57-82. doi: 10.1016/b978-0-12-394596-9.00003-2

Russo, E., Gitto, R., Citraro, R., Chimirri, A., & De Sarro, G. (2012). New AMPA antagonists in epilepsy. *Expert Opin Investig Drugs, 21*(9), 1371-1389. doi: 10.1517/13543784.2012.705277

Schmidt, D. (2010). Effect of antiepileptic drugs on the postictal state. A critical overview. *Epilepsy Behav, 19*(2), 176-181. doi: 10.1016/j.yebeh.2010.06.019

Schmidt, D., & Noachtar, S. (2010). Outlook: the postictal state--future directions for research. *Epilepsy Behav, 19*(2), 191-192. doi: 10.1016/j.yebeh.2010.06.015

Seiffert, E., Dreier, J. P., Ivens, S., Bechmann, I., Tomkins, O., Heinemann, U., & Friedman, A. (2004). Lasting blood-brain barrier disruption induces epileptic focus in the rat somatosensory cortex. *J Neurosci, 24*(36), 7829-7836. doi: 10.1523/JNEUROSCI.1751-04.2004

Stamoulis, C., & Chang, B. S. (2012). Space-time adaptive processing for improved estimation of preictal seizure activity. *Conf Proc IEEE Eng Med Biol Soc, 2012*, 6157-6160. doi: 10.1109/embc.2012.6347399

Steinhauser, C., Seifert, G., & Bedner, P. (2012). Astrocyte dysfunction in temporal lobe epilepsy: K+ channels and gap junction coupling. *Glia, 60*(8), 1192-1202. doi: 10.1002/glia.22313

Stork, T., Bernardos, R., & Freeman, M. R. (2012). Analysis of glial cell development and function in Drosophila. *Cold Spring Harb Protoc, 2012*(1), 1-17. doi: 10.1101/pdb.top067587

Surges, R., & Sander, J. W. (2012). Sudden unexpected death in epilepsy: mechanisms, prevalence, and prevention. *Curr Opin Neurol, 25*(2), 201-207. doi: 10.1097/WCO.0b013e3283506714

Thom, M., Blumcke, I., & Aronica, E. (2012). Long-term epilepsy-associated tumors. *Brain Pathol, 22*(3), 350-379. doi: 10.1111/j.1750-3639.2012.00582.x

Timofeev, I., Bazhenov, M., Seigneur, J., & Sejnowski, T. (2012). Neuronal Synchronization and Thalamocortical Rhythms in Sleep, Wake and Epilepsy. In J. L. Noebels, M. Avoli, M. A. Rogawski, R. W. Olsen & A. V. Delgado-Escueta (Eds.), *Jasper's Basic Mechanisms of the Epilepsies*. Bethesda MD: Michael A Rogawski, Antonio V Delgado-Escueta, Jeffrey L Noebels, Massimo Avoli and Richard W Olsen.

Trinka, E., Hofler, J., & Zerbs, A. (2012). Causes of status epilepticus. *Epilepsia, 53 Suppl 4*, 127-138. doi: 10.1111/j.1528-1167.2012.03622.x

Widdess-Walsh, P., & Devinsky, O. (2010). Historical perspectives and definitions of the postictal state. *Epilepsy Behav, 19*(2), 96-99. doi: 10.1016/j.yebeh.2010.06.037

Chapter 1 Figures and Tables

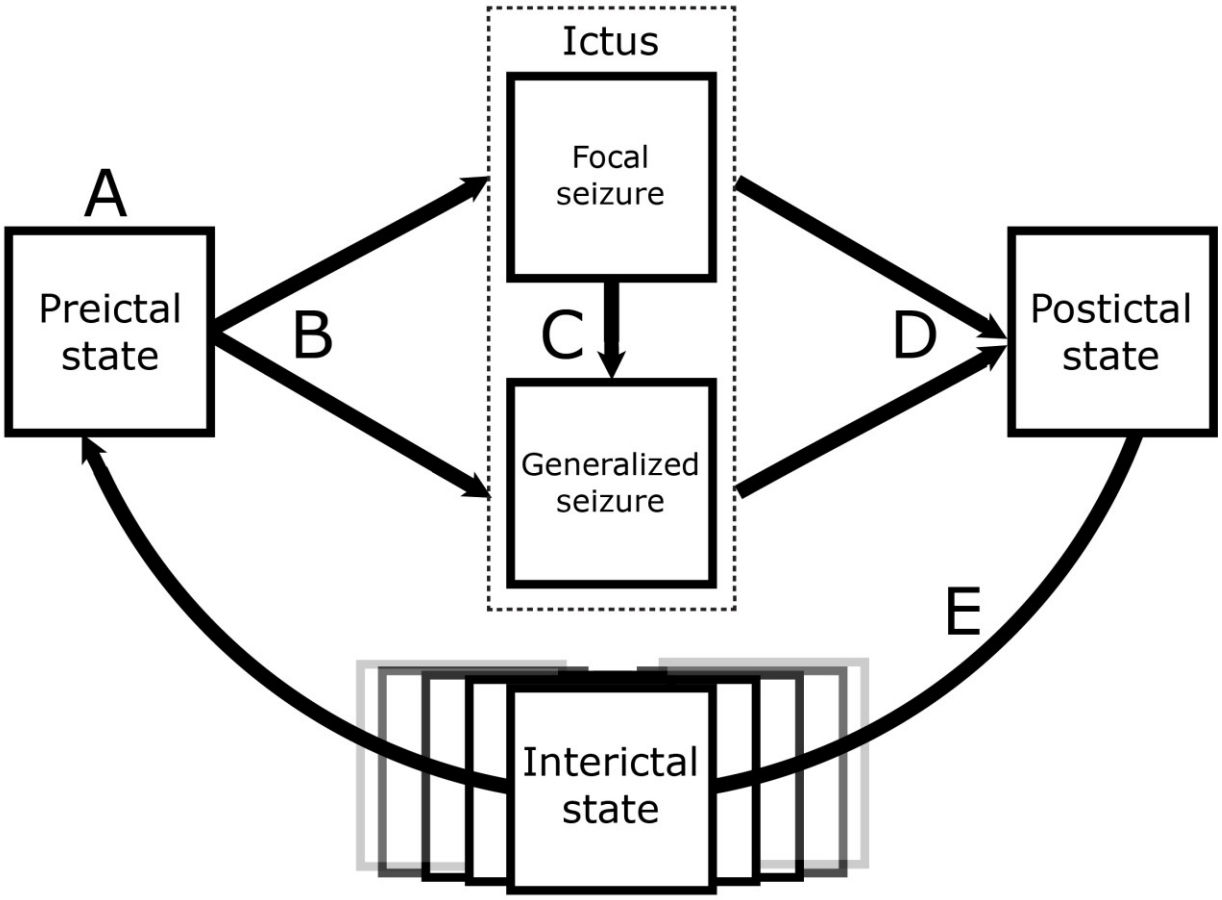

Figure 1.1: State diagram for general epileptic states. ***A***) Unique neural activity and behavior exist during periods leading up to a seizure. Undesirable sensations may accompany this preictal state. ***B***) Unprovoked paroxysmal events of neuronal hyperexcitability and hypersynchronicity occur in confined areas of the nervous system (focal seizures), or involve most regions simultaneously (generalized seizures). Behavioral output depends on seizure localization and circuit interplay, which could sometimes lead to a permanent seizure state (status epilepticus) and death (not shown). ***C***) Focal seizures may evolve into generalized seizures in a process called secondary-generalization. ***D***) Ictal events terminate giving rise to a period infamous for confusion, paralysis, fear and psychosis; the postictal state. ***E***) Epileptics spend most of their time functioning in the interictal state where they are still traumatized and repressed by the prospect of future seizures.

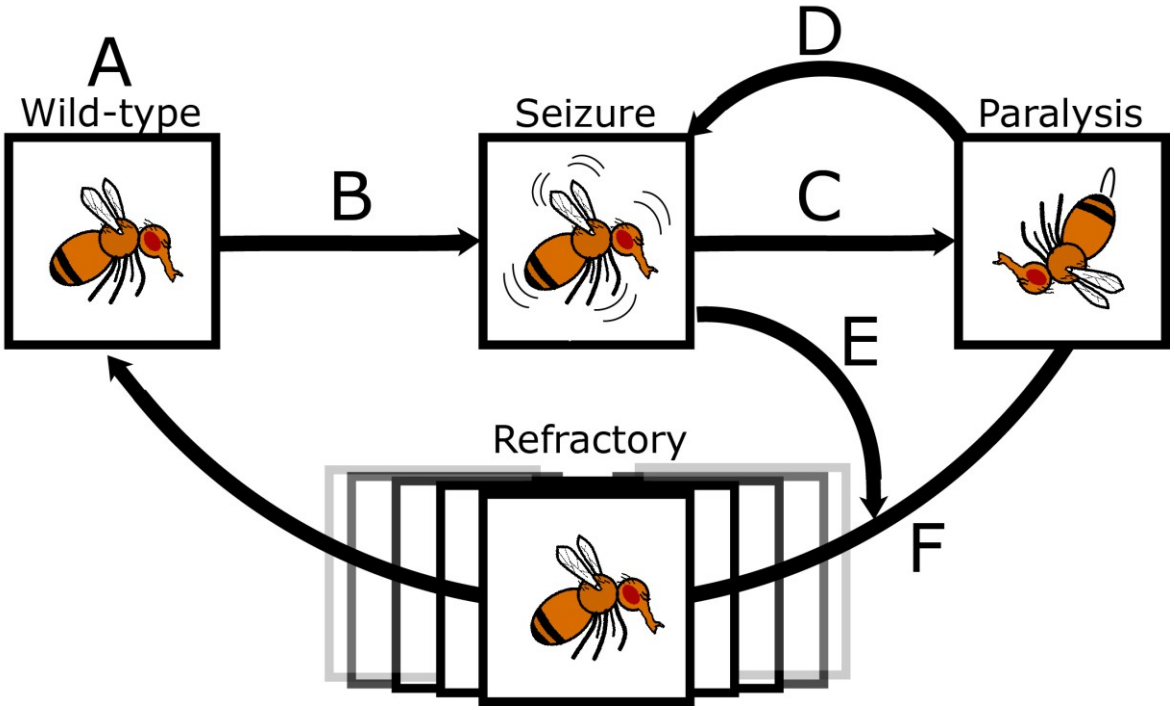

Figure 1.2: State diagram for general *Drosophila* behavioral seizure states. ***A***) Even the most seizure-susceptible flies often exhibit behavior comparable to that of wild-type prior to seizures. ***B***) An adequate stimulus induces a paroxysmal event characterized by rapid wing-beating, contraction of the abdomen, egg-laying and extension of proboscis and limbs. Bang-sensitives are a class of mutant flies that suffer a seizure given a 10 s mechanical agitation on a vortexer called a "bang". ***C***) Seizures terminate autonomously resulting in a paralytic state. Wings, proboscises and limbs are often extended with only minor twitching seen. ***D***) Seizure bouts can follow paralysis as part of a seizure-paralysis cycle known as "tonic-clonic-like" behavior characteristic of the most seizure-sensitive genotypes. ***E***) A "recovery seizure" can also follow a single seizure-paralysis transition prior to recovery in some mutants. ***F***) Recovery is sudden with flies regaining upright-posture, walking, flying, climbing and grooming. However, reduced performance scores for these behaviors compared with wild-type, and general hypoactivity, defines this post-seizure state. A bang can no longer trigger a seizure for the duration of this state, hence dubbing it the seizure refractory period.

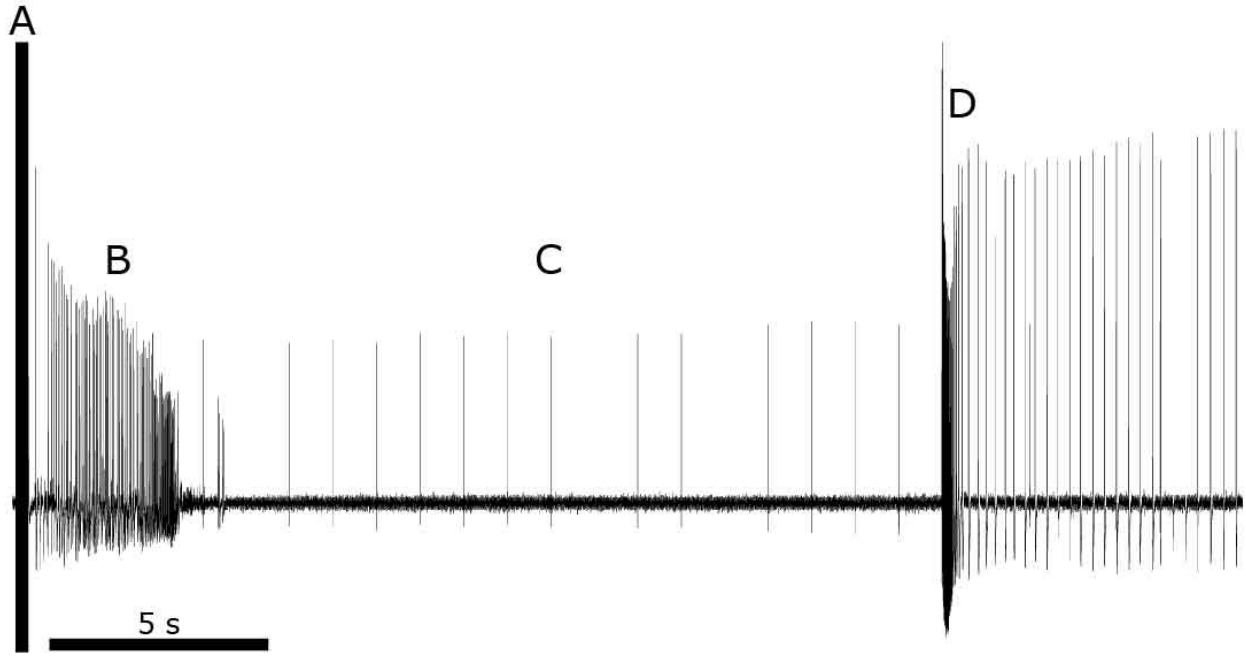

Figure 1.3: Electrophysiologically-recorded seizure phases in DLM. ***A***) HFS stimulus artifact. ***B***) Ectopic high-frequency DLM response corresponding to the behavioral seizure state follows an HFS of sufficient threshold. ***C***) DLM response arrest and inability to trigger DLM responses through GF stimulation, corresponding to the behavioral paralysis period. Only GF stimulation artifacts are recorded at 1 Hz. ***D***) Delayed DLM discharges often accompanying recovery of 1:1 relationship between GF stimulation and DLM response.

Genotype	Gene product	%BS paralysis	Seizure voltage threshold	Notes
para^{bss1}	Voltage-gated Na^+ channel	100	3.2	Gain-of-function, semi-dominant
eas^{PC80}	Ethanolamine kinase	100	3.4	Null, Recessive
bas^{2}	Unknown	100	3.8	
sda$^{iso7.8}$	Aminopeptidase N	100	6.7	Recessive
tko^{25t}	Ribosomal protein S12	100	9.9	Mitochondrial protein translation
jbug	Unknown	100	10.5	Temperature-sensitive
cpo^{EG1}	RNA-binding protein	30	11.1	
kcc^{DHS1}	K^+/Cl^- cotransporter	4-38	17.0	Hypomorph, Temperature-sensitive, seizures suppressed with age.
kdn	Citrate synthase	Unknown	20.2	
ATPalpha^{H64}	Na^+/K^+ ATPase	100	Unknown	Homozygous lethal, dominant seizure phenotype in heterozygotes
pk^{sple}	LIM domain protein	100	Unknown	
sesB^{1}	Adenine nucleotide translocase	100	Unknown	Duration of paralysis increases with age
zydeco^{1}	$Na^+/Ca2^+$, K^+ exchanger	94	Unknown	Glial cell specific
Canton Special	N/A	0	40.7	Wild-type

Table 1.1: Seizure-susceptibility of *Drosophila* mutants and affected gene products.

Chapter 2
Loss of Cation-Chloride Cotransporters in Glia or Neurons During Development Increases Seizure-Susceptibility in *Drosophila*

Introduction

Cation-chloride cotransporters (CCC) are nine members of the SLC12 family of transmembrane proteins (SLC12a1-9). Evolutionarily ancient, these solute carriers have been described for vertebrates, arthropods, worms, plants, fungi, and bacteria (Colmenero-Flores et al., 2007; Hebert, Mount, & Gamba, 2004; Park & Saier, 1996; Q. Sun, Tian, Turner, & Ten Hagen, 2010). CCCs are symporters serving the unidirectional transport of Cl^- ions together with Na^+ and/or K^+ ions across the plasma membrane. The Na^+-coupled CCCs (NCC, NKCC1 and NKCC2 in vertebrates) utilize the large inwardly-directed electrochemical gradient for Na^+ to transport Cl^- into the cell. They are capable of raising intracellular Cl^- to concentrations greater than the Nernst equilibrium value. K^+/Cl^- cotransporters (KCC1 through 4 in vertebrates) mainly act to transport K^+ and Cl^- out of the cell utilizing the outwardly-directed electrochemical gradient for K^+. These electroneutral transporters are capable of lowering intracellular Cl^- to concentrations below the electrochemical equilibrium value. The CCCs CIP1 and CCC9 remain poorly understood (Blaesse, Airaksinen, Rivera, & Kaila, 2009).

CCCs are involved in a wide range of physiological and pathological mechanisms in humans and experimental models (Benarroch, 2013; Gagnon & Delpire, 2013). Different CCCs acting together actively regulate intracellular concentration gradients of Cl^-, the most abundant anion in biological systems. CCCs play cell-type specific roles in the control of many fundamental processes including cell volume homeostasis, cell migration, neural circuit development and neuronal excitability (Blaesse et al., 2009; Zdebik, 2011). For example, CCCs regulate cell volume with cell swelling countered by an efflux of Cl^-, K^+, and water, mediated by KCC3 and ion channels (Benesova et al., 2012; Macaulay & Zeuthen, 2012; Ringel & Plesnila, 2008). Cell shrinkage is countered by an influx of Cl^-, Na^+, K^+, and water, mediated by NKCC1 and ion exchangers (Jayakumar et al., 2011; Kahle, Rinehart, & Lifton, 2010). All cells tightly regulate their size and shape because even small changes can be catastrophic to the myriad of cell and organ functions (Byun & Delpire, 2007; Kahle et al., 2008; Pasantes-Morales & Tuz, 2006).

A generally accepted neuronal function of the CCCs NKCC1 and KCC2 is the regulation of synaptic signaling by ligand-gated Cl^- channels, such as $GABA_A$ receptors (Ben-Ari, Woodin, et al., 2012; Blaesse et al., 2009; Kahle et al., 2008). During development, gamma-aminobutyric acid (GABA) may have excitatory action, signaling thought to be critical for neuronal maturation and integration into neural circuits (Cancedda, Fiumelli, Chen, & Poo, 2007; Tanis, Bellemer, Moresco, Forbush, & Koelle, 2009; Zhang, Wei, Xia, & Du, 2010). Excitatory GABA signaling occurs via high intracellular Cl^-, largely through NKCC1 transport function. Opening of $GABA_A$ receptors causes Cl^- to exit the cell as an excitatory current depolarizing the immature neuron. By contrast, in mature cortex, GABA is the major inhibitory

neurotransmitter. Inhibitory GABA signaling occurs via low intracellular Cl^- largely through KCC2 transport function. Opening of $GABA_A$ receptors allows Cl^- to enter the cell as an inhibitory current that hyperpolarizes the adult neuron. The polarity change in GABA action has been dubbed the "The GABA Excitatory/Inhibitory Shift" (Ben-Ari, Khalilov, et al., 2012), and is accompanied, among other changes, by expression up-regulation of *KCC2* (Rivera, Voipio, & Kaila, 2005; Tanis et al., 2009). An aberrant GABA shift is believed to be a major component of neuronal hyperexcitability and seizure-genesis resulting from CCC dysfunction. However, given the ubiquitous and dynamic expression of CCC encoding genes, it is likely that failure of several CCC mechanisms have the capacity to foster a multi-cellular phenomena like seizures (Boettger et al., 2003; Gagnon, Adragna, Fyffe, & Lauf, 2007; Hochman, 2012; Loscher, Puskarjov, & Kaila, 2012; Lucas, Hilaire, Delpire, & Scamps, 2012; Shekarabi et al., 2012; Y. T. Sun, Lin, Tzeng, Delpire, & Shen, 2010).

CCC function may be elucidated by studying model organisms such as *Drosophila*. In *Drosophila*, there are five CCCs including: *kcc* (*kazachoc*), an ortholog of vertebrate KCCs; *ncc69*, an ortholog of vertebrate NKCCs; and three other less understood members (*CG12773*, *CG31547*, and *CG10413*) (Featherstone, 2011; Filippov, Aimanova, & Gill, 2003; Hekmat-Scafe, Lundy, Ranga, & Tanouye, 2006; Hekmat-Scafe et al., 2010; W. M. Leiserson & Keshishian, 2011; William M. Leiserson, Forbush, & Keshishian, 2011). For example, animals carrying *kcc* loss-of-function mutations, such as kcc^{DHS1}, have been found to be seizure-sensitive, displaying seizure-like behavioral phenotypes with a reduced threshold for seizures induced by electroconvulsive shock (Hekmat-Scafe et al., 2006). Genetic and pharmacological experiments suggested that the increased seizure sensitivity of kcc^{DHS1} flies occurred via excitatory GABAergic signaling. The seizure phenotype for kcc^{DHS1} could be partially rescued by ectopic, spatially-restricted expression of a UAS-kcc^+ transgene in neurons, especially in the mushroom body (MB) (Hekmat-Scafe et al., 2010). These results for *Drosophila* resemble those of vertebrates and other organisms that implicate excitatory GABAergic signaling in the genesis of neonatal seizures, temporal lobe epilepsy, and seizures occurring after ischemic-hypoxic insult (Ben-Ari, Khalilov, et al., 2012; Gagnon & Delpire, 2013; Kahle et al., 2008)

Here, I show that seizure-sensitivity due to *kcc* loss-of-function in *Drosophila* is more complex than previously described. In the present experiments, seizure-sensitivity was induced by ectopic, spatially and temporally restricted expression of UAS-kcc-RNAi transgenes. This RNAi-induced seizure-sensitivity, in several instances, supports conclusions that differ from those obtained from previously reported kcc^+ rescue of seizure-sensitivity in mutants. I argue that although defective GABAergic signaling may raise overall seizure-sensitivity, other cellular abnormalities contribute substantially to the neuropathology. Particularly important factors in

Drosophila seizure-susceptibility found here appear to be the roles that *kcc* and *ncc69* play in glial function and volume control in the developing nervous system. I discuss a model of seizure-sensitivity that provides a more complete description of seizure-susceptibility due to CCC dysfunction.

Materials and Methods

Fly strains

Genotypes of the *Drosophila* strains used in this study, their referred to names and their sources are given in Table 2.1. Unless otherwise indicated, flies were maintained on standard cornmeal-molasses medium at ~23-25 °C in a humidified incubator. The kcc^{DHS1} mutation is a 13-bp insertion in intron 11 of *kcc* (*kazachoc*). The mutation leads to an approximate two-fold reduction in transcript and an approximate four-fold reduction in protein; phenotypically it behaves as a hypomorph (Hekmat-Scafe et al 2006). The kcc^{Ad4} and $kcc^{EY08304}$ embryonic lethal mutations are not molecularly mapped and are likely to be nulls (Figure 2.6). The *para* (*paralyzed*) gene encodes a voltage-gated Na^+ channel. The semidominant $para^{bss1}$ gain-of-function mutation is a missense mutation that results in an amino acid substitution, L1699F, causing a more persistent Na^+ current after normal activation (Parker, Padilla, et al., 2011). Genotypes were combined by following standard *Drosophila* crossing schemes using common strains with balancer chromosomes as needed (data not shown). The *A307-GAL4>UAS-kcc-RNAi-V/CyO* seizure-sensitive strain was generated by breeding seizure-sensitive F1 recombinants from *A307-GAL4>UAS-kcc-RNAi-V* virgin females crossed to noc^{Sco}*/CyO* males.

Behavioral assays

Behavioral testing for bang-sensitive (BS) paralysis was performed as described previously (Kuebler & Tanouye, 2000). Briefly, flies were collected <1 day post-eclosion then placed in a 25 °C humidified incubator to recover from CO_2–induced anesthesia until tested for BS paralysis the following day. No more than 15 individual flies were tested per vial since larger numbers seemed to dampen the mechanical stimulus (Zeid M. Rusan and Louise Parker, unpublished observations). Mechanical stimuli ("bangs") were 10 s vial agitations using a VWR vortexer set to maximum speed. Pools of data were combined (in total n > 100 for each genotype, unless stated otherwise) to yield a final measure of %BS paralysis for each genotype, 24-48 hours old. For determining the duration of post-seizure paralysis, no more than 6 individual flies were tested per vial so the time each fly took to restore normal posture after a bang could be documented accurately. Pools of paralysis time data were combined (in total n > 100 for each genotype, as noted in Figure 2.4*A*). Flies kept at 30 °C for TARGET experiments were moved to fresh vials after each BS paralysis test due to the rapid

deterioration of vial conditions under those circumstances (McGuire, Le, Osborn, Matsumoto, & Davis, 2003).

Electrophysiology

in vivo electrophysiological assays were from the giant fiber system, a well characterized fly escape circuit (Allen, Godenschwege, Tanouye, & Phelan, 2006). Seizure threshold and following frequency tests were based on previous studies but with a variation in specimen preparation (Allen & Godenschwege, 2010; Kuebler & Tanouye, 2000). Using a blunted hypodermic needle attached to a vacuum line, a fly 1 day post-eclosion was suctioned onto a random body position with a swift insert into the vial. When needed, suction was aligned onto the head by gentle handling of the fly. The fly was then repeatedly passed head-first through a trough made in dental wax covering a glass slide. Once the thorax of the struggling fly was at an appropriate upright orientation during a given pass, the fly was sandwiched in the wax by gently pushing one edge of the trough wall using forceps until the needle detached. Pieces of wax were then added to secure the head and abdomen of the trapped fly, keeping the targets of electrodes exposed. I found that this modification saves time and reduces injury to specimens. Stimulating and ground metal electrodes were of uninsulated tungsten (WPI), and recording electrodes were of Borosillicate glass (WPI) filled with 3 M KCl. Seizure-like activity was evoked by high-frequency (HF) electrical brain stimulation (0.5 ms pulses at 200 Hz for 300 ms) of varying voltage and monitored by DLM (dorsal longitudinal muscle) recordings as described previously. Flies were given a maximum of four HF stimuli with 7-10 minutes of rest between HF stimuli before being discarded, unless otherwise noted. During the course of each experiment, the giant fiber (GF) circuit was monitored continuously as a proxy for holobrain function. Seizures were declared with the occurrence of aberrant high-frequency DLM activity and subsequent failure of GF stimulation to elicit a DLM response. For each fly, DLM following frequencies were determined by averaging 4 trials per stimulation frequency, where each trial consisted of 10 trains of 12 stimuli. Stimulation duration of a Grass 44S stimulator was controlled by a Molecular Devices digidata 1440a under the command of custom protocols implemented in Strathclyde Electrophysiology Software, WinWCP V4.5.8. Pulse width, stimulation frequency and voltage settings on the stimulator were set manually. Recordings were amplified with Dagan Electro 705 preamplifiers, digitized with the digidata 1440a and acquisition data stored by WinWCP V4.5.8. Data were filtered at 1000 Hz for presented traces. n>10 for each genotype tested.

Histology

Staining of whole mount *Drosophila* embryos was performed by following Bossing's whole-mount protocol (Abcam). Third instar larvae were dissected

in hemolymph-like solution (Feng, Ueda, & Wu, 2004) then stained according to standard procedures (Grant Kauwe, personal communication). Immuno-staining of adult *Drosophila* nervous systems was performed as described previously (Wu & Luo, 2006). The Kcc antibody is rabbit polyclonal anti-Kcc, a gift from Dr. Daria Hekmet-Scafe. The antibody is predicted to recognize all four Kcc isoforms (Kcc-A, -B, -C, and -D) at their C-termini (RGGGREVITIYS). Control experiments with *kcc* deletion mutations show specificity to Kcc protein under the staining conditions used (Figure 2.6). Other primary antibodies used were: Ab13970 chicken polyclonal anti-GFP (1:1000; Abcam), nc82 mouse anti-bruchpilot (1:500; Developmental Studies Hybridoma Bank developed under the auspices of the National Institute of Child Health and Human Development [NICHD] and maintained by the Department of Biology, University of Iowa [Iowa City, IA]) and anti-HRP-Cy3 (1:100; Invitrogen). Secondary antibodies were highly cross-adsorbed IgG (H+L) Alexa Fluor 488 goat anti-chicken (1:1000; Jackson Immunoresearch), Alexa Fluor 546 goat anti-mouse (1:1000; Life technologies) and Alexa Fluor 647 goat anti-rabbit (1:1000; Life technologies). n>9 for each genotype and condition tested.

Imaging

Images were acquired using the following microscopes and imaging software: Zeiss LSM 5-Live with LSM 5 software (embryo images) and Zeiss LSM 780 with ZEN software (all other images). Cross-channel bleed-through for each stained tissue type was tested by single antibody stainings (data not shown). Fluorescent micrographs were processed using ImageJ software (National Institute of Health). Confocal slice and Z-stack sizes used are noted in figure legends. Image files were imported into Adobe Illustrator CS6 for figure composition. Microscopes were calibrated and maintained by the Berkeley Molecular Imaging Center.

Results

Neuronal expression of UAS-kcc-RNAi induces behavioral seizure-like activity

Loss of K^+/Cl^- cotransporter function, for example, via the kcc^{DHS1} *Drosophila* hypomorphic mutation, raises seizure-susceptibility through a reduction in *kcc* expression. The kcc^{DHS1} mutant displays seizure-sensitivity as evidenced by a lowered threshold to evoked electrophysiologically-recorded seizure-like activity, and a bang-sensitive (BS) paralytic behavioral seizure-like activity phenotype hereafter referred to as 'BS paralysis' (Hekmat-Scafe et al., 2006; Hekmat-Scafe et al., 2010). Here, I dissect spatial aspects of induced seizure-sensitivity using different GAL4 drivers and UAS-kcc-RNAi transgenes to generate *kcc* loss-of-function in subsets of cells (Brand & Perrimon, 1993). I examined a total of 64 different GAL4 drivers in combination with 2 UAS-kcc-RNAi constructs (Table 2.1). This is a robust

method of inducing seizure-sensitivity, particularly using UAS-kcc-RNAi-B (Bloomington Stock Center #34584), which appears to be more efficacious than UAS-kcc-RNAi-V (Vienna Drosophila RNAi Center #101742) (Table 2.2). Twenty-eight of the 64 GAL4 drivers tested were found to induce lethal and/or paralytic phenotypes (Figure 2.1). The other 36 GAL4 drivers gave rise to viable flies without BS paralytic or morphological phenotypes.

Several GAL4/UAS combinations resulted in lethal phenotypes, especially the ubiquitous driver Act5C (First to third instar, and embryonic lethal with UAS-kcc-RNAi-V and UAS-kcc-RNAi-B, respectively) and the pan-neuronal driver elav^{c155} (late larval to late pupal and embryonic lethal with UAS-kcc-RNAi-V and UAS-kcc-RNAi-B, respectively). Third instar larvae of *elav^{c155}*-GAL4>*UAS-kcc-RNAi-V* and of several other genotypes often burrowed to the bottom of their vials before perishing (Figure 2.2*A*). The cholinergic neuron drivers, Cha [1] and Cha [2], caused semi-lethality and 100% BS paralysis in escapers with UAS-kcc-RNAi-V, and produced late pupal lethality with UAS-kcc-RNAi-B. In addition, *Cha-GAL4>UAS-kcc-RNAi-V* flies are sterile and have a completely penetrant juvenile-wing phenotype identical to that of flies with perturbed CCAP neuropeptide-producing/-receptive neurons (Figure 2.2*B*). These observations further demonstrate the criticality of *kcc* functions in the *Drosophila* nervous system.

Resembling the observations using the Cha-GAL4 drivers, I note unusual findings with the ellipsoid body driver, c507, the motor neuron driver, OK6, and the MB drivers, 201Y, MB247, OK107, and c772: for each of these GAL4 drivers, the weaker UAS-kcc-RNAi-V is largely ineffective in inducing BS paralytic behavior. In contrast, in combination with the stronger UAS-kcc-RNAi-B, the MB drivers induce complete (100%) or nearly complete (> 90%) BS paralysis and the c507 and OK6 drivers cause lethality. These data suggest that a threshold of *kcc* RNAi in a particular neuronal population must be reached in order for phenotypes to manifest. Despite this unusual observation between the two UAS-kcc-RNAi constructs, the MB GAL4 drivers did not appear to be markedly more effective at inducing BS paralysis phenotypes in these experiments than any other neural drivers.

Examination of 49 GAL4/UAS combinations using MB and other neuronal drivers showed no obvious spatial tendencies in the induction of seizure-sensitivity by UAS-kcc-RNAi. However, there is a clear correlation between the extent of expression with regards to the number of neurons constituting a driver expression domain, and the emergence of BS paralysis. Drivers expressing in small sets of neurons, including GABAergic, U/CQ and Pdf-expressing neurons failed to illicit BS paralysis with UAS-kcc-RNAi. Non-nervous system drivers, including those with robust hemocyte, salivary gland, fat body, muscle, tracheal and adipokinetic hormone-secreting cell expression failed to generate BS paralysis phenotypes (Table 2.2). Cumulatively, it appears that phenotypes are mainly associated with the number of neurons deficient in *kcc* function, and the magnitude of this

deficiency. It also appears that some *kcc*$^{+}$ function is required for the nervous system to exhibit seizure-sensitive phenotypes; a more severe loss of function causes lethality.

BS paralysis of *A307-GAL4>UAS-kcc-RNAi-V*

Experiments using the A307 GAL4 driver indicate that loss of *kcc* function in glia, as well as in neurons, causes seizure-sensitivity. A307 had been thought to have a limited expression profile, only consistently expressing GAL4 in the few neurons of the giant fiber (GF) circuit and not many other neurons in adults (Allen, Drummond, Sweetman, & Moffat, 2007; Phelan et al., 1996). I initiated investigation using *A307-GAL4>UAS-kcc-RNAi-V* to explore contributions of the GF circuit to seizure-susceptibility. Using this driver UAS-kcc-RNAi-B is lethal in 1x dose and UAS-kcc-RNAi-V is lethal in 2x doses. UAS-kcc-RNAi-V in 1X dose (genotype: *A307-GAL4>UAS-kcc-RNAi-V*) flies displayed 100% BS paralytic behavior. In addition, recovery time, an indicator of severity, was prolonged, comparable to the most severe of BS mutants *para*^{bss1} (Figure 2.4*A*). Taken together, these phenotypes are substantially more severe than had initially been anticipated for GF system knockdown of *kcc*.

Part of the A307 severity appears to be explained by a broader neuronal expression profile than had been expected. Using a sensitive reporter, *40xUAS-mCD8::GFP*, I confirmed expression in GF circuit neurons and thoracic and abdominal sensory neurons (data not shown) (Phelan et al., 1996; Figure 2.4*D*, *E*). In addition, I found ubiquitous GFP expression in the antennal lobe (AL, Figure 2.4*C*), and lamina (Lam, Figure 2.4*G1*), as well as expression in subsets of MB Kenyon cells (arrows, Figure 2.4*C*, *D*, *E*), and medulla (Med, Figure 2.4*F1*). Taking advantage of A307 expression diversity, I used GAL80 (inhibitor of GAL4) transgenes to restrict the A307 expression domain driving UAS-kcc-RNAi-V. For example, UAS-kcc-RNAi-V was expressed in all A307 cells and then Gad1-GAL80 was used to eliminate RNAi from A307 GABAergic neurons (genotype: *A307-GAL4>UAS-kcc-RNAi-V/+;Gad1-GAL80/+*). Experimental flies showed 97% BS paralysis, suggesting that inhibitory interneurons within the A307 domain contribute little to the behavioral phenotype. Similarly, when cholinergic neurons were removed from the A307 domain using Cha-GAL80, experimental flies showed 80% BS paralysis, indicating that these neurons also contribute little to the behavioral phenotype. In contrast, greater suppression of the A307 phenotype was observed with tsh-GAL80 (thoracic ganglion, 20% BS paralysis) and MB-GAL80 (mushroom body, 7% BS paralysis). Thus, different types of neurons contribute to A307 %BS paralysis. Elav-GAL80 (all neurons) caused extensive, but incomplete, suppression (9.4% BS paralysis). This incomplete suppression suggested that within the limitations of the GAL80 technique, A307 drives UAS-kcc-RNAi-V in non-neuronal tissues and this may also contribute to seizure-sensitivity.

Non-neuronal expression of A307 was found in confocal sections comparing its expression to that of the neuronal membrane marker horseradish peroxidase (HRP). Example fluorescent micrographs taken from the optic ganglia show A307 expression in both neuronal and non-neuronal cell types (Figure 2.4*F3*, *G3*). Non-neuronal cell processes may belong to glia since previous studies in these brain structures have reported similar patterns surrounding neurons (T. N. Edwards, Nuschke, Nern, & Meinertzhagen, 2012). I tested repo-GAL80 (all glia except midline glia) expecting the result to serve as a negative control for my running hypothesis of neuronal contributions to seizure-sensitivity. I made the serendipitous discovery that the *A307>UAS-kcc-RNAi-V* behavioral phenotype was substantially suppressed by repo-GAL80 (7% BS paralysis, Figure 2.4*B*). These observations provide the first indication for the potential involvement of glial CCC function in seizure-susceptibility. Tentatively, these findings expand the cell-numerical hypothesis for *kcc* loss-of-function and seizure-susceptibility to include the glial cell-type. A joint threshold requirement for seizures via *kcc* RNAi in neurons and glia could explain the incomplete suppression seen with elav-GAL80 and with repo-GAL80.

BS paralysis caused by glial expression of UAS-kcc-RNAi

Experiments using glial-specific GAL4 drivers indicate directly that loss of *kcc* function in this tissue causes seizure-sensitivity. repo-GAL4 drives expression in all glia except for midline glia. When used to drive UAS-kcc-RNAi, I find that *repo-GAL4>UAS-kcc-RNAi-V* and *repo-GAL4>UAS-kcc-RNAi-B* cause substantial BS paralytic behavior, 70% and 85% BS paralysis, respectively (Figure 2.1). Seizure refractory periods were also prolonged in these flies compared with those of mutants in the BS collection (Kuebler & Tanouye, 2000). These are surprising findings, particularly since expressing kcc^{+} in glial cells was not especially effective in rescuing kcc^{DHS1} mutant BS phenotypes, although some rescue was observed (Hekmat-Scafe et al., 2010).

Several glial subtypes distinguished by transcriptome, proteome, morphology and function are present in *Drosophila* (DeSalvo, Mayer, Mayer, & Bainton, 2011; T. N. Edwards et al., 2012; Hartenstein, 2011; Stork et al., 2012). Particularly interesting are the subperineurial glia (SPG) that comprise the main blood-brain barrier cell type. Intercellular diffusion barrier integrity is maintained by septate junctions, protein complexes organized between SPG cells and analogous to mammalian tight junctions. GAL4 drivers apparently specific for cells that express septate junction genes, including SPG cells, were particularly effective at causing BS paralytic behavioral phenotypes in combination with UAS-kcc-RNAi. Thus, Gli-GAL4 and Moody-GAL4 each driving UAS-kcc-RNAi-B gave rise to 100% and 65% BS paralysis, respectively (Figure 2.1). *Gli-GAL4>UAS-kcc-RNAi-B* flies often had malformed wings (Figure 2.2*C*) and were especially prone to behavioral

seizure-like activity. Gentle handling of their vial was sufficient to trigger seizures; this appears to be the most severely seizure-sensitive genotype that has been observed for *Drosophila* to date. *Gli-GAL4>UAS-kcc-RNAi-B* flies also exhibited the longest refractory period reported, with inability to illicit a second seizure with the same stimulus taking up to one hour following the first (data not shown). Although *Gli-GAL4>UAS-kcc-RNAi-B* flies always had locomotor difficulties, they only exhibited stereotyped BS paralysis if their previous seizure was more than an hour past. The result points to a potential causative link between BBB function and seizure refractory period.

Substantial (90%) BS paralysis was also observed with *NP2222-GAL4>UAS-kcc-RNAi-B*. NP2222-GAL4 is reported to drive expression in cortex glia surrounding neuronal cell bodies (Melom & Littleton, 2013). I also observed BS paralysis using *nrv2-GAL4>UAS-kcc-RNAi-B* (cortex and neuropile glia, 88% BS paralysis), *mz709-GAL4>UAS-kcc-RNAi-B* (ensheathing glia, 60% BS paralysis) and *alrm-GAL4>UAS-kcc-RNAi-B* (astrocyte-like glia, 22% BS paralysis). Taken together, these combined results suggest that proper *kcc* function is required in glial cells, and that loss-of-function causes seizure-sensitivity. Further, within the limitations of GAL4 glial driver specificity, several glial subtypes may contribute to the seizure-sensitive phenotype due to *kcc* loss of function.

Electrophysiology with UAS-kcc-RNAi

The BS paralytic phenotype is an indicator of seizure-sensitivity: flies displaying a strong BS behavioral phenotype generally display a substantially reduced threshold to evoked seizure-like neuronal activity in electrophysiological tests (Kuebler & Tanouye, 2000; Pavlidis & Tanouye, 1995). Here, seizure-like activity was evoked by high frequency electrical stimulation (HFS) of the brain and recorded as abnormal firing of the dorsal longitudinal flight muscle (DLM) (Figure 2.3*A*). 24-48 hour old wild-type Canton-Special flies had a relatively high seizure threshold, 40.7±2.7 V HFS (Figure 2.3*B*). Example DLM traces following sub-threshold and supra-threshold HF stimuli administered to Canton Special flies are shown in Figure 2.3*C*. A seizure was scored if DLM activity following an HFS was of abnormally high frequency, followed by failure to illicit a DLM response via GF circuit stimulation (Figure 2.3*C*, red inset) unlike prior to HFS delivery or sub-threshold stimulation (Figure 2.3*C*, green inset). Experimental flies of the genotype: *A307-GAL4>UAS-kcc-RNAi-V* showed a relatively low evoked seizure threshold, 10.7±2.1V HFS (Figure 2.3*B*). An example seizure from *A307-GAL4>UAS-kcc-RNAi-V* flies is shown in Figure 2.3*C*. The threshold of the A307-GAL4 knockdown is significantly lower than that of the hypomorphic mutation kcc^{DHS1}, 17.0±1.4V HFS (Hekmat-Scafe et al., 2006). In comparison, the seizure threshold of control flies (genotype: *UAS-kcc-RNAi-V*) is 37.8±2.7 V HFS, similar to that of wild-type Canton Special.

Thus, knockdown of *kcc* in a subset of fly cells can result in more severe seizure-susceptibility than that caused by any reported *kcc* mutation.

Low seizure thresholds were measured when CCC expression was reduced in glial cells (Figure 2.3*B*). Seizure threshold for *repo-GAL4>UAS-kcc-RNAi-B* flies was 17.5±1.5 V HFS. An example of a *repo-GAL4>UAS-kcc-RNAi-B* seizure is shown in Figure 2.3*C.* The seizure threshold of *Gli-GAL4>UAS-kcc-RNAi-B* was also low, 9.9±1.9V HFS. *repo-GAL4>UAS-kcc-RNAi-B* and *Gli-GAL4>UAS-kcc-RNAi-B* flies were mounted in wax then left to rest in a humidified chamber for one hour prior to testing because of their long seizure refractory periods (see previous section). Still, *Gli-GAL4>UAS-kcc-RNAi-B* flies often had seizures during electrode placement and so could not be probed for seizure susceptibility and were discarded. Hence, I believe the measured threshold for these flies to be a gross overestimate because some contaminating data points pertained to the elevated thresholds during refractory periods seen previously (Kuebler & Tanouye, 2000). Flies that did not suffer from an initial seizure were only given one HFS. An example of a *Gli-GAL4>UAS-kcc-RNAi-B* seizure is shown in Figure 2.3*C.* Seizure threshold of control flies (genotype: *UAS-kcc-RNAi-B*) is 38.5±3.3 V HFS, not significantly different from that of wild-type Canton-Special. These electrophysiological results confirm behavioral observations indicating that reducing expression of *kcc* by *RNAi* in either nerve cells or glial cells causes seizure-sensitivity. To my knowledge, this is the first causative link between glial cell CCC disruption and increased seizure-susceptibility.

I also assayed the ability of the GF system from each genotype to follow stimuli of a particular frequency, detected as 1:1 responses in the DLMs, as described previously (Allen & Godenschwege, 2010). Specifically, I gave each fly four sets of 10 trains of 12 GF threshold stimuli at 100, 200 and 300 Hz. Two sets were administered before the first HFS, and two were administered 7-10 minutes after (i.e. just before the second HFS in Canton S and *A307-GAL4>UAS-kcc-RNAi-V* flies*,* and prior to discarding *Gli-GAL4>UAS-kcc-RNAi-B* flies). The number of DLM responses for each genotype was quantified and expressed as a successful-following percentage for each frequency. I compared successful-following percentages of wild-type Canton S, *A307-GAL4>UAS-kcc-RNAi-V* and *Gli-GAL4>UAS-kcc-RNAi-B* (Figure 2.2*D*). Wild-type control genotype DLM percent-following was ~100%, 30% and 10% for 100, 200 and 300 Hz, respectively. *A307-GAL4>UAS-kcc-RNAi-V* percent-following for each frequency was not significantly different than those of Canton S. *Gli-GAL4>UAS-kcc-RNAi-B* DLMs failed to follow GF stimulation as well at 100 Hz, but was not significantly different at 200 Hz and 300 Hz. This result suggests a convoluted temporal relationship for DLM following in this genotype. Some *Gli-GAL4>UAS-kcc-RNAi-B* flies had wild-type following frequencies at 100 Hz, whereas others had much lower percent-following, reflecting variability between flies. However, most of the reduction in the total average percent-

following frequency relative to Canton S comes from variability within one fly; between the two pairs of the four sets of stimuli. Thus, I speculate that the reduction in percent-following is linked to the seizure refractory periods of *Gli-GAL4>UAS-kcc-RNAi-B* flies, with the worst following performances observed after administration of an HFS. Variability between flies could be due to some flies being in the seizure refractory state prior to administration of any stimuli.

kcc is expressed in glial cells, as well as neurons

Kcc immunoreactivity is present throughout the nervous system and it is this expression which is responsible for loss-of-function seizure-sensitivity seen in this tissue (Hekmat-Scafe et al., 2006; Hekmat-Scafe et al., 2010). To examine Kcc localization in more detail, a Kcc-specific polyclonal antibody was generated that should recognize the four predicted Kcc isoforms (Kcc-A, -B, -C and –D) (Figure 2.6). Here, I find that Kcc immunoreactivity is also present in larval and adult glial cells; this expression is presumably responsible for phenotypes observed with glial GAL4 drivers driving UAS-kcc-RNAi. Figure 2.5 shows Kcc antibody staining present in both neuronal and glial cells in third instar larvae and adult brains. Prominent Kcc staining is present in the ventral nerve cord (VNC) and peripheral nerves (PNs), as well as in neuronal cell bodies of the VNC (Figure 2.5*A*). Weaker Kcc colocalization with the neuropile marker, anti-nc82, is seen in the VNC. However, the neuropile reveals Kcc protein when examined at higher magnification and gain settings (data not shown).

Glial expression of Kcc is salient at the motor nerve terminal and neuromuscular junction (NMJ) of third instar larvae (Figure 2.5*B3*). The peripheral nerve and individual sensory and motor axons display robust GFP signal (Figure 2.5*B1*). Although the nerve contains some Kcc, the synaptic region appears largely devoid of Kcc (magenta-labeling via anti-Kcc antibody staining, Figure 2.5*B2*). Neither sensory neuron cell bodies nor axons appear to show Kcc staining. Strong anti-Kcc immunoreactivity is present in layers ensheathing the peripheral nerve (arrowheads, Figure 2.5*B2*, *B3*) that appear to terminate before the motor neurons soma. Larval muscle also had a covering of Kcc that was often continuous with nerve Kcc (arrow, Figure 2.5*B2, B3*). Taken together, I tentatively identify most Kcc at the periphery as belonging to SPG cells, which are thought to ensheath both nerve and muscle (Pereanu, Shy, & Hartenstein, 2005).

Kcc immunoreactivity is observed throughout the adult brain present apparently in glial, as well as neuronal cell types. For clarity—since magenta and green merged images provide the best indication of colocalization—all of the following triple-stained adult brain image series were bordered by merged images, with the shared Kcc image at the center of each series. Figure 2.5*C3* depicts the general pattern of Kcc in the adult mushroom body. Kcc is labeled by anti-Kcc and neuronal membranes are labeled with GFP

(and anti-GFP) utilizing the mushroom body driver OK107 (genotype: *OK107-GAL4>UAS-mCD8::GFP*). Kcc staining is abundant in the mushroom body neuropile and in the cell body region (Figure 2.5*C1*, calyx, labeled Cyx). Kcc staining is also observed in a subset of optic lobe medulla (labeled Med) neurons and their processes (Figure 2.5*C1*). Merge shows apparent colocalization of neuronal and Kcc signal in the mushroom body cell bodies and neuropile; a general arrangement found in many brain regions examined (see below and data not shown). Surrounding the MB cell body region appears to be a layer of non-neuronal Kcc expression (arrow, Figure 2.5*C1*). I tentatively identify this expression as belonging to PG and/or SPG cells, which are thought to ensheathe the CNS (DeSalvo et al., 2011). DIC image of the same slice shows white granular regions of cell bodies, and dark regions of neuropile (Figure 2.5*C4*). Colocalization of cell bodies is often associated with the undulated Kcc patterns found in adult central brain (Figure 2.5*C5*). Similarly, in the optic medulla, *OK107-GAL4>UAS-mCD8::GFP* drives GFP in a subset of neurons (Figure 2.5*D2*) and Kcc signal in the same cross-section slice (Figure 2.5*D3*) colocalizes with GFP (Figure 2.5*D1*). The anatomical layout of the medulla lends to better spatial resolution for marked neurons. Kcc is detected in proximity to neuronal cell bodies, which resembles cortex glia, although could be due to unlabeled medulla neurons (arrows, Figure 2.5*D1*). Neuropile staining in the same medulla region (Figure 2.5*D4*) colocalizes with Kcc (Figure 2.5*D5*). Kcc interlacing neuropile is seen which resembles expression in neuropile glial processes (T. N. Edwards et al., 2012).

For exploring glial cell Kcc I additionally co-stained brains expressing 1) membrane-bound GFP exclusively in glia (repo-GAL4>mCD8::GFP), 2) anti-Kcc antibody, and 3) the neuronal membrane marker horseradish peroxidase (HRP). Again, merged images bordered the image series, with GFP and HRP staining both presented in green for clarity when merged with magenta (Kcc staining, in the middle of each series). Imaging of the posterior central brain confirmed that Kcc is enriched in PG and/or SPG cells and cortex glia (arrows and arrowheads, respectively, Figure 2.5*E1*, *E2*, *E3*). Identification of Kcc-positive glial subtypes was performed by manual tracing of structures in GFP/HRP merge Z-stacks based on the known stereotyped anatomical relationships between glial subtypes and neurons (data not shown). Optic medulla surface glia were highlighted in the lateral brain by Kcc staining (Med, Figure 2.5*F3*). Apparent processes of fenestrated and pseudocartridge glia, the surface glia of the optic lamina, also react with anti-Kcc (Lam, Figure 2.5*F1* and T. N. Edwards et al., 2012). High-magnification images of the inner optic lamina expose a non-uniform distribution of Kcc in glia and neurons (Figure 2.5*G1*, *G5*). Neuronal processes contain Kcc foci (Figure 2.5*G5*), while glial Kcc in this region could belong to astrocyte-like glial processes mingling with synapses (Figure 2.5*G1*). In summary, brain Kcc was membrane bound and found

ubiquitously in both neurons and glia. Cell bodies and their glial partners, cortex and surface glia, had the highest concentrations of Kcc. Neuropile occupying internal brain regions contained Kcc when examined with higher magnification and gain settings.

UAS-kcc-RNAi during development has consequences in the young adult, including: neuronal and whole-brain volume increase, and BBB degradation

What cellular dysfunctions arising from *kcc* RNAi throughout development persist into the adult stage? I dissected and imaged brains of 24-48 hour old flies of different GAL4/UAS-kcc-RNAi genotypes to explore this question. Whole-brain volume increases were seen in several genotypes, including the brains of *A307-GAL4>UAS-kcc-RNAi-V,40xUAS-mCD8::GFP* (Figure 2.7*B1*), *OK107-GAL4>UAS-kcc-RNAi-B,UAS-mCD8::GFP* (Figure 2.7*D1*), and *repo-GAL4>UAS-kcc-RNAi-B,UAS-mCD8::GFP* (Figure 2.7*F1*) in comparison with brains of control genotypes (Figure 2.7*A1, C1, E1,* respectively). For example, I estimate an approximately 2.5-fold volume increase for *A307-GAL4>UAS-kcc-RNAi-V,40xUAS-mCD8::GFP* compared to wild-type (n = 13). Undulated Kcc patterns of PG and SPG cell membranes appeared qualitatively more extreme in *A307-GAL4>UAS-kcc-RNAi-V,40xUAS-mCD8::GFP* and *OK107-GAL4>UAS-kcc-RNAi-B,UAS-mCD8::GFP* brains (Figure 2.7*B1*, *D1,* respectively); the glial cells appear to have more foldings, and thus, might have a larger surface area than surface glia in wild-type (Figure 2.7*A1*, C*1,* respectively). In optical slices of the same size, shorter stretches and smaller sheets of Kcc signal are present around enlarged brains, whereas, wild-type Kcc signal stretches are longer and there is a higher probability of observing larger contiguous planes of surface glia. Expanded surface area of surface glia and the secreted extracellular matrix, the neural lamella, could be a physiological compensation mechanism for enhancing the ion permeability and cation-selectivity barriers upon neuronal loss of Kcc (Juang & Carlson, 1994). PGs continue to proliferate to accommodate brain size, but not much is known about morphological optimization of their functions (DeSalvo et al., 2011). Upon reexamination, it is interesting to note that embryos homozygous for *kcc* null mutations were usually bigger than their non-homozygous siblings, reminiscent of mutant embryos lacking mesoderm and its derived PGs (Figure 2.6 and J. S. Edwards, Swales & Bate, 1993).

The soma and processes of neurons expressing *kcc* RNAi have wild-type anatomical positions with respect to brain size. However, some morphological differences appear to be caused by *kcc* RNAi. Identified cells, GF and lateral pace-making neurons (LNs), expressing *kcc* RNAi were enlarged and misshapen (Figure 2.7*B2* and Figure 2.8*B1*), as seen previously in an *in vivo* mammalian system (Cancedda et al., 2007). Diffuse and elongated dendrites lacking distinctive spines were also evident in the

GF neuron deficient in Kcc (insets, Figure 2.7*B2*) similar to reports of "filopodia-like" dendritic spines in mice (Fiumelli et al., 2013; Li et al., 2007). Cellular abnormalities due to *kcc* knockdown were clearest in the MB calyx, perhaps because the ratio of Kcc in the tightly-sequestered neuronal processes to glial membrane Kcc is higher than elsewhere in the brain (Figure 2.7*C3*, *D3*). It was common to find the undulated Kcc signal on the brain surface at a distance from Kcc deficient neurons, separated by signal-devoid regions (Figure 2.7*B4*, *D4* and Figure 2.8*B3*).

Glial cell anatomical changes in oversized *repo-GAL4>UAS-kcc-RNAi-B,UAS-mCD8::GFP* adult brains are revealed at higher magnification. MB Kenyon cell bodies and calyxes are wrapped and interlaced with glial membranes in wild-type brains, but these associations are largely absent when glia express *kcc* RNAi (labeled Cyx, Figure 2.7*E2* and *F2,* respectively). Thus, the signal-devoid regions observed in such inner brain confocal slices are expected to be enlarged extracellular space (ECS). Enlarged ECS could be what is observed in the brains of *A307-GAL4>UAS-kcc-RNAi-V,40xUAS-mCD8::GFP* and *OK107-GAL4>UAS-kcc-RNAi-B,UAS-mCD8::GFP* flies as well, however, glial membranes were not visualized in these genotypes. The possibility of a compensatory increase in total glial cell volume to accommodate larger brain sizes in those genotypes could not be excluded. Enlarged ECS is aberrant and suggests the possibility of water retention due to ionic imbalances compared with tightly-packaged wild-type brains, and likely degradation of BBB functions, due to *kcc* loss-of-function (Figure 2.7*A4*, *C4*, *E4* and Figure 2.8*A3*).

ncc69 RNAi in glia, but not in neurons, causes seizures

A glial function for *kcc* had not been previously described for *Drosophila*. However, another fly CCC has been described for glia, *ncc69*, a $Na^+/K^+/2Cl^-$ cotransporter and an ortholog of the well-studied mammalian NKCCs (Gamba et al., 1993; Park & Saier, 1996; Xu et al., 1994).The *ncc69* gene product works together with the Serine/Threonine kinase, Fray, to regulate extracellular volume (Cruz-Rangel et al., 2011; William M. Leiserson et al., 2011). NKCC1 was shown to be involved in seizure-genesis previously (Dzhala et al., 2005). So, I examined *ncc69* loss-of-function for BS paralysis by driving two UAS-ncc69-RNAi constructs*,* UAS-ncc69-RNAi-B and UAS-ncc69-RNAi-V*,* with different GAL4 drivers (Figure 2.1). UAS-ncc69-RNAi driven by repo-GAL4 in glial cells caused substantial BS paralysis, with up to 58% of animals paralyzed by mechanical stimulation. Gli-GAL4 also caused BS paralysis in some flies (4%). In contrast, unlike the case for *kcc*, loss of *ncc69* function in neurons causes no BS paralytic behavioral phenotype. In particular, flies carrying *elav^{C155}-GAL4>UAS-ncc69-RNAi-V* showed no evidence of increased seizure-sensitivity (Figure 2.1).

Electrophysiological tests on *repo-GAL4>UAS-ncc69-RNAi-V* showed that these flies also have a low seizure threshold, as suggested by the BS

paralytic behavior test. Their seizure refractory periods was comparable to that of *repo-GAL4>UAS-kcc-RNAi-B*, so each fly was given only one HFS as well (data not shown). The seizure threshold for *repo-GAL4>UAS-ncc69-RNAi-V* flies was found to be 20.9±2.2 V HFS, lower than control flies (genotype: *UAS-ncc69RNAi-V*, seizure threshold: 44.7±2.7 V HFS,). Therefore, seizure-sensitivity by UAS-ncc69-RNAi parallels volume regulation phenotypes seen with utilizing the same RNAi construct: knockdown of *ncc69* in glia causes seizures and cell volume enlargement, but knockdown in neurons does not cause any detectable hyperexcitability or cell volume phenotypes (Figure 2.1*,* Figure 2.3*B* and William M. Leiserson et al., 2011).

UAS-kcc-RNAi perturbs cell volume homeostasis and causes a "frayed-nerve" phenotype in third instar larval peripheral nerves

Leiserson et. al. (2011) found that third instar larvae lacking glial *ncc69* expression have abnormalities in the abdominal peripheral nerves associated with these glia. The nerves show prominent localized swellings, a so-called "bulging" phenotype, and marked defasciculation of neuronal processes, a so-called "frayed-nerve" phenotype. Abnormalities in this minimal system may be rescued by restoring Ncc69 to subperineural (SPG) glial cells forming the blood-nerve barrier (BNB). The inability of glia to transport K^+ out of the ECS due to *ncc69* loss-of-function, and the enlargement of glia from the subsequent water flux, is one suggested explanation for these abnormalities occurring during development (W. M. Leiserson & Keshishian, 2011).

Here, I find similarly that *kcc* loss-of-function in glial cells causes swelling and frayed-nerve like phenotypes. Figure 2.9 compares glia and neurons of third instar larvae abdominal nerves of different genotypes. *repo-GAL4>UAS-kcc-RNAi-B,UAS-mCD8::GFP* larvae display an increase in the average nerve diameter along the entire length of their nerves (Figure 2.9*B1*, *B2*, *B4*, *B5*), without localized bulges, relative to those of wild-type (Figure 2.9*A1, A2*, *A4*, *A5*). The phenotype is completely penetrant with volume increases appearing in the abdominal nerves of all animals examined (n = 12). Defasciculation of neuronal processes is also visible within the enlarged nerves revealed by Kcc and HRP staining (Figure 2.9*B3*, *B4* and Figure 2.10*B2*, respectively). These phenotypes were less severe than those of nerve bulges in glial *ncc69* RNAi larvae (Figure 2.9*C1-C5* and Figure 2.10*C1-C4*). The ion-homeostasis/osmoregulation model for larval nerves proposed by Leiserson and Keshishian points to glial transport of K^+ and Cl^- into hemolymph. The findings suggest that Kcc might contribute to, this transport function. The PN ion-homeostasis/osmoregulation model proposed by Leiserson and Keshishian, modified to include the role of Kcc, is found in Figure 2.11*A*.

I also found that *kcc* knockdown in neuronal cells caused frayed-nerve phenotypes in larval PNs. Defasciculated nerves labeled by membrane-bound GFP were observed in PNs of *elav^{C155}>UAS-kcc-RNAi-V,UAS-mCD8::GFP*

third instar larval fillets stained with anti-GFP and anti-Kcc (Figure 2.9*E2* and *E3*, respectively). Although total PN size and nerve bundles in the neuronal *kcc* knockdown condition did not appear to be altered without fine measurements, the observed signal-devoid regions between neural processes might reflect obvious confined enlargement of ECS (Figure 2.9*E4*, *E5*). Conceivably, frayed nerves could be a consequence of localized disruptions in ion-homeostasis and consequent water-retention confined to PN neuronal compartments. The PN ion-homeostasis/osmoregulation model proposed by Leiserson and Keshishian postulates simultaneous K^+/Cl^- efflux from neurons, and this transport might in part be provided by neuronal Kcc function as illustrated in the updated model (Figure 2.11*A*). This *kcc* loss-of-function result bolsters the connection between abnormalities in the simple larval nerve system and adult seizure-susceptibility noted earlier in the case of glial *ncc69* knockdown, but not neuronal *ncc69* knockdown; *kcc* knockdown in glia or neurons positively correlates with larval phenotypes as well as adult seizure-sensitivity.

Discussion

Seizure disorders, including the epilepsies, are tragedies suffered by about 1% of a given human population. These debilitating disorders exist for numerous genetic, epigenetic and environmental reasons. Inhibitory mechanisms of the nervous system are critical for neural circuit computation, but a price for computational complexity is the potential loss of inhibition; an imbalance favoring neuronal excitability may lead to a detrimental cataclysmic feed-back loop, or seizure. Existence of a multitude of pathways ending in hyperexcitability and disinhibition may be a reason why seizures or peroxismal events are seen in many animals, *in vitro* systems and computational models of neural activity. Seizures are multi-cellular phenomena most effectively examined *in vivo*. Neuroscientists have long recognized the complexity of regulating the electrochemical milieu governing the performance of nervous tissue. Hundreds of molecules contribute to mechanisms controlling a few biological ion species. Seizure disorder research with intact model organisms and fine molecule manipulation provides some hope for cures (Raol & Brooks-Kayal, 2012). When surgery is not an option, or when current anti-epileptic drugs (AEDs) are ineffective, as is the case with a third of epilepsies, novel therapeutics tailored to elucidated pathways could be vital to 1% of the population (Parker, Howlett, et al., 2011).

The loop-diuretics bumetanide and furosemide have well-known antiepileptic properties. These molecules are capable of suppressing seizures generated by synaptic and non-synaptic mechanisms in several systems (Hochman, 2012). As with most new pharmaceuticals, loop-diuretics are being considered for prescription as AEDs for their positive outcomes and nonfatal side-effects, without exact knowledge of how they work at the

molecular level or of long-term side-effects (Loscher et al., 2012). They are inhibitors of NKCCs and KCCs, however, as portrayed earlier, CCCs embody nervous system complexity; they offer all the challenges in defining their precise physiological and pathological roles. Blockade of two main pathways is suggested for loop-diuretic seizure suppression, the first being increased potency of inhibitory GABAergic synaptic signaling by diminishing uptake of Cl^- by NKCC1 in neurons (Blaesse et al., 2009). The second—osmoregulation and volume control of the extracellular space (ECS) by glia—is hypothesized to be necessary for sustained epileptiform activity *in vivo*, regardless of the activity's source. Antagonism of glial NKCC1 and concomitant limitation of ECS shrinkage due to glial cell swelling may underlie this general non-synaptic antiepileptic effect (Hochman, 2012).

Understanding the exact ways in which CCCs are involved in epilepsies could aid in the design of less toxic cures for seizures that are caused by CCC dysfunction. The *Drosophila* experimental model for CCC loss-of-function studies can provide insight into glial CCC mechanisms. A major finding here that reducing Kcc or Ncc69 via targeted RNAi in glial cells positively correlates with seizure-sensitivity. Although biochemical properties and loss-of-function phenotypes of glial CCCs have been explored previously *in vitro*, I am unaware of other studies exclusively targeting glial CCC functions *in vivo* besides this work presented here and that of Leiserson et al. in *Drosophila* (Gagnon et al., 2007; Jayakumar & Norenberg, 2010; Jayakumar et al., 2011; William M. Leiserson et al., 2011; Ringel & Plesnila, 2008). The conservation of glial function and the currently unmatched genetic tools for manipulating them in *Drosophila* make the fly a superb model for elucidating physiological and pathological *in vivo* CCC mechanisms.

I focused on the role that Kcc plays in seizure-susceptibility. My first question regarding this role concerned whether glial Kcc-deficiency could cause seizures, i.e. is targeted glial cell *kcc* knockdown sufficient for induction of seizure-sensitivity in *Drosophila*? Indeed, I found that knockdown in nearly all glia, or exclusively in several glial subtypes, induced robust behavioral and electrophysiologically-recorded seizures. Behavior and electrophysiology experiments culminated in the hypothesis that seizure-susceptibility due to Kcc loss in *Drosophila* depends on the number of glia and neurons with Kcc-deficiency. A Kcc-specific antibody revealed Kcc in neurons and glia at different stages of development, meeting the expectation from cell type-specific *kcc* knockdown results. The second question concerned whether the mechanisms of seizure-genesis due to neuronal or glial *kcc* knockdown were separable. To address this question in one way, I explored anatomical changes in neurons and glia correlating with *kcc* RNAi in those cells and found similarities between the two conditions. Mainly, I found likely indications of perturbed ion-homeostasis and subsequent osmoregulation phenotypes in larval and adult nervous systems.

As a whole, the investigation expands the knowledge base of Kcc-deficiency phenotypes in *Drosophila*, and thus in turn, suggests a widespread role for glial K^+/Cl^- cotransporter loss in seizure-genesis across phyla.

Glial abnormalities, especially those of CNS astrocytes, have previously been correlated with seizures of different etiologies, but whether these defects are a cause or a consequence of them is undetermined (Kovacs et al., 2012; Steinhauser et al., 2012). It is unclear if the ionic mechanisms targeted by loop-diuretics are the same as those affected by glial K^+/Cl^- loss. For example, it is possible that glial K^+/Cl^- cotransport loss could have non-cell-autonomous effects on neuronal intracellular $[Cl^-]$ via ECS $[Cl^-]$ changes, thereby affecting inhibitory GABAergic synaptic transmission. Loop-diuretics could also inhibit ECS ion-homeostasis provided by K^+/Cl^- cotransporter glia causing deleterious K^+ concentrations and cell swelling leading to neuronal hyperexcitability. Structural functions provided by K^+/Cl^- cotransporters could contribute to loss-of-function seizure pathology as well, given that KCC2 has ion transport-independent functions (Fiumelli et al., 2013; Horn, Ringstedt, Blaesse, Kaila, & Herlenius, 2010; Li et al., 2007). Elimination of KCC2 C-terminus interaction with the cytoskeleton-associated protein 4.1N is responsible for these ion transport-independent phenotypes. *coracle*, the *Drosophila* ortholog of cytoskeleton-associated protein 4.1N-encoding genes, is a critical component of *Drosophila* septate junctions (SJs) and the BBB (Baumgartner et al., 1996; Oshima & Fehon, 2011). Kcc could be important for structural and/or ion-transport functions at the SJ akin to those of the Na^+/K^+ ATPase; perhaps Kcc is a member of the protein complex comprising the SJ. These possibilities have yet to be tested, but it is interesting to mention that of the four KCCs, only mutations causing KCC3 C-terminus truncations have been linked to certain human seizures (Benarroch, 2013; Galanopoulou, 2010; Shekarabi et al., 2012), and in addition, that of the three KCC3 isoforms (KCC3a-c) KCC3a is exclusively present in glia (Shekarabi et al., 2011).

It is clear that there are several important questions regarding *kcc* loss-of-function and seizure-susceptibility still unanswered. Particularly, how important are the cellular dysfunctions arising from early loss of Kcc for generating seizures in the adult? I attempted to answer this questions using different temporally-controlled expression systems, including the heat-schock GAL4 system and the TARGET system based on a temperature sensitive GAL80 ($GAL80^{ts}$) protein (McGuire et al., 2003). However, I was unable to induce seizures through presumed exclusive expression of *kcc* RNAi in neurons, glia or in all cells using these temperature-dependent systems (Figure 2.12*A*). I was also unable to ameliorate seizures upon restoration of kcc^+ expression in flies born as BS paralytics (Figure 2.12*B*). Although *kcc* mutant seizure-sensitivity was shown to be temperature-sensitive, with higher temperatures ameliorating seizures, another possible explanation for these data is the lack of a major role for acutely dampened

inhibitory synaptic GABAergic signaling in *Drosophila* seizure-susceptibility (Hekmat-Scafe et al., 2006). A speculative model incorporating known and proposed CCC dysfunctions, from *Drosophila* and other systems, is illustrated in Figure 2.11*B*. The work presented here sets the stage for thorough *in vivo* structure/function studies focused on CCCs using already available techniques. For example, the mosaic analysis using a repressible cell-marker (MARCM) system, combined with temperature-independent temporally-controlled gene expression of transgenes, can test phenotypic rescue in specific kcc^{-}/ kcc^{-} cells coexisting amongst a modifiable number of kcc^{+}/kcc^{+} cells in an individual fly. Interestingly, at least one of the four *kcc* transcripts exhibits two drastic developmental peaks in expression, one at the end of the embryonic stage and one at the end of the larval stage; two periods associated with vast restructuring of the nervous system in preparation for larval and adult stages, respectively (Roy et al., 2010). Further investigations utilizing the advantages of the *Drosophila* model of CCC-related dysfunction will be beneficial for unraveling the complex pleiotropic functions of the ancient CCCs in the nervous system. For, some phenomena are best examined under *in vivo* conditions using minimally-invasive and reversible manipulations, whilst marginalizing the significance of evolutionary-distance relative to humans. In particular, it would be of benefit to measure the extent of excitatory GABAergic transmission due to acute Kcc loss in adults and the impact this has on seizure-susceptibility.

Acknowledgments

This study was supported by awards from the McKnight Foundation and the NIH (NS31231) to M.A.T. I thank Angelica I. Anguiano, Ryan J. Arant, Roland J. Bainton, Diana M. Bautista, Brandon D. Bunker, Damian O. Elias, Jose E. Estrada, Marc R. Freeman, Kristin A. Gerhold, Tanja A. Godenschwege, Michael G. Gorczyca, Aaron M. Hamby, Liam J. Holt, Grant Kauwe, Louise Parker, Mu-ming Poo, Allan-Hermann Pool, Nasser M. Rusan, Kristin Scott, Maximilian H. Ulbrich, Scott Waddell and members of the Tanouye lab past and present for fruitful discussions and sharing of unpublished data. I would also like to thank Marc R. Freeman, Tanja A. Godenschwege, Gary H. Karpen, Haig Keshishian, Tzumin Lee, Louise Parker, Donald C. Rio, Nasser M. Rusan, Kristin Scott, Scott Waddell, the Bloomington Drosophila Stock Center, the Vienna Drosophila RNAi Center and the Developmental Studies Hybridoma Bank for reagents. I am grateful to Peter J. Chou, Ali E. Esmaeili, Jose E. Estrada, Daria Hekmat-Scafe, Olivia A. Kingsford, Akemi M. Kunibe, Tyler Liu, Graciela Medrano, Hong-An Truong, Richard E. Price, Jefferson "Matt" Taliaferro and Erin H. Welter for aid in acquiring preliminary data. And finally, I am grateful to John Dempster

for creating and sharing the open-source Strathclyde Electrophysiology Software, WinWCP.

REFERENCES

Allen, M. J., Drummond, J. A., Sweetman, D. J., & Moffat, K. G. (2007). Analysis of two P-element enhancer-trap insertion lines that show expression in the giant fibre neuron of Drosophila melanogaster. *Genes Brain Behav, 6*(4), 347-358. doi: 10.1111/j.1601-183X.2006.00263.x

Allen, M. J., & Godenschwege, T. A. (2010). Electrophysiological recordings from the Drosophila giant fiber system (GFS). *Cold Spring Harb Protoc, 2010*(7), pdb prot5453. doi: 10.1101/pdb.prot5453

Allen, M. J., Godenschwege, T. A., Tanouye, M. A., & Phelan, P. (2006). Making an escape: development and function of the Drosophila giant fibre system. *Semin Cell Dev Biol, 17*(1), 31-41. doi: 10.1016/j.semcdb.2005.11.011

Baumgartner, S., Littleton, J. T., Broadie, K., Bhat, M. A., Harbecke, R., Lengyel, J. A., . . . Bellen, H. J. (1996). A Drosophila neurexin is required for septate junction and blood-nerve barrier formation and function. *Cell, 87*(6), 1059-1068.

Ben-Ari, Y., Khalilov, I., Kahle, K. T., & Cherubini, E. (2012). The GABA excitatory/inhibitory shift in brain maturation and neurological disorders. *Neuroscientist, 18*(5), 467-486. doi: 10.1177/1073858412438697

Ben-Ari, Y., Woodin, M. A., Sernagor, E., Cancedda, L., Vinay, L., Rivera, C., . . . Cherubini, E. (2012). Refuting the challenges of the developmental shift of polarity of GABA actions: GABA more exciting than ever! *Front Cell Neurosci, 6*, 35. doi: 10.3389/fncel.2012.00035

Benarroch, E. E. (2013). Cation-chloride cotransporters in the nervous system: General features and clinical correlations. *Neurology, 80*(8), 756-763. doi: 10.1212/WNL.0b013e318283bb1c

Benesova, J., Rusnakova, V., Honsa, P., Pivonkova, H., Dzamba, D., Kubista, M., & Anderova, M. (2012). Distinct expression/function of potassium and chloride channels contributes to the diverse volume regulation in cortical astrocytes of GFAP/EGFP mice. *PLoS One, 7*(1), e29725. doi: 10.1371/journal.pone.0029725

Blaesse, P., Airaksinen, M. S., Rivera, C., & Kaila, K. (2009). Cation-chloride cotransporters and neuronal function. *Neuron, 61*(6), 820-838. doi: 10.1016/j.neuron.2009.03.003

Boettger, T., Rust, M. B., Maier, H., Seidenbecher, T., Schweizer, M., Keating, D. J., . . . Jentsch, T. J. (2003). Loss of K-Cl co-transporter KCC3 causes deafness, neurodegeneration and reduced seizure threshold. *EMBO J, 22*(20), 5422-5434. doi: 10.1093/emboj/cdg519

Brand, A. H., & Perrimon, N. (1993). Targeted gene expression as a means of altering cell fates and generating dominant phenotypes. *Development, 118*(2), 401-415.

Byun, N., & Delpire, E. (2007). Axonal and periaxonal swelling precede peripheral neurodegeneration in KCC3 knockout mice. *Neurobiol Dis, 28*(1), 39-51. doi: 10.1016/j.nbd.2007.06.014

Cancedda, L., Fiumelli, H., Chen, K., & Poo, M. M. (2007). Excitatory GABA action is essential for morphological maturation of cortical neurons in vivo. *J Neurosci, 27*(19), 5224-5235. doi: 10.1523/jneurosci.5169-06.2007

Colmenero-Flores, J. M., Martinez, G., Gamba, G., Vazquez, N., Iglesias, D. J., Brumos, J., & Talon, M. (2007). Identification and functional characterization of cation-chloride cotransporters in plants. *Plant J, 50*(2), 278-292. doi: 10.1111/j.1365-313X.2007.03048.x

Cruz-Rangel, S., Melo, Z., Vazquez, N., Meade, P., Bobadilla, N. A., Pasantes-Morales, H., . . . Mercado, A. (2011). Similar effects of all WNK3 variants on SLC12 cotransporters. *Am J Physiol Cell Physiol, 301*(3), C601-608. doi: 10.1152/ajpcell.00070.2011

DeSalvo, M. K., Mayer, N., Mayer, F., & Bainton, R. J. (2011). Physiologic and anatomic characterization of the brain surface glia barrier of Drosophila. *Glia, 59*(9), 1322-1340. doi: 10.1002/glia.21147

Dzhala, V. I., Talos, D. M., Sdrulla, D. A., Brumback, A. C., Mathews, G. C., Benke, T. A., . . . Staley, K. J. (2005). NKCC1 transporter facilitates seizures in the developing brain. *Nat Med, 11*(11), 1205-1213. doi: 10.1038/nm1301

Edwards, J. S., Swales, L. S., & Bate, M. (1993). The differentiation between neuroglia and connective tissue sheath in insect ganglia revisited: the neural lamella and perineurial sheath cells are absent in a mesodermless mutant of Drosophila. *J Comp Neurol, 333*(2), 301-308. doi: 10.1002/cne.903330214

Edwards, T. N., Nuschke, A. C., Nern, A., & Meinertzhagen, I. A. (2012). Organization and metamorphosis of glia in the Drosophila visual system. *J Comp Neurol, 520*(10), 2067-2085. doi: 10.1002/cne.23071

Featherstone, David E. (2011). Glial solute carrier transporters in drosophila and mice. *Glia, 59*(9), 1351-1363. doi: 10.1002/glia.21085

Feng, Y., Ueda, A., & Wu, C. F. (2004). A modified minimal hemolymph-like solution, HL3.1, for physiological recordings at the neuromuscular junctions of normal and mutant Drosophila larvae. *J Neurogenet, 18*(2), 377-402. doi: 10.1080/01677060490894522

Filippov, V., Aimanova, K., & Gill, S. S. (2003). Expression of an Aedes aegypti cation-chloride cotransporter and its Drosophila homologues. *Insect Mol Biol, 12*(4), 319-331.

Fiumelli, H., Briner, A., Puskarjov, M., Blaesse, P., Belem, B. J., Dayer, A. G., . . . Vutskits, L. (2013). An ion transport-independent role for the cation-chloride cotransporter KCC2 in dendritic spinogenesis in vivo. *Cereb Cortex, 23*(2), 378-388. doi: 10.1093/cercor/bhs027

Gagnon, K. B., Adragna, N. C., Fyffe, R. E., & Lauf, P. K. (2007). Characterization of glial cell K-Cl cotransport. *Cell Physiol Biochem, 20*(1-4), 121-130. doi: 10.1159/000104160

Gagnon, K. B., & Delpire, E. (2013). Physiology of SLC12 Transporters: Lessons from Inherited Human Genetic Mutations and Genetically-Engineered Mouse Knockouts. *Am J Physiol Cell Physiol*. doi: 10.1152/ajpcell.00350.2012

Galanopoulou, A. S. (2010). Mutations affecting GABAergic signaling in seizures and epilepsy. *Pflugers Arch, 460*(2), 505-523. doi: 10.1007/s00424-010-0816-2

Gamba, G., Saltzberg, S. N., Lombardi, M., Miyanoshita, A., Lytton, J., Hediger, M. A., . . . Hebert, S. C. (1993). Primary structure and functional expression of a cDNA encoding the thiazide-sensitive, electroneutral sodium-chloride cotransporter. *Proc Natl Acad Sci U S A, 90*(7), 2749-2753.

Hartenstein, V. (2011). Morphological diversity and development of glia in Drosophila. *Glia, 59*(9), 1237-1252. doi: 10.1002/glia.21162

Hebert, S. C., Mount, D. B., & Gamba, G. (2004). Molecular physiology of cation-coupled Cl- cotransport: the SLC12 family. *Pflugers Arch, 447*(5), 580-593. doi: 10.1007/s00424-003-1066-3

Hekmat-Scafe, D. S., Lundy, M. Y., Ranga, R., & Tanouye, M. A. (2006). Mutations in the K+/Cl- cotransporter gene kazachoc (kcc) increase seizure susceptibility in Drosophila. *J Neurosci, 26*(35), 8943-8954. doi: 10.1523/JNEUROSCI.4998-05.2006

Hekmat-Scafe, D. S., Mercado, A., Fajilan, A. A., Lee, A. W., Hsu, R., Mount, D. B., & Tanouye, M. A. (2010). Seizure sensitivity is ameliorated by targeted expression of K+-Cl- cotransporter function in the mushroom body of the Drosophila brain. *Genetics, 184*(1), 171-183. doi: 10.1534/genetics.109.109074

Hochman, D. W. (2012). The extracellular space and epileptic activity in the adult brain: explaining the antiepileptic effects of furosemide and bumetanide. *Epilepsia, 53 Suppl 1*, 18-25. doi: 10.1111/j.1528-1167.2012.03471.x

Horn, Z., Ringstedt, T., Blaesse, P., Kaila, K., & Herlenius, E. (2010). Premature expression of KCC2 in embryonic mice perturbs neural development by an ion transport-independent mechanism. *Eur J Neurosci, 31*(12), 2142-2155. doi: 10.1111/j.1460-9568.2010.07258.x

Jayakumar, A. R., & Norenberg, M. D. (2010). The Na-K-Cl Co-transporter in astrocyte swelling. *Metab Brain Dis, 25*(1), 31-38. doi: 10.1007/s11011-010-9180-3

Jayakumar, A. R., Panickar, K. S., Curtis, K. M., Tong, X. Y., Moriyama, M., & Norenberg, M. D. (2011). Na-K-Cl cotransporter-1 in the mechanism of cell swelling in cultured astrocytes after fluid percussion injury. *J*

Neurochem, 117(3), 437-448. doi: 10.1111/j.1471-4159.2011.07211.x
Juang, J. L., & Carlson, S. D. (1994). Analog of vertebrate anionic sites in blood-brain interface of larval Drosophila. *Cell Tissue Res, 277*(1), 87-95.
Kahle, K. T., Rinehart, J., & Lifton, R. P. (2010). Phosphoregulation of the Na-K-2Cl and K-Cl cotransporters by the WNK kinases. *Biochim Biophys Acta, 1802*(12), 1150-1158. doi: 10.1016/j.bbadis.2010.07.009
Kahle, K. T., Staley, K. J., Nahed, B. V., Gamba, G., Hebert, S. C., Lifton, R. P., & Mount, D. B. (2008). Roles of the cation-chloride cotransporters in neurological disease. *Nat Clin Pract Neurol, 4*(9), 490-503. doi: 10.1038/ncpneuro0883
Kovacs, R., Heinemann, U., & Steinhauser, C. (2012). Mechanisms underlying blood-brain barrier dysfunction in brain pathology and epileptogenesis: role of astroglia. *Epilepsia, 53 Suppl 6*, 53-59. doi: 10.1111/j.1528-1167.2012.03703.x
Kuebler, D., & Tanouye, M. A. (2000). Modifications of seizure susceptibility in Drosophila. *J Neurophysiol, 83*(2), 998-1009.
Leiserson, W. M., & Keshishian, H. (2011). Maintenance and regulation of extracellular volume and the ion environment in Drosophila larval nerves. *Glia, 59*(9), 1312-1321. doi: 10.1002/glia.21132
Leiserson, William M., Forbush, Biff, & Keshishian, Haig. (2011). Drosophila glia use a conserved cotransporter mechanism to regulate extracellular volume. *Glia, 59*(2), 320-332. doi: 10.1002/glia.21103
Li, H., Khirug, S., Cai, C., Ludwig, A., Blaesse, P., Kolikova, J., . . . Rivera, C. (2007). KCC2 interacts with the dendritic cytoskeleton to promote spine development. *Neuron, 56*(6), 1019-1033. doi: 10.1016/j.neuron.2007.10.039
Loscher, W., Puskarjov, M., & Kaila, K. (2012). Cation-chloride cotransporters NKCC1 and KCC2 as potential targets for novel antiepileptic and antiepileptogenic treatments. *Neuropharmacology*. doi: 10.1016/j.neuropharm.2012.05.045
Lucas, O., Hilaire, C., Delpire, E., & Scamps, F. (2012). KCC3-dependent chloride extrusion in adult sensory neurons. *Mol Cell Neurosci, 50*(3-4), 211-220. doi: 10.1016/j.mcn.2012.05.005
Macaulay, N., & Zeuthen, T. (2012). Glial K(+) clearance and cell swelling: key roles for cotransporters and pumps. *Neurochem Res, 37*(11), 2299-2309. doi: 10.1007/s11064-012-0731-3
McGuire, S. E., Le, P. T., Osborn, A. J., Matsumoto, K., & Davis, R. L. (2003). Spatiotemporal rescue of memory dysfunction in Drosophila. *Science, 302*(5651), 1765-1768. doi: 10.1126/science.1089035

Melom, J. E., & Littleton, J. T. (2013). Mutation of a NCKX eliminates glial microdomain calcium oscillations and enhances seizure susceptibility. *J Neurosci, 33*(3), 1169-1178. doi: 10.1523/JNEUROSCI.3920-12.2013

Oshima, K., & Fehon, R. G. (2011). Analysis of protein dynamics within the septate junction reveals a highly stable core protein complex that does not include the basolateral polarity protein Discs large. *J Cell Sci, 124*(Pt 16), 2861-2871. doi: 10.1242/jcs.087700

Park, J. H., & Saier, M. H., Jr. (1996). Phylogenetic, structural and functional characteristics of the Na-K-Cl cotransporter family. *J Membr Biol, 149*(3), 161-168.

Parker, L., Howlett, I. C., Rusan, Z. M., & Tanouye, M. A. (2011). Seizure and epilepsy: studies of seizure disorders in Drosophila. *Int Rev Neurobiol, 99*, 1-21. doi: 10.1016/b978-0-12-387003-2.00001-x

Parker, L., Padilla, M., Du, Y., Dong, K., & Tanouye, M. A. (2011). Drosophila as a model for epilepsy: bss is a gain-of-function mutation in the para sodium channel gene that leads to seizures. *Genetics, 187*(2), 523-534. doi: 10.1534/genetics.110.123299

Pasantes-Morales, H., & Tuz, K. (2006). Volume changes in neurons: hyperexcitability and neuronal death. *Contrib Nephrol, 152*, 221-240. doi: 10.1159/000096326

Pavlidis, P., & Tanouye, M. A. (1995). Seizures and failures in the giant fiber pathway of Drosophila bang-sensitive paralytic mutants. *J Neurosci, 15*(8), 5810-5819.

Pereanu, W., Shy, D., & Hartenstein, V. (2005). Morphogenesis and proliferation of the larval brain glia in Drosophila. *Dev Biol, 283*(1), 191-203. doi: 10.1016/j.ydbio.2005.04.024

Phelan, P., Nakagawa, M., Wilkin, M. B., Moffat, K. G., O'Kane, C. J., Davies, J. A., & Bacon, J. P. (1996). Mutations in shaking-B prevent electrical synapse formation in the Drosophila giant fiber system. *J Neurosci, 16*(3), 1101-1113.

Raol, Y. H., & Brooks-Kayal, A. R. (2012). Experimental models of seizures and epilepsies. *Prog Mol Biol Transl Sci, 105*, 57-82. doi: 10.1016/b978-0-12-394596-9.00003-2

Ringel, F., & Plesnila, N. (2008). Expression and functional role of potassium-chloride cotransporters (KCC) in astrocytes and C6 glioma cells. *Neurosci Lett, 442*(3), 219-223. doi: 10.1016/j.neulet.2008.07.017

Rivera, C., Voipio, J., & Kaila, K. (2005). Two developmental switches in GABAergic signalling: the K+-Cl- cotransporter KCC2 and carbonic anhydrase CAVII. *J Physiol, 562*(Pt 1), 27-36. doi: 10.1113/jphysiol.2004.077495

Roy, S., Ernst, J., Kharchenko, P. V., Kheradpour, P., Negre, N., Eaton, M. L., . . . Kellis, M. (2010). Identification of functional elements and

regulatory circuits by Drosophila modENCODE. *Science, 330*(6012), 1787-1797. doi: 10.1126/science.1198374

Shekarabi, M., Moldrich, R. X., Rasheed, S., Salin-Cantegrel, A., Laganiere, J., Rochefort, D., . . . Rouleau, G. A. (2012). Loss of neuronal potassium/chloride cotransporter 3 (KCC3) is responsible for the degenerative phenotype in a conditional mouse model of hereditary motor and sensory neuropathy associated with agenesis of the corpus callosum. *J Neurosci, 32*(11), 3865-3876. doi: 10.1523/jneurosci.3679-11.2012

Shekarabi, M., Salin-Cantegrel, A., Laganiere, J., Gaudet, R., Dion, P., & Rouleau, G. A. (2011). Cellular expression of the K+-Cl- cotransporter KCC3 in the central nervous system of mouse. *Brain Res, 1374*, 15-26. doi: 10.1016/j.brainres.2010.12.010

Steinhauser, C., Seifert, G., & Bedner, P. (2012). Astrocyte dysfunction in temporal lobe epilepsy: K+ channels and gap junction coupling. *Glia, 60*(8), 1192-1202. doi: 10.1002/glia.22313

Stork, T., Bernardos, R., & Freeman, M. R. (2012). Analysis of glial cell development and function in Drosophila. *Cold Spring Harb Protoc, 2012*(1), 1-17. doi: 10.1101/pdb.top067587

Sun, Q., Tian, E., Turner, R. J., & Ten Hagen, K. G. (2010). Developmental and functional studies of the SLC12 gene family members from Drosophila melanogaster. *Am J Physiol Cell Physiol, 298*(1), C26-37. doi: 10.1152/ajpcell.00376.2009

Sun, Y. T., Lin, T. S., Tzeng, S. F., Delpire, E., & Shen, M. R. (2010). Deficiency of electroneutral K+-Cl- cotransporter 3 causes a disruption in impulse propagation along peripheral nerves. *Glia, 58*(13), 1544-1552. doi: 10.1002/glia.21028

Tanis, J. E., Bellemer, A., Moresco, J. J., Forbush, B., & Koelle, M. R. (2009). The potassium chloride cotransporter KCC-2 coordinates development of inhibitory neurotransmission and synapse structure in Caenorhabditis elegans. *J Neurosci, 29*(32), 9943-9954. doi: 10.1523/jneurosci.1989-09.2009

Wu, J. S., & Luo, L. (2006). A protocol for dissecting Drosophila melanogaster brains for live imaging or immunostaining. *Nat Protoc, 1*(4), 2110-2115. doi: 10.1038/nprot.2006.336

Xu, J. C., Lytle, C., Zhu, T. T., Payne, J. A., Benz, E., Jr., & Forbush, B., 3rd. (1994). Molecular cloning and functional expression of the bumetanide-sensitive Na-K-Cl cotransporter. *Proc Natl Acad Sci U S A, 91*(6), 2201-2205.

Zdebik, A. A. (2011). Beyond ion transport: KCC2 makes cells walk and talk. *J Physiol, 589*(Pt 24), 5903. doi: 10.1113/jphysiol.2011.221754

Zhang, R. W., Wei, H. P., Xia, Y. M., & Du, J. L. (2010). Development of light response and GABAergic excitation-to-inhibition switch in zebrafish

retinal ganglion cells. *J Physiol, 588*(Pt 14), 2557-2569. doi: 10.1113/jphysiol.2010.187088

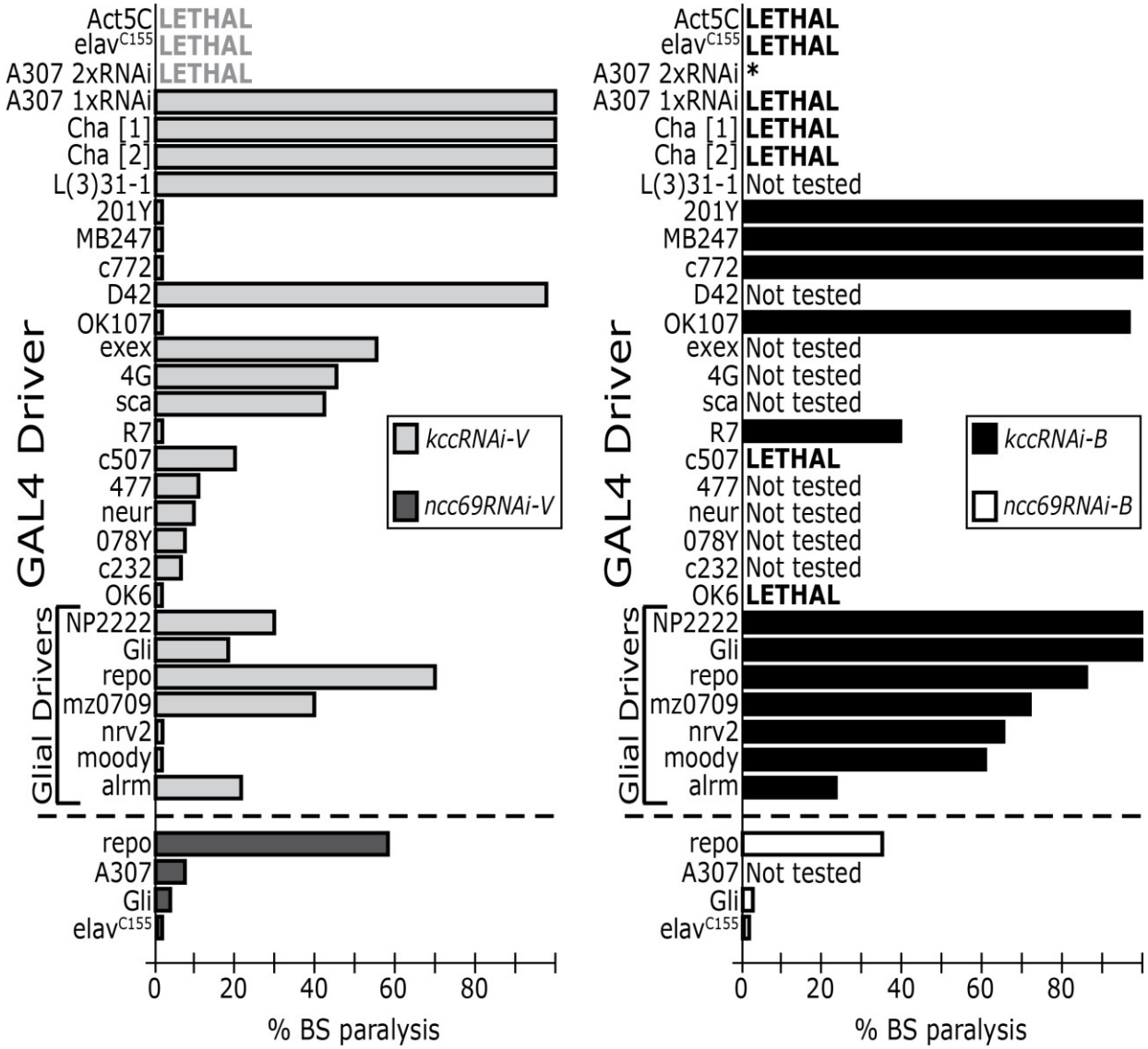

Figure 2.1: Reducing *kcc* expression by RNAi causes behavioral seizure-like activity and lethality. Various GAL4 driver males were crossed to virgin females carrying either UAS-kcc-RNAi-V (light gray bars) or UAS-kcc-RNAi-B (black bars). The resulting progeny (1 day old) were tested for BS paralysis. Lethal combinations are denoted "LETHAL", and the font color indicates the causative RNAi transgene. Positive results, where GAL4 drivers caused lethal or BS paralytic phenotypes, are depicted in this figure. Drivers and their expression domains are: Act5C (all cells), elav^{C155} (all post-mitotic neurons), A307 (GF circuit and others, see Figure 2.5; "*" denotes an impossible genotype), Cha[1] and Cha[2] (cholinergic neurons), L(3)31-1

(neuroblasts and neurons), 201Y (MB neurons), MB247 (MB neurons), c772 (MB neurons), D42 (motor neurons), OK107 (all MB neurons, lateral pace-maker neurons and medulla neurons), exex (subsets of motor neurons and interneurons), 4G (pan-neural in late embryos, in a subset of motor neurons in 3rd instar larvae, and enriched in MBs in adults), sca (some proneural clusters and sensory organ precursors), R7 (R7 photoreceptors), c507 (ring neurons, large field neurons and ellipsoid body), 477 (subset of dendritic arborization neurons), neur (all sensory neurons and their precursors), 078Y (ellipsoid body and other central nervous system neurons), c232 (ellipsoid body, ring neurons, large field neurons), OK6 (motor neurons), NP2222 (cortex glia), Gli (subperineurial glia), repo (all glia except midline glia), mz0709 (ensheathing glia and neurons), nrv2 (cortex and neuropile glia), moody (subperineurial glia), alrm (astrocyte-like glia). See Table 2.2 for complete set of tested drivers, including negative GAL4-UAS combinations (viable with no BS paralytic phenotypes).

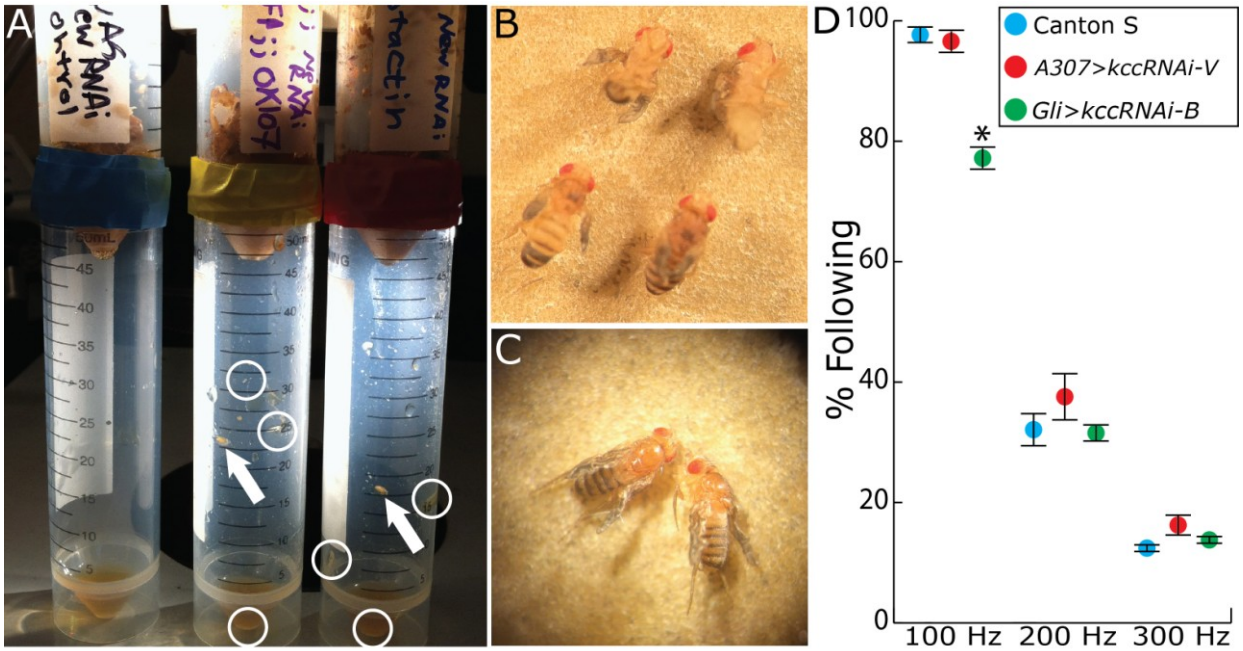

Figure 2.2: Other phenotypes associated with nervous system *kcc* loss of function. ***A***, Larvae of all stages were often found dead at the bottom of their vials. Several genotypes exhibited this phenotype including *A307-GAL4>UAS-kcc-RNAi-V, Cha-GAL4>UAS-kcc-RNAi-V* (not shown), *OK107-GAL4>UAS-kcc-RNAi-B* (middle), *repo>UAS-kcc-RNAi-B* (not shown) and *Gli-GAL4>UAS-kcc-RNAi-B* (right). Such larvae (circles) exhibited aberrant geotaxis, evidenced by others crawling through a hole made in the bottom of their vials to the space below where some pupated (arrows). Wild-type Canton-Special (left) larvae exhibited negative geotaxis and avoided the foodless space beneath. ***B***, *A307-GAL4>UAS-kcc-RNAi-V* and *Cha-GAL4>UAS-kcc-RNAi-V* flies often had a juvenile wing and cuticle phenotype lasting throughout adulthood. Shown are four *A307-GAL4>UAS-kcc-RNAi-V* flies. ***C***, *repo-GAL4>UAS-kcc-RNAi-B* and *Gli-GAL4>UAS-kcc-RNAi-B* often had a different deflated wing phenotype. Shown are two *Gli-GAL4>UAS-kcc-RNAi-B* flies. ***D,*** GF circuit following frequency data for Canton S, *A307-GAL4>UAS-kcc-RNAi-V* and *Gli-GAL4>UAS-kcc-RNAi-B*, at 100, 200 and 300 Hz. *Gli-GAL4>UAS-kcc-RNAi-B* failed to follow as well as control genotypes at 100Hz. Error bars are S.E.M. and significance for student's t-tests are * = $p<0.05$.

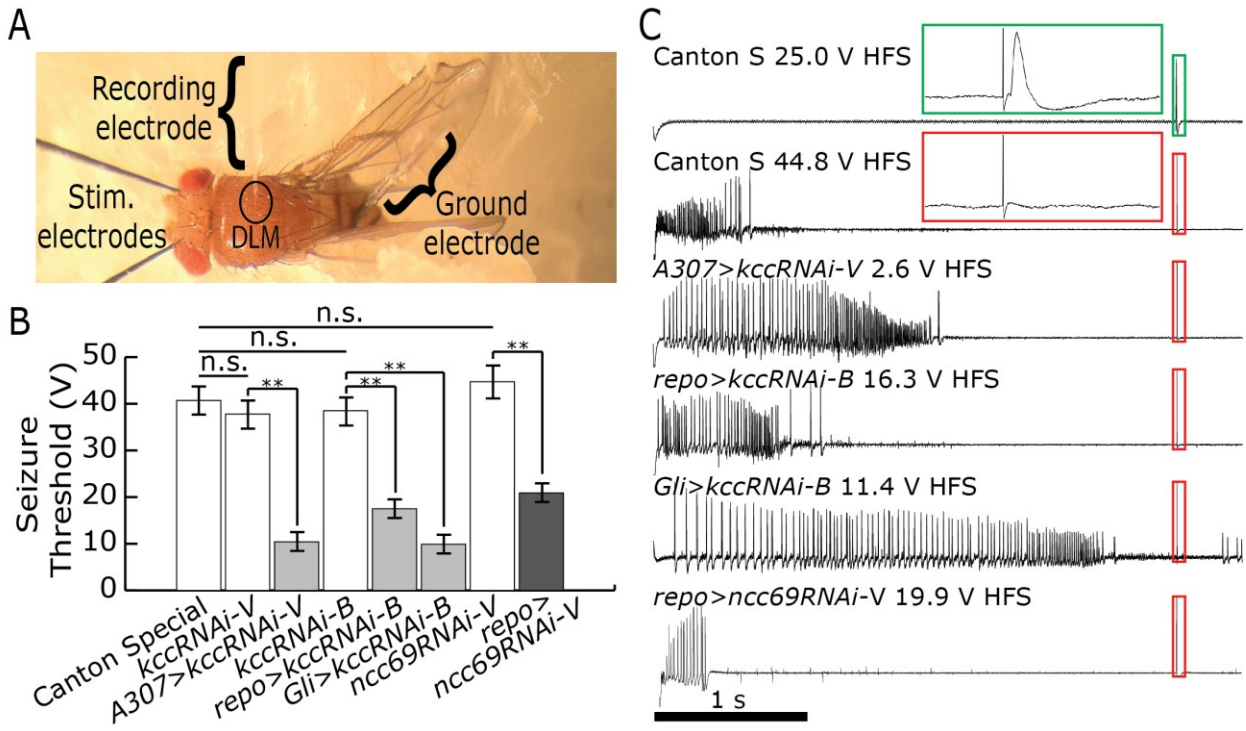

Figure 2.3: Reducing *kcc* expression by RNAi causes lowered seizure thresholds and electrophysiologically-recorded seizure-like activity. ***A***, *in vivo* stimulation and recordings from the GF system of a fly mounted in dental wax. ***B***, HFS (200 Hz for 300 ms) seizure thresholds for select UAS-kcc-RNAi and UAS-ncc69-RNAi expressing genotypes and control genotypes (white bars). Error bars are S.E.M. and significance for student's t-tests was: ** = $p<0.005$. n.s. = not significant. ***C***, representative seizures recorded in DLMs from flies of select genotypes, as indicated. Green insert is an enlargement of the region enclosed by a green rectangle illustrating a DLM response following a GF threshold stimulus pulse (~2 V, 0.3 ms pulse-width). Red insert is an enlargement of the region enclosed by the first red rectangle illustrating a DLM failure following a single GF threshold stimulus pulse. Remaining red rectangles indicate failures following seizures in other genotypes.

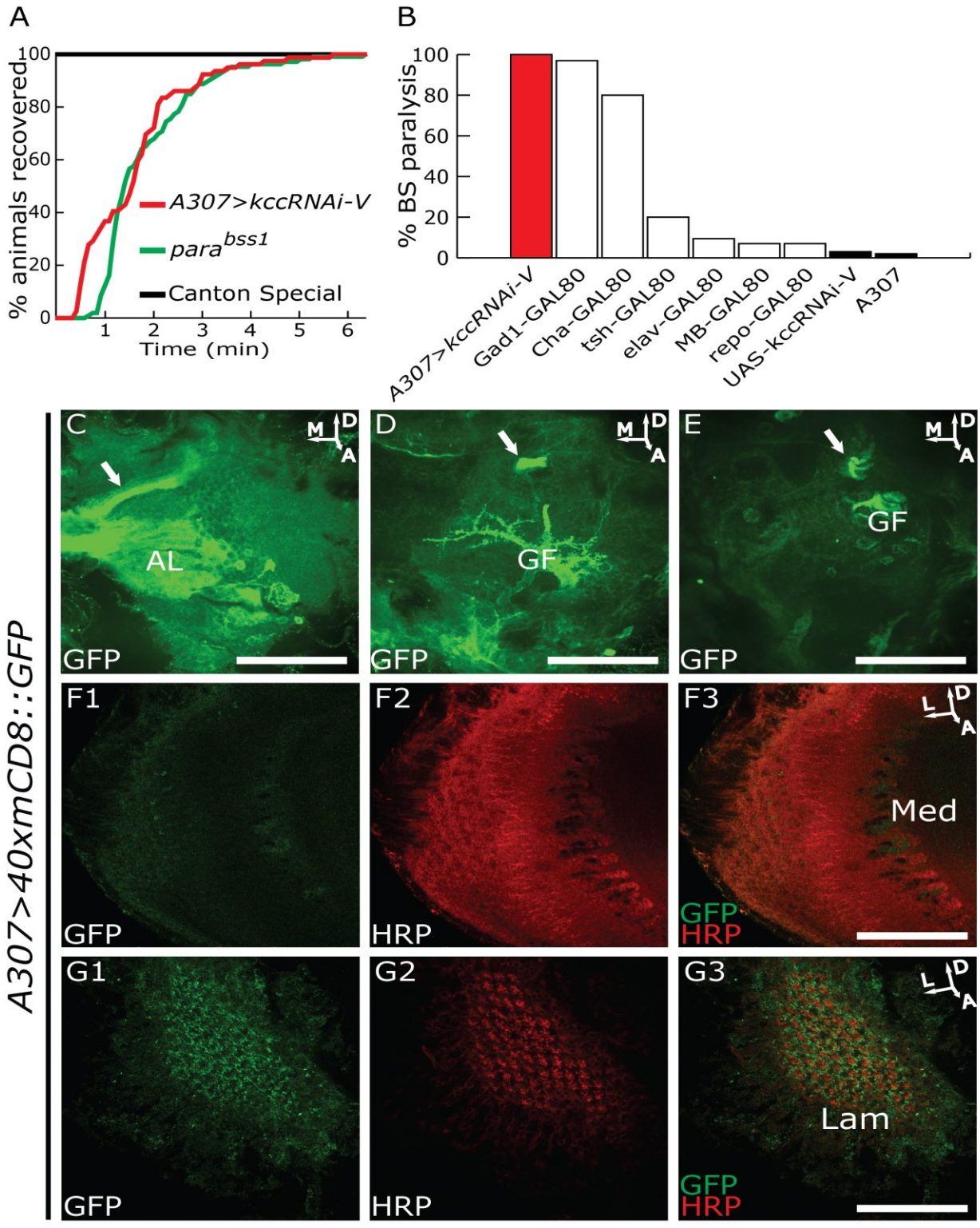

Figure 2.4: *A307-GAL4>UAS-kcc-RNAi-V* BS paralysis arises from RNAi in various cell types, including glia. ***A***, *A307-GAL4>UAS-kcc-RNAi-V* (labeled *A307>kccRNAi-V*, red curve, n = 102) flies show severe BS paralysis. A 10 s mechanical stimulus causes BS paralysis in 100% of

mutant flies and recovery times are prolonged and comparable to the severe BS mutant *para*^{bss1} (green curve, n = 100). In contrast, control wild-type strain Canton Special flies (black line, n = 27) show no BS paralysis. ***B***, Effect on BS paralysis of A307>kccRNAi-V by GAL80 transgenes. In each instance, the A307 expression domain is restricted by GAL80 expression under control of different promoters, as indicated (black bars). A307>kccRNAi-V (red bar) is UAS-kcc-RNAi-V expressed in the A307 expression domain without GAL80 restriction. Gad1-GAL80 is *A307>kccRNAi-V/+;Gad1-GAL80/+* with the Gad1-GAL80 eliminating RNAi from A307 GABAergic neurons (see text). Cha-GAL80 is *A307>kccRNAi-V/+;Cha-GAL80/+.* tsh-GAL80 is *A307>kccRNAi-V/tsh-GAL80*. elav-GAL80 is *A307>kccRNAi-V/+;elav-GAL80/+.* MB-GAL80 is *A307>kccRNAi-V/MB-GAL80*. repo-GAL80 is *A307>kccRNAi-V/+; repo-GAL80/+.* UAS-kcc-RNAi-V and A307 are control genotypes (green bars). ***C-E,*** A307 expression is shown as green-labeled cell membranes using anti-GFP on *A307-GAL4>40xUAS-mCD8::GFP* (labeled *A307>40xmCD8::GFP*) adult brains. **C**, Anterior section depicting A307 expression in antennal lobe glomeruli (AL) and a subset of MB Kenyon cells (arrow). **D**, A307 expression in GF processes (GF) and a subset of MB Kenyon cells (arrow). **E**, Posterior section depicting A307 expression in the GF cell body (GF) and a subset of MB Kenyon cells (arrow). **F-G**, A307 expression is shown as green-labeled cell membranes using *A307>40xmCD8::GFP*. Neurons are shown as red-labeled cell membranes using Cy3-conjugated anti-HRP. **F1**, A307 expression in the medulla (labeled Med). **F2**, HRP staining in the medulla. **F3**, GFP/HRP merge in the medulla. **G1**, A307 expression in the lamina (labeled Lam). **G2**, HRP-staining in the lamina. **G3**, GFP/HRP merge in the lamina. D and E are each 9 μm Z-projections. C, F1-3 and G1-G3 confocal slices are of 0.25 μm. Scale bars are 50 μm. For orientation, A: Anterior, D: Dorsal, L: Lateral and M: Medial.

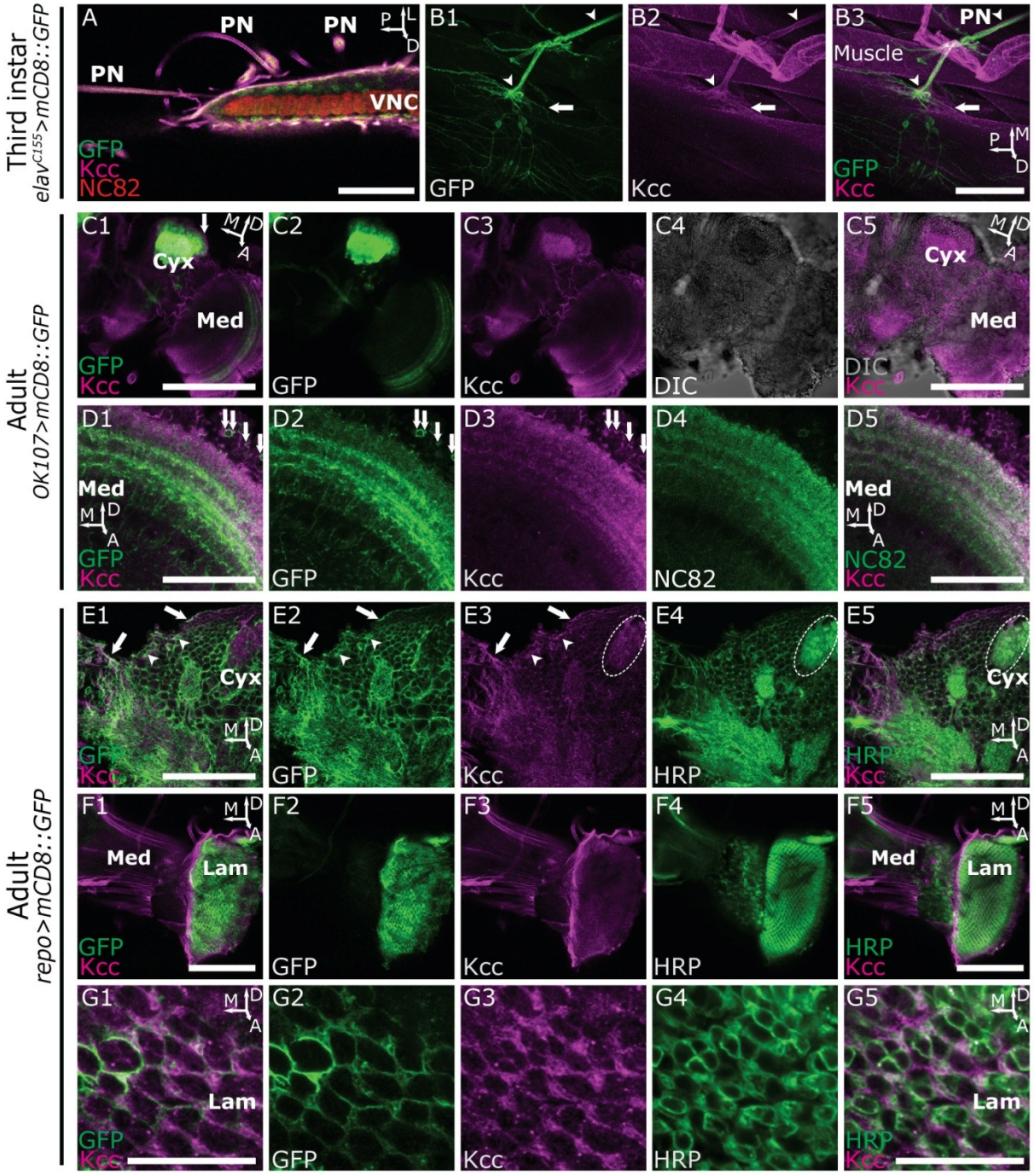

Figure 2.5: Immunohistochemistry with confocal fluorescence microscopy reveals neuronal and glial Kcc. ***A***, 0.75 μm slice of third instar larval nervous system stained for Kcc (magenta-labeling with anti-Kcc antibody), neuronal membranes (green-labeling with elav^{C155}>mCD8::GFP

and anti-GFP), and neuropile synaptic active zones (red-labeling with anti-bruchpilot, NC82). Kcc/neuronal membrane colocalization appears white. Kcc is observed in peripheral nerves (PN). Kcc signal is also prominent in ventral nerve cord (VNC) apparently in the neuronal cell body region. Little Kcc signal colocalizes with the neuropile active zone marker NC82. ***B1-3,*** Third instar larval motor nerve terminal and neuromuscular junction in 55 μm Z-stack projection. ***B1***, Neuronal membranes labeled with GFP (green-labeling with elav^{C155}>mCD8::GFP and anti-GFP). ***B2***, Kcc protein (magenta-labeling with anti-Kcc antibody). ***B3,*** Neuronal (green)/Kcc (magenta) merge. Peripheral nerve and synaptic terminal show strong GFP signaling, as do sensory neuron cell bodies, dendrites and axons; these structures appear to be largely devoid of Kcc. Kcc surrounds neuronal axons (arrow heads) and larval muscle (arrow) supporting the notion that it is mainly in SPGs, thought to ensheath both. ***C1-5,*** 0.5 μm adult posterior central brain slice showing especially the calyx of the mushroom body (Cyx) and the medulla optic lobe (Med). ***C1,*** Mushroom body neuronal membranes (green-labeling with OK107>mCD8::GFP)/Kcc (magenta-labeling with anti-Kcc antibody) merge. Kcc/neuronal membrane colocalization appears white. Colocalization appears in the calyx neuropile and soma. Note that a thin layer of magenta-labeling is seen to surround the outside of the mushroom body calyx (arrow). ***C2***, Neuronal membranes of the mushroom body are labeled with GFP (green-labeling with OK107>mCD8::GFP and anti-GFP). The OK107 driver also causes labeling in a subset of medulla neurons. ***C3,*** Central brain Kcc (magenta-labeling with anti-Kcc antibody). ***C4,*** DIC image showing the lighter and granular somatic regions, and the darker and uniform neuropile regions of the adult brain. ***C5,*** DIC (grey)/Kcc (magenta) merge. Kcc is widespread in adult brain, with prominent undulated pattern on the brain surface and adjacent to cell soma. ***D1-D5,*** 0.5 μm adult optic lobe medulla slice. ***D1,*** Neuronal (green)/Kcc (magenta) merge. Kcc has an enriched foci or punctate pattern on neuronal membranes (arrows) and stains green-labeled portions of neuropile as well. ***D2,*** Medulla neuron membranes labeled with GFP (green-labeling with OK107>mCD8::GFP and anti-GFP). ***D3,*** Medulla Kcc (magenta-labeling with anti-Kcc antibody). ***D4,*** Medulla NC82 (green-labeling with anti-NC82 antibody). ***D5,*** Neuropile (green)/Kcc (magenta) merge. Kcc is in neuropile and interlaces it. ***E1-E5***, 0.5 μm adult posterior central brain slice. ***E1***, Glial (green)/Kcc (magenta) merge. Kcc is present in PGs and/or SPGs (arrows), and in cortex glia surrounding neuronal soma (arrowheads). ***E2***, Glial membranes labeled with GFP (green-labeling with repo>mCD8::GFP and anti-GFP). ***E3***, Kcc protein (magenta-labeling with anti-Kcc antibody). ***E4***, Neuronal membranes (green-labeling with anti-HRP). ***E5***, Neural (green)/Kcc (magenta) merge. Kcc is present in neuropile and has a punctate pattern on MB cell soma. ***F1-F5***, 0.5 μm lateral brain slice. ***F1***, Glial (green)/Kcc (magenta) merge. Kcc is present in medulla surface glia and fenestrated and/or pseudocartridge glia of the optic lamina

(labeled Lam). ***F2***, Glial membranes labeled with GFP (green-labeling with repo>mCD8::GFP and anti-GFP) ***F3***, Kcc protein (magenta-labeling with anti-Kcc antibody). ***F4***, Neuronal membranes (green-labeling with anti-HRP). ***F5***, Neural (green)/Kcc (magenta) merge. Kcc is mostly in and around neuronal soma, and surrounding neuropile. ***G1-G5***, 0.5 μm high-magnification inner lamina slice. ***G1***, Glial (green)/Kcc (magenta) merge. Kcc is present in what are presumed to be astrocyte-like glia processes married to synaptic neuropile. ***G2***, Glial membranes labeled with GFP (green-labeling with repo>mCD8::GFP and anti-GFP). ***G3***, Kcc protein (magenta-labeling with anti-Kcc antibody). ***G4***, Neuronal membranes (green-labeling with anti-HRP). ***G5***, Neural (green)/Kcc (magenta) merge. Kcc puncta are also present on neuronal processes. Scale bars are 20 μm (H1 and H5), 50 μm (E1, E5, G1 and G5) and 100 μm (all others). For orientation, A: anterior, D: dorsal, L: lateral, M: medial, P: posterior.

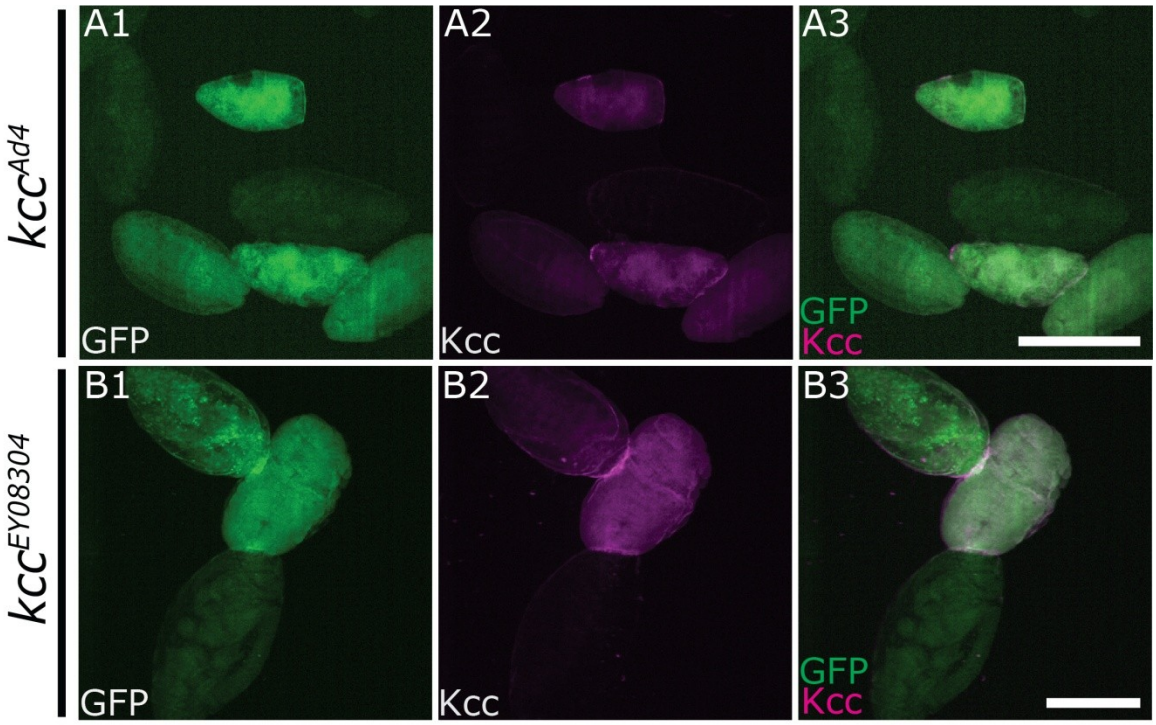

Figure 2.6: Rabbit polyclonal anti-kcc is largely Kcc-specific. ***A1-3***, Representative images of 20-22 h old F1 embryos of self-crossed *kcc*^{Ad4}/Cyo, Act-GFP stained with anti-GFP and anti-Kcc. ***A1***, Cytoplasmic GFP (green-labeling via Act-GFP and anti-GFP antibody). Faint auto-fluorescence in GFP-negative embryos arising from developing gut can be seen in the GFP channel confirming that they, and other similarly scored specimens, were not unfertilized eggs. GFP-negative embryos are presumably *kcc*^{Ad4}/*kcc*^{Ad4}. ***A2***, Kcc protein (magenta-labeling with anti-Kcc antibody). Marginal Kcc signal was detected surrounding all embryos of any genotype suggesting a negligible degree of non-specific staining or presence of lingering maternally deposited Kcc. ***A3***, GFP/Kcc merge. GFP-negative embryos were almost always Kcc-negative (n = 42 out of 51). Thus, *kcc*^{Ad4} appears to be a null mutation. ***B1-3*****,** Representative images of 20-22 h old F1 embryos of self-crossed *kcc*^{EY08304}/Cyo, Act-GFP stained with anti-GFP and anti-Kcc. ***B1***, Cytoplasmic GFP (green-labeling with Act-GFP and anti-GFP antibody). GFP-negative embryos are presumably *kcc* ^{EY08304}/*kcc* ^{EY08304}. ***B2***, Kcc protein (magenta-labeling with anti-Kcc antibody). ***B3***, GFP/Kcc merge. GFP-negative embryos were almost always Kcc-negative (n = 28 out of 33). Thus, *kcc* ^{EY08304} appears to be a null mutation.

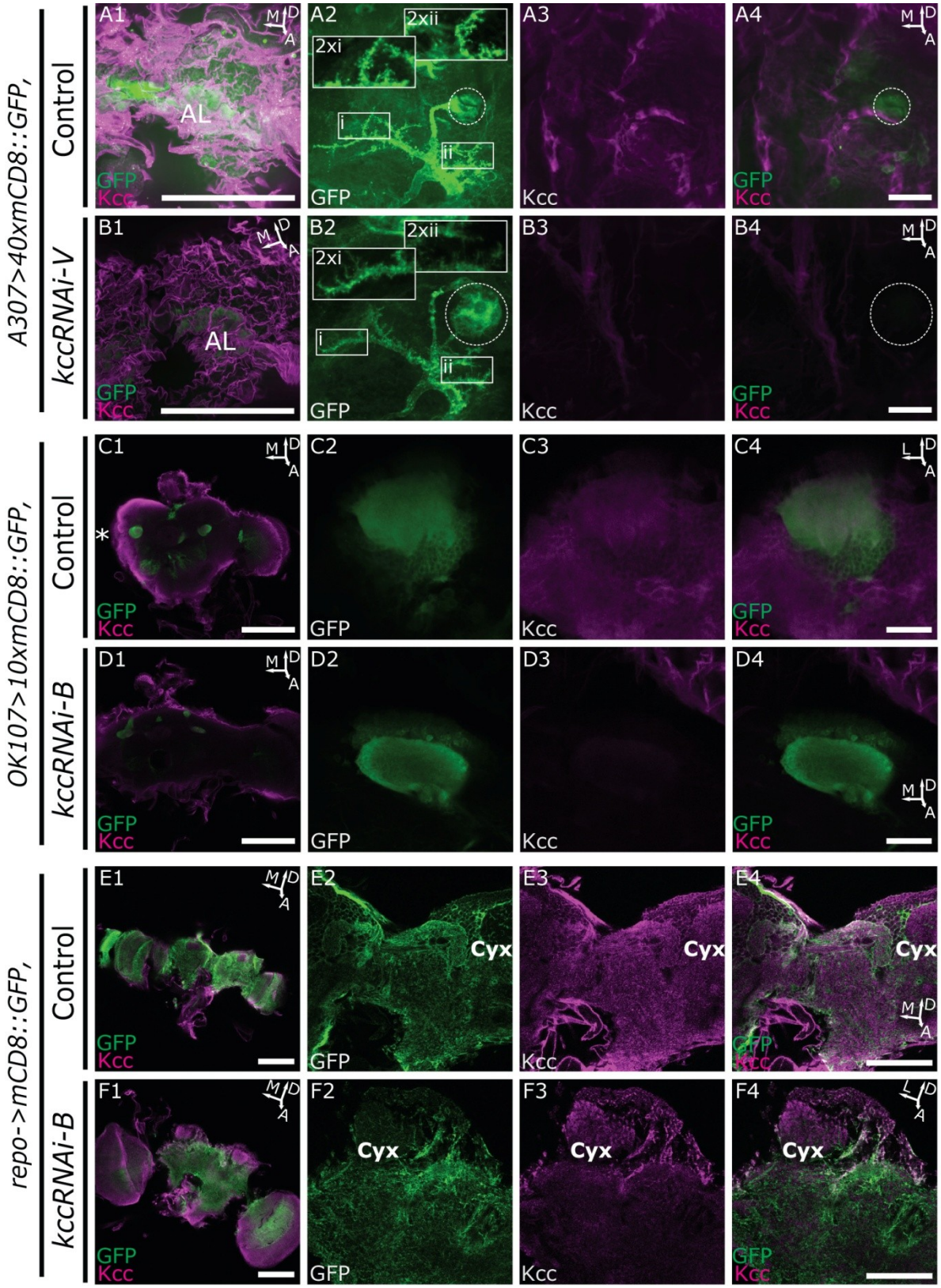

Figure 2.7: *kcc* knockdown during development leads to whole-brain swelling and BBB degradation in 24-48 hour old adults. *A1-A4*,

A307>40xUAS-mCD8::GFP probed with anti-GFP and anti-Kcc. ***A1***, 0.5 μm anterior brain slice of GFP/Kcc merge at low magnification. ***A2,*** 34 μm GFP Z-stack projection (green-labeling with A307>40xUAS-mCD8::GFP and anti-GFP). Wild-type GF neurons soma (circle) and dendrites with spines (insets, i and ii) are shown. ***A3***, 0.5 μm slice of Kcc on the posterior central brain surface (magenta-labeling with anti-Kcc). ***A4***, GFP/Kcc merge of posterior-most slice from GFP Z-stack and the corresponding Kcc slice. Kcc-rich structures are around neuronal soma and overlap at small contact points on soma. ***B1-B4***, *A307>40xUAS-mCD8::GFP, UAS-kcc-RNAi-V* probed with anti-GFP and anti-Kcc**.** ***B1***, 0.5 μm anterior brain slice of GFP/Kcc merge at low magnification. Kcc is absent from antennal lobe neurons, and surface glia Kcc is more undulated. ***B2,*** 34 μm GFP Z-stack projection (green-labeling with A307>40xUAS-mCD8::GFP and anti-GFP). Gargantuan GF neuron soma (circle) and absent/diffuse dendritic spines (insets, i and ii) are shown. ***B3***, 0.5 μm slice of Kcc on the posterior central brain surface (magenta-labeling with anti-Kcc). ***B4***, GFP/Kcc merge of posterior-most slice from GFP Z-stack and the corresponding Kcc slice. Extracellular space (ECS) appears to be enlarged and close proximity of glia to neurons is lost. ***C1-C4***, *OK107>UAS-mCD8::GFP* probed with anti-GFP and anti-Kcc. ***C1***, 0.5 μm interior brain slice of GFP/Kcc merge at low magnification. *: optic lobes of either test or control brains were often severed during dissection to distinguish brain groups mixed in the same tubes. ***C2,*** 0.5 μm slice of MB calyx GFP (green-labeling with OK107>UAS-mCD8::GFP and anti-GFP). Wild-type calyx is shown. ***C3***, 0.5 μm slice of Kcc in the MB calyx (magenta-labeling with anti-Kcc). ***C4***, GFP/Kcc merge. ***D1-D4***, *OK107>UAS-mCD8::GFP, UAS-kcc-RNAi-B* probed with anti-GFP and anti-Kcc. ***D1***, 0.5 μm interior brain slice of GFP/Kcc merge at low magnification. Brains are larger than their wild-type counterparts. ***D2,*** 0.5 μm slice of MB calyx GFP (green-labeling with OK107>UAS-mCD8::GFP and anti-GFP). ***D3***, 0.5 μm slice with dearth of Kcc in *kcc* RNAi expressing MB calyx, but Kcc abundance on the visible brain surface (magenta-labeling with anti-Kcc). ***D4***, GFP/Kcc merge with calyx isolated and distant from any Kcc signal. ***E1-E4***, *repo>UAS-mCD8::GFP* probed with anti-GFP and anti-Kcc. ***E1***, 0.5 μm posterior brain slice of GFP/Kcc merge at low magnification. Intimate anatomical relationship between glia and neurons in wild-type. ***E2,*** 0.5 μm slice of surface and internal glial GFP (green-labeling with repo>UAS-mCD8::GFP and anti-GFP). ***E3***, 0.5 μm slice of Kcc in MB calyx as well as in surface and cortex glia (magenta-labeling with anti-Kcc). ***E4***, GFP/Kcc merge. ***F1-F4***, *repo>UAS-mCD8::GFP, UAS-kcc-RNAi-B* probed with anti-GFP and anti-Kcc. ***F1***, 0.5 μm posterior brain slice of GFP/Kcc merge at low magnification. Brains were much bigger than controls. ***F2,*** 0.5 μm slice of surface and internal glial GFP (green-labeling with repo>UAS-mCD8::GFP and anti-GFP). ***F3***, 0.5 μm slice of Kcc in MB calyx and soma, but largely eliminated in surface and cortex glia (magenta-labeling with anti-Kcc). ***F4***, GFP/Kcc

merge. Gaps in between glia and neurons evident, unlike the densely-packed wild-type brain. Test and corresponding control specimens were always imaged with the same settings. Scale bars are 100 μm (A1, B1, C1, D1, E1 and F1), 50 μm (E4 and F4) and 20 μm (A4, B4, C4 and D4). For orientation, A: anterior, D: dorsal, L: lateral, M: medial.

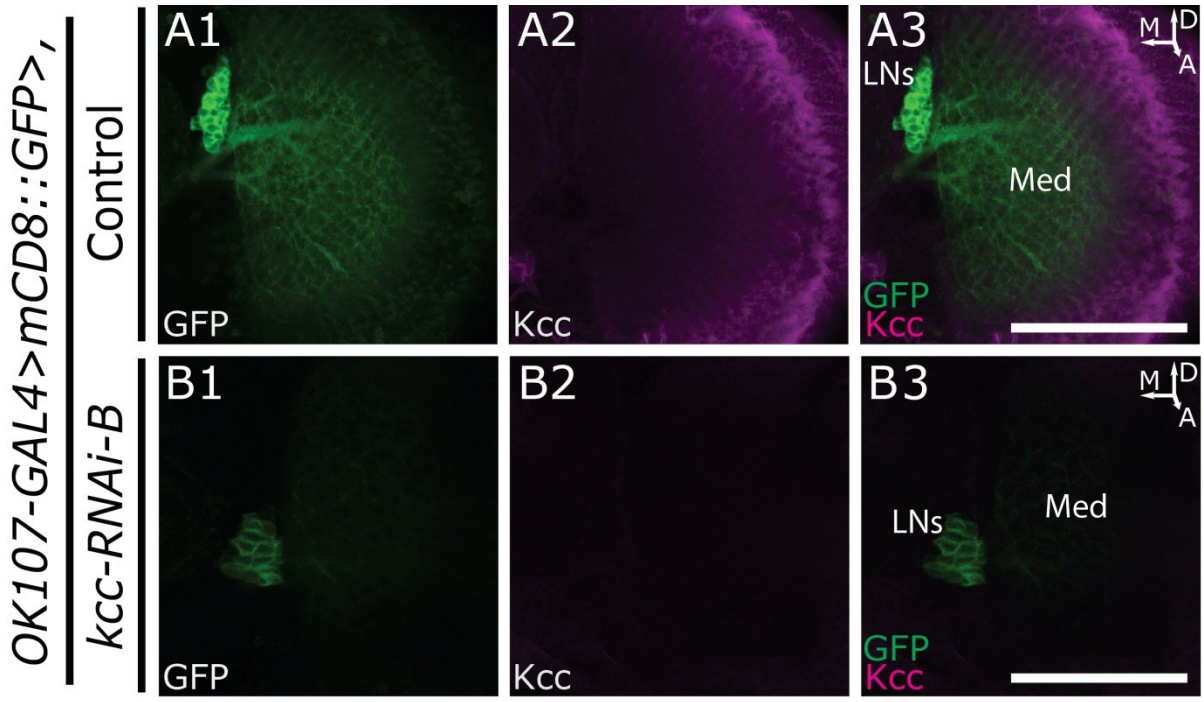

Figure 2.8: Lateral pace-making neurons (LNs) deficient in Kcc are enlarged and misshapen. ***A1-3***, wildtype LNs are spherical. ***A1***, GFP in membranes of LNs (green-labeled via *OK107-GAL4>UAS-mD8::GFP* and anti-GFP). ***A2***, Kcc in and around LNs and the medulla (magenta-labeling by anti-Kcc). ***A3***, GFP/Kcc merge. ***B1-3***, LNs expressing *kcc* RNAi are misshapen. ***B1***, GFP in membranes of LNs (green-labeled via *OK107-GAL4>UAS-mD8::GFP* and anti-GFP). LNs are swollen and non-spherical. ***B2***, Kcc in and around LNs and the medulla (magenta-labeling by anti-Kcc). Kcc signal is more diffuse than in the wild-type scenario, likely due to water retention in these brains. ***B3***, GFP/Kcc merge. LNs are not immediately surrounded by Kcc-rich structures. Scale bars are 50 μm. For orientation, A: anterior, D: dorsal, L: lateral, M: medial.

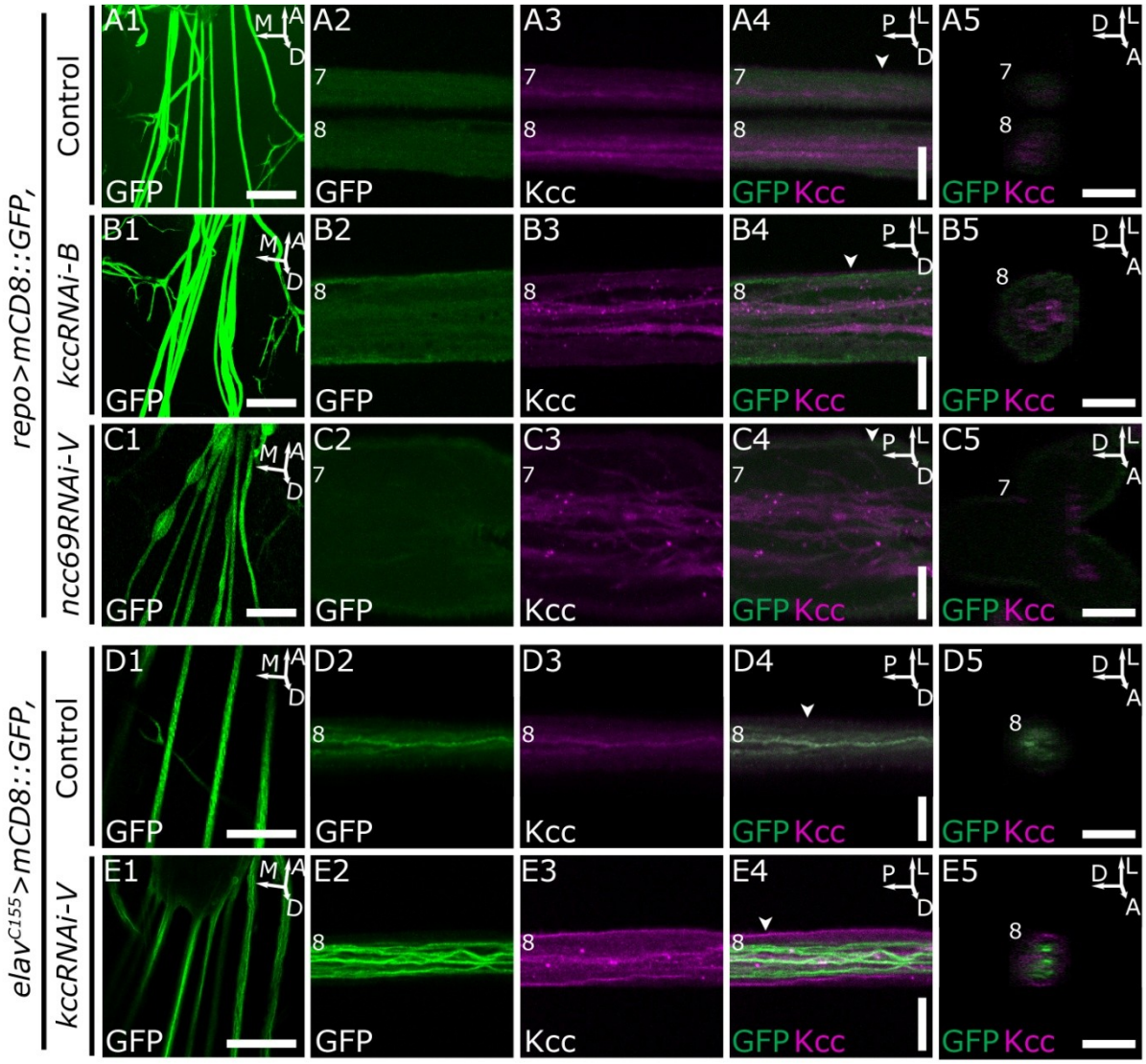

Figure 2.9: *kcc* knockdown in third instar larval peripheral nerves causes nerve swelling and neuronal process defasciculation. *A1-A5*, Wild-type *repo>UAS-mCD8::GFP* larval fillet probed with anti-GFP, anti-Kcc and anti-HRP (Figure 2.10). ***A1***, Glial GFP illuminating wild-type peripheral nerves (PNs) at low magnification 40 μm slice (green-labeling with repo>UAS-mCD8::GFP and anti-GFP). ***A2***, In high magnification 2μm slice, PN glia (PGs, SPGs and wrapping/neuropile glia) are sources of GFP florescence. ***A3***, Ubiquitous Kcc present in wild-type PN glia and bundled neuronal processes (magenta-labeling with anti-Kcc). ***A4***, GFP/Kcc merge. ***A5,*** Orthogonal view of ***A4*** at the indicated position (arrowhead, ***A4***) outputted by ImageJ software using whole PN Z-stack. ***B1-B5***, *repo>UAS-mCD8::GFP,UAS-kcc-RNAi-B* larval fillet probed with anti-GFP, anti-Kcc and anti-HRP. ***B1***, Glial GFP of swollen PNs in 40 μm slice at low magnification (green-labeling with repo>UAS-mCD8::GFP and anti-GFP). ***B2***, 2μm slice of

enlarged PN with circumferential glial GFP at high magnification. ***B3***, Kcc in frayed nerve and reduced in surface glia (magenta-labeling with anti-Kcc). ***B4***, GFP/Kcc merge. Ratio of GFP to Kcc in surface glia is increased with respect to controls. ***B5,*** Orthogonal view of ***B4*** at the indicated position (arrowhead, ***B4***) using whole PN Z-stack. ***C1-C5***, *repo>UAS-mCD8::GFP,UAS-ncc69-RNAi-V* larval fillets probed with anti-GFP, anti-Kcc and anti-HRP. ***C1***, Glial GFP of PN in 40 μm slice at low magnification (green-labeling with repo>UAS-mCD8::GFP and anti-GFP). ***C2***, GFP in a PN bulge. ***C3***, Frayed nerve as seen by Leiserson et al. revealed by Kcc signal (magenta-labeling with anti-Kcc). ***C4***, GFP/Kcc merge. ***C5,*** Orthogonal view of ***C4*** at the indicated position (arrowhead, ***C4***) using whole PN Z-stack. ***D1-D5***, Wild-type *elav^{c155}>UAS-mCD8::GFP* larval fillets probed with anti-GFP, and anti-Kcc. ***D1***, Neuronal GFP of PN s in 40 μm slice at low magnification (green-labeling with elav^{c155}>UAS-mCD8::GFP and anti-GFP). ***D2***, Wild-type neuronal processes tightly bundled along core of a PN. ***D3***, Kcc in and surrounding PN neuronal processes (magenta-labeling with anti-Kcc). ***D4***, GFP/Kcc merge. Kcc is in glia and neurons. ***D5,*** Orthogonal view of ***D4*** at the indicated position (arrowhead, ***D4***) using whole PN Z-stack. ***E1-E5***, *elav^{c155}>UAS-mCD8::GFP,UAS-kcc-RNAi-V* larval fillets probed with anti-GFP and anti-Kcc. ***E1***, Neuronal GFP of PN s in 40 μm slice at low magnification (green-labeling with elav^{c155}>UAS-mCD8::GFP and anti-GFP). ***E2***, Frayed neuronal processes within PN. ***E3***, Kcc mostly in surface and wrapping glia (magenta-labeling with anti-Kcc). ***E4***, GFP/Kcc merge. Kcc is plentiful in glia, but frayed neuronal processes are mostly Kcc-negative. Miniscule GFP/Kcc overlap is believed to be confounding signal from wrapping glia Kcc. ***E5,*** Orthogonal view of ***E4*** at the indicated position (arrowhead, ***E4***) using whole PN Z-stack. White numbers indicate abdominal nerve number. Scale bars are 50 μm (A1, B1, C1, D1 and E1), and 10 μm (A4-5, B4-5, C4-5, D4-5 and E4-5). For orientation, A: anterior, D: dorsal, L: lateral, M: medial, P: posterior.

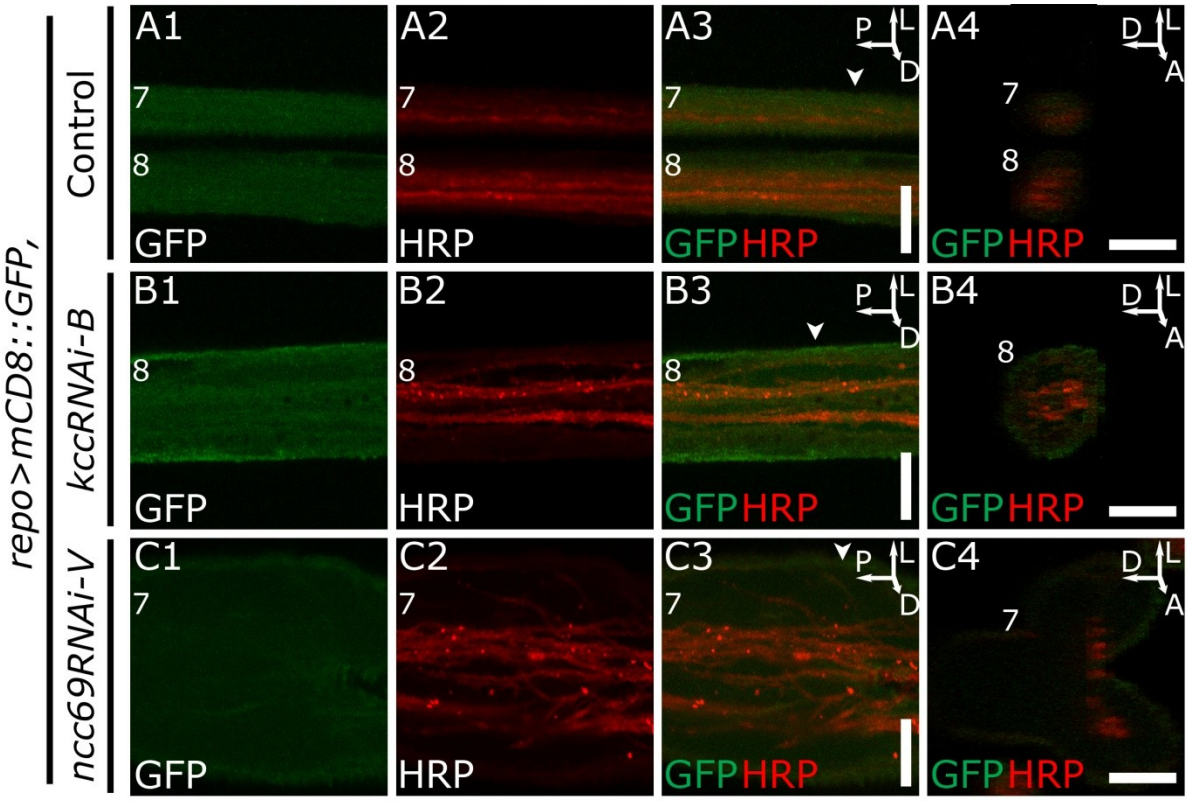

Figure 2.10: HRP staining in specimens from Figure 2.9 confirms frayed-nerve phenotypes with glial *kcc* RNAi. *A1-A4*, Wild-type *repo>UAS-mCD8::GFP* larval fillet probed with anti-GFP and anti-HRP. ***A1***, 2μm slice of PN glia (PGs, SPGs and wrapping/neuropile glia) that are sources of GFP florescence (green-labeling with repo>UAS-mCD8::GFP and anti-GFP). ***A2***, Robust HRP staining present in bundled wild-type neuronal processes (red-labeling with anti-HRP). ***A3***, GFP/HRP merge. ***A4,*** Orthogonal view of ***A3*** at the indicated position (arrowhead, ***A3***) outputted by ImageJ software using whole Z-stack of the PN. ***B1-B4***, *repo>UAS-mCD8::GFP,UAS-kcc-RNAi-B* larval fillet probed with anti-GFP and anti-HRP. ***B1***, 2μm slice of enlarged PN glial GFP (green-labeling with repo>UAS-mCD8::GFP and anti-GFP). ***B2***, Robust HRP staining present in defasciculated or frayed neuronal processes (red-labeling with anti-HRP). ***B3***, GFP/HRP merge. ***B4,*** Orthogonal view of ***B3*** at the indicated position (arrowhead, ***B3***) using whole Z-stack of the PN. ***C1-C4***, *repo>UAS-mCD8::GFP,UAS-ncc69-RNAi-V* larval fillet probed with anti-GFP and anti-HRP. ***C1***, 2μm slice of PN bulge glial GFP (green-labeling with repo>UAS-mCD8::GFP and anti-GFP). ***C2***, Robust HRP staining present in frayed neuronal processes (red-labeling with anti-HRP). ***C3***, GFP/HRP merge. ***C4,*** Orthogonal view of ***C3*** at the indicated position (arrowhead, ***C3***) using whole Z-stack of the PN. Scale bars are 10 μm. For orientation, A: anterior, D: dorsal, L: lateral, M: medial, P: posterior.

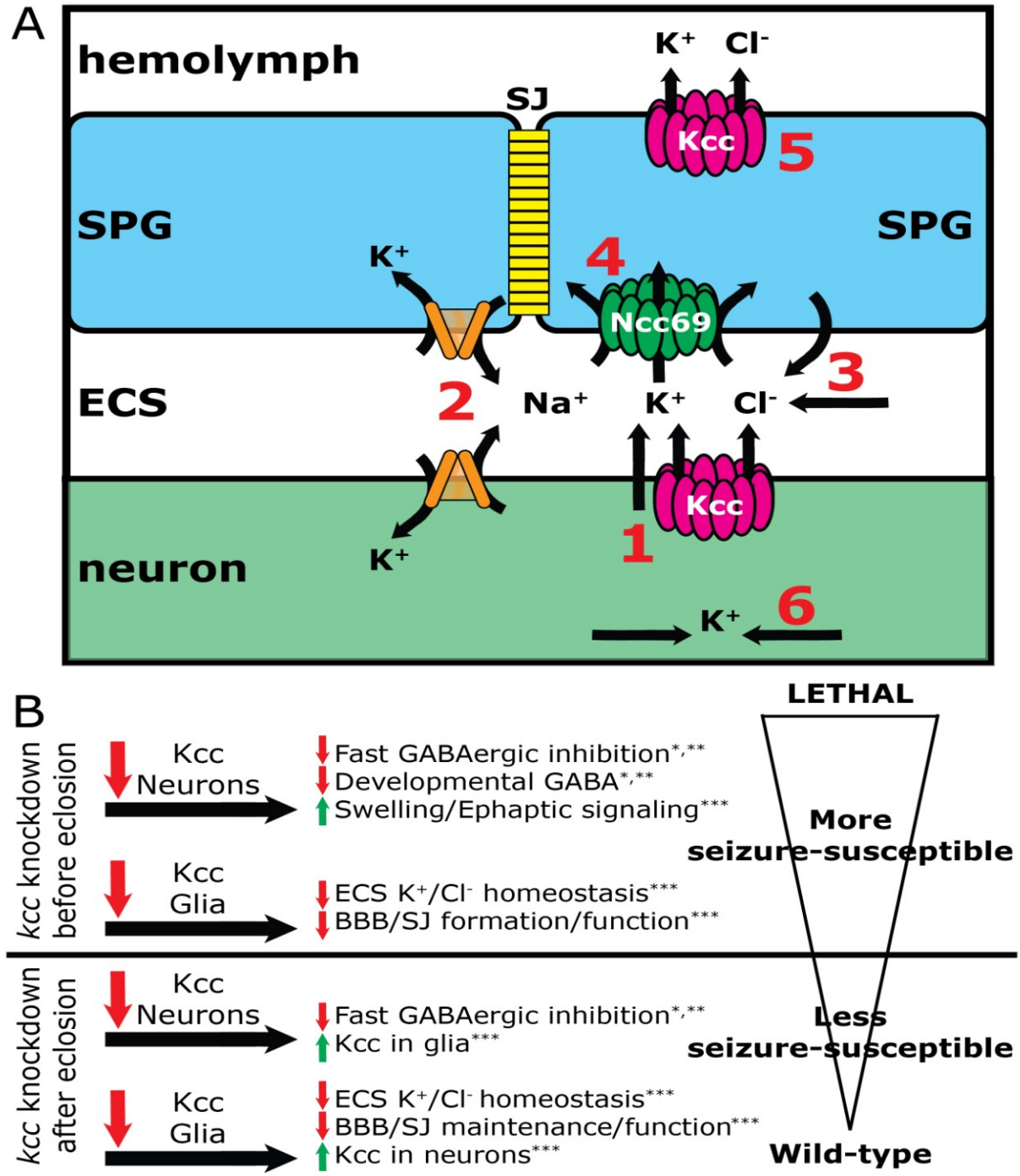

Figure 2.11: Larval PN osmoregulation model and speculative model of seizure-susceptibility due to *kcc* knockdown. ***A***, A model of Kcc and Ncc69 function in larval PNs, showing how the Na^+/K^+ ATPase may create

the need for solute removal from the PN ECS. Shown is a simple model of a PN, consisting of an axon and SPGs whose septate junctions (SJ) prevent pericellular ion flow. **1**: Beginning with the action potential, the ECS has increased extracellular K^+ due to flow through voltage-gated K^+ channels, and also perhaps, through Kcc. **2**: The Na^+/K^+ ATPase transports 2 K^+ ions from the ECS, and replaces them with 3 Na^+ ions, and functions in both neurons and SPGs presumably. **3**: Cl^- ions balance the gain in positive charge. These Cl^- ions could flow from other parts of the ECS and/or from intracellular locations, e.g., through Cl^- channels or Kcc. **4**: Ncc69 in SPGs transports solutes into SPGs from the ECS. **5**: SPGs efflux solutes into the hemolymph, perhaps in part via Kcc, to maintain volume homeostasis. **6**: The K^+ lost in axons is replenished by flow from other parts of the neuron. ***B***, Speculative model showing confirmed, and presumed, cellular dysfunctions arising from CCC loss and their connection with seizure-susceptibility. *kcc* knockdown before eclosion: less fast GABAergic signaling through Cl^--permeable $GABA_A$ receptors, and loss of trophic effects of GABA found in many other systems may increase seizure-susceptibility. Larger neurons are usually more excitable, and swelling has been shown to enable ephaptic signaling (neuronal synchronization due to strengthening of local field potentials), both factors which facilitate seizures. High extracellular $[K^+]/[Cl^-]$ due to ECS or BBB abnormalities are likely to be critical factors governing neuronal excitability. *kcc* knockdown after eclosion: fast GABAergic signaling, BBB function and ECS ion-homeostasis should all be impacted. However, the properly developed brain—with glia and neurons in close-proximity—may be able to compensate for Kcc-deficiencies by upregulation of other properly-developed mechanisms and/or upregulation of *kcc* in the opposing cell type; glial or neuronal. *: in part from (Hekmat-Scafe et al., 2006). **: in part from (Hekmat-Scafe et al., 2010).***: mainly suggested by this study.

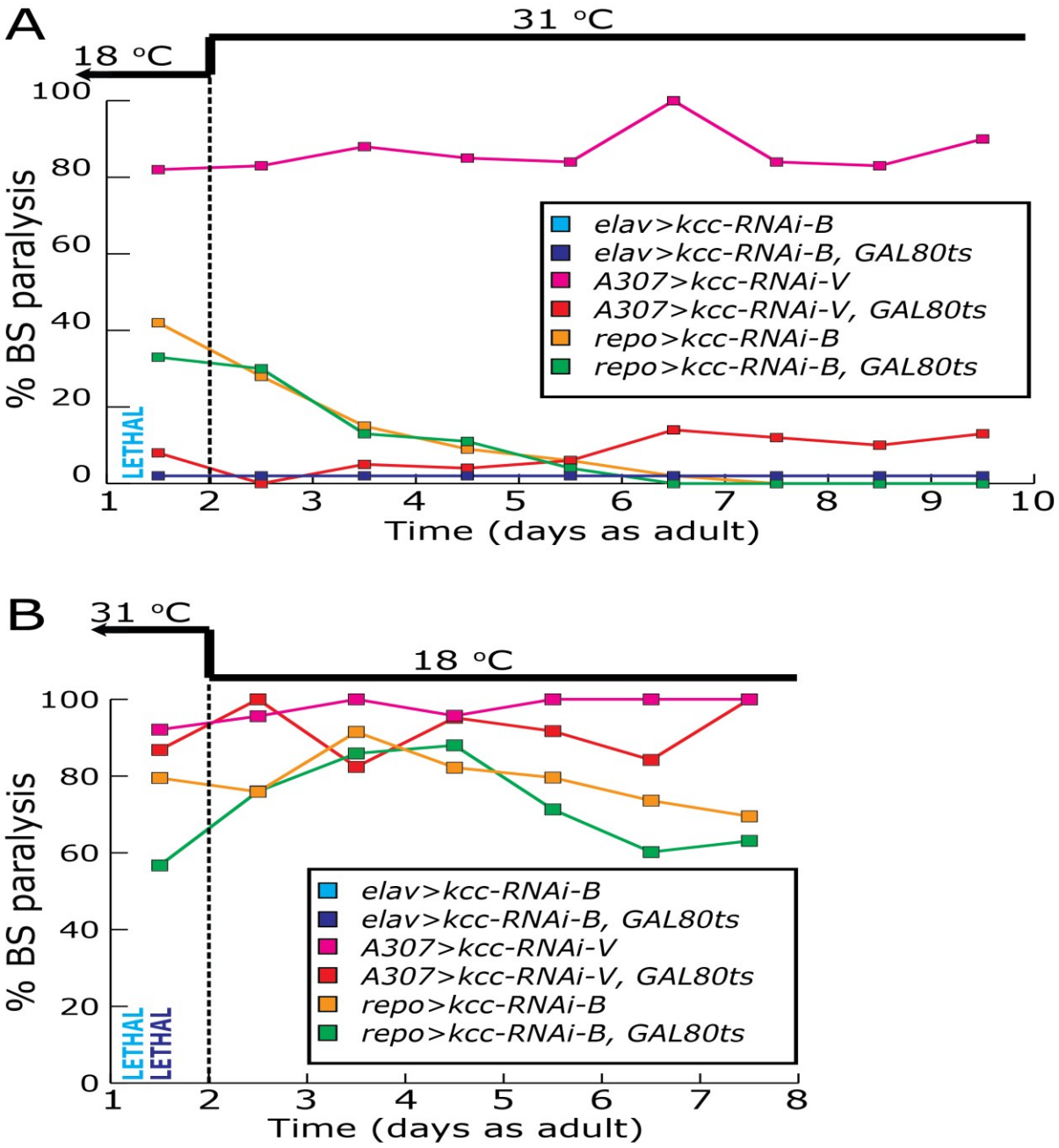

Figure 2.12: %BS paralysis via *kcc* RNAi and the TARGET system in glia or neurons cannot be altered after eclosion. *A*, %BS paralysis is fixed at eclosion; %BS paralysis cannot significantly be increased or induced in adult flies having developed with restricted *kcc* RNAi. ***B***, %BS paralysis cannot be ameliorated upon presumed restoration of kcc^{+} expression.

Referred to as	Genotype	Stock (source, ID)
078Y	*w*; P{GawB}078Y*	Bloomington, 30821
104Y	*w*;104Y-GAL4*	Tanouye, T161
109(2)80	*y^1 w*; P{GawB}109(2)80*	Bloomington, 8769
10xmCD8::GFP	*w*; P{10XUAS-IVS-mCD8::GFP}su(Hw)attP5*	Bloomington, 32188
201Y	*w^{1118}; P{GawB}Tab2^{201Y}*	Bloomington, 4440
221	*w*; Pin^1/CyO; P{?GawB}221w-*	Bloomington, 26259
40xmCD8::GFP	*w*; P{40XUAS-IVS-mCD8::GFP}attP2*	Bloomington, 32195
43	*w*; P{GawB}43*	Bloomington, 7148
477	*w*; P{GawB}477/CyO*	Bloomington, 8737
4G	*w*; P{GawB}4G*	Bloomington, 6927
5-HT	*w*; P{GAL4-5-HTR1B.Y}2*	Bloomington, 27636
A307	*w*;A307-GAL4*	Tanouye, T061
A307>kccRNAi-V	*w*; A307-GAL4, P{KK107965}VIE-260B/CyO*	This study, ZMR002
Act5C	*y^1 w*; P{Act5C-GAL4-w}E1/CyO*	Bloomington, 25374
Akh	*y^1 w*; P{Akh-gal4.L}2/CyO, y^+*	Bloomington, 25683
alrm	*w*;alrm-GAL4 (#3)/CyO;Dr/TM3, Sb^1, e*	Marc Freeman
c061	*w*; P{GawB}c061*	Bloomington, 30845

c17	*w*; P{GAL4}c17/CyO*	Bloomington, 39690
c21	*P{GAL4-Eh.2.4}C21*	Bloomington, 6301
c232	*w*; P{GawB}Aph-4^{c232}*	Bloomington, 30828
c346	*w*; P{GawB}c346*	Bloomington, 30831
c507	*w*; P{GawB}Aph-4^{c507}*	Bloomington, 30840
c632a	*w*; P{GawB}c632a*	Bloomington, 30846
c739	*y^{1} w^{67c23}; P{GawB}Hr39^{c739}*	Bloomington, 7362
c772	*w*;c772-GAL4/CyO*	Tanouye, T165
Canton Special	Wild-type	Tanouye, T801
Cha [1]	*w*; P{Cha-GAL4.7.4}19B P{UAS-GFP.S65T}Myo31DF^{T2}*	Bloomington, 6793
Cha [2]	*w^{1118}; P{Cha-GAL4.7.4}19B/CyO, P{sevRas1.V12}FK1*	Bloomington, 6798
Cha-GAL80	*w*;;Cha-GAL80/TM3, Sb^{1}*	Kristin Scott
CQ2 [1]	*y^{1} w*; P{CQ2-GAL4}O*	Bloomington, 7466
CQ2 [2]	*y^{1} w*; P{CQ2-GAL4}H*	Bloomington, 7468
CyO, Act-GFP	*w*; In(2LR)noc^{4L}Sco^{rv9R}, b^{1}/CyO, P{ActGFP}JMR1*	Bloomington, 4533
D42	*w*; P{GawB}D42*	Bloomington, 8816
DJ761	w^{1118}; P{GawB}DJ761	Bloomington, 8185
elav^{C155}	*P{GawB}elav^{C155}*	Bloomington, 458
elav^{C155}>mCD8::GFP	*P{GawB}elav^{C155}, P{UAS-mCD8::GFP.L}Ptp4E^{LL4}, P{hsFLP}1, w**	Bloomington, 5146

elav-GAL80	*w*;;elav-GAL80/TM6, b*	Kristin Scott
elav^{GS}	*y^{1}w*;;elav$^{Gene-Switch}$*	Haig Keshishian
Exex	*w*; P{GawB}exex^{GAL4} P{lacW}wah$^{S009\ 413}$/TM3, P{GAL4-Kr.C}DC2, P{UAS-GFP.S65T}DC10, Sb^{1}*	Bloomington, 32555
Gad1	*w*;Gad1-GAL4*	Tanouye, T152
Gad1-GAL80	*w*;;Gad1-GAL80/TM6, b*	Kristin Scott
Gcm	*y^{1} w*; P{GawB}gcm$^{rA87.C}$/CyO*	Bloomington, 35541
Gli	*w*;gliotactin-GAL4 (RL82-GAL4)*	Vanessa Auld (via Marc Freeman)
GMR	*w^{1118}; P{GMR-GAL4.w^{-}}2/CyO*	Bloomington, 9146
Gr66a	*w*; P{Gr66a-GAL4.D}2; Gr93a^{3}*	Bloomington, 28801
He	*w*; P{He-GAL4.Z}85, P{UAS-GFP.nls}8*	Bloomington, 8700
hsp-70	*w*;hsp-70-GAL4/CyO*	Louise Parker
kcc^{Ad-4}/CyO, Act-GFP	*dp^{ov1} cn^{1} bw^{1} kcc^{Ad-4}/ CyO, P{ActGFP}JMR1*	This study, ZMR000
kcc^{Ad-4}/SM6a	*dp^{ov1} cn^{1} bw^{1} kcc^{Ad-4}/SM6a*	Bloomington, 5207
kcc^{EY08304}/CyO	*y^{1} w^{67c23}; P{EPgy2}kcc^{EY08304}/CyO*	Bloomington, 16887
kcc^{EY08304}/CyO, Act-GFP	*y^{1} w^{67c23}; P{EPgy2}kcc^{EY08304}/ CyO, P{ActGFP}JMR1*	This study, ZMR001
L(3)31-1	*w*; P{GawB}l(3)31-1$^{31-1}$/TM6C, Sb^{1} Tb^{1}*	Bloomington, 5820
Lsp2	*y^{1} w^{1118}; P{Lsp2-GAL4.H}3*	Bloomington, 6357
MB247	*w*;;MB247-GAL4*	Tanouye, T160
MB-GAL80	*w*;MB-GAL80/SM5, Cy*	Scott Waddell
moody	*w*;spg-GAL4 [B-1]*	Roland

		Bainton (via Marc Freeman), C/9/A
mz0709	*w*;;mz0709-GAL4*	Kai Ito (via Marc Freeman)
Mz97	*w*; P{GawB}Mz97 P{UAS-Stinger}2*	Bloomington, 9488
nan	*w*; P{nan-GAL4.K}2; nan^{dy5}*	Bloomington, 24903
neur	*w^{1118}; P{GawB}neur$^{GAL4-A101}$ Kg^{V}/TM3, Sb^{1}*	Bloomington, 6393
ninaE	*w*; P{ninaE-GAL4.D}2; P{UAS-41Q.HA}3*	Bloomington, 30540
NP2222	*w*;NP2222-GAL4/CyO*	Marc Freeman, C/10/D
nrv2	*w*; P{nrv2-GAL4.S}3*	Bloomington, 6800
OK107	*w*; P{GawB}ey^{OK107}/In(4)ci^{D}, ci^{D} pan^{c} ^{iD} sv$^{spa-pol}$*	Bloomington, 854
OK6	*w*;OK6-GAL4*	Grant Kauwe
Or83b	*w*; P{Orco-GAL4.W}11.17; TM2/TM6B, Tb^{1}*	Bloomington, 26818
pain	*w*; P{GawB}pain^{GAL4}*	Bloomington, 27894
para^{bss1}	*w*, para^{bss1}, f^{1}*	Tanouye, T808
pdf	*y^{1} w*; P{Pdf-GAL4.P2.4}2*	Bloomington, 6900
ppk	*w*; P{ppk-GAL4.G}3*	Bloomington, 32079
ppk [1]	*Df(1)pod1$^{\Delta 17}$, w^{1118} pod1$^{\Delta 17}$ P{FRT(w^{hs})}9-2/FM7c, P{GAL4-Kr.C}DC1, P{UAS-GFP.S65T}DC5,*	Bloomington, 8749

	sn^{+}; P{ppk-GAL4.G}2, P{UAS-mCD8::GFP.L}LL5/CyO	
ppk [2]	*w*; P{ppk-GAL4.G}2*	Bloomington, 32078
R1	*P{rh1-GAL4}1; ry^{506}*	Bloomington, 8688
R7	*w*; P{Pan-R7-GAL4}2/CyO*	Bloomington, 8603
Rdl	*w*;;Rdl-GAL4-2-1(3)*	Tanouye, T352
Repo	*w*;;repo-GAL4/TM3, Sb^{1}*	Kai Ito (via Marc Freeman)
repo-GAL80	*y^{1}w*;repo-GAL80/CyO*	Tzumin Lee
Sca	*y^{1} w*; P{GawB}sca$^{109-68}$/CyO*	Bloomington, 6479
SG18	*w*; P{GawB}SG18.1*	Bloomington, 6405
Sgs3	*w^{1118}; P{Sgs3-GAL4.PD}TP1*	Bloomington, 6870
TH	*w*; P{ple-GAL4.F}3*	Bloomington, 8848
tim	*y^{1} w*; P{GAL4-tim.E}62*	Bloomington, 7126
tsh-GAL80	*w*;tsh-GAL80/CyO; TM2/TM6, b*	Kristin Scott
tub-GAL80^{ts} [1]	*w*; sna^{Sco}/CyO; P{tubP-GAL80^{ts}}7*	Bloomington, 7018
tub-GAL80^{ts} [2]	*w*; P{tubP-GAL80^{ts}}20; TM2/TM6B, Tb^{1}*	Bloomington, 7019
UAS-kcc-RNAi-B	*y^{1} sc* v^{1}; P{TRiP.HMS01058}attP2*	Bloomington, 34584
UAS-kcc-RNAi-B,tubulin-GAL80^{ts}[2	*w*; P{tubP-GAL80^{ts}}20; P{TRiP.HMS01058}attP2*	This study, ZMR004
UAS-kcc-RNAi-V	*P{KK107965}VIE-260B*	VDRC, 101742

UAS-kcc-RNAi-V,tubulin-GAL80^{ts}[1]	*w*; P{KK107965}VIE-260B; P{tubP-GAL80^{ts}}7*	This study, ZMR003
UAS-ncc69-RNAi-B	*y^{1} v^{1}; P{TRiP.JF03097}attP2*	Bloomington, 28682
UAS-ncc69-RNAi-V	*w^{1118}; P{GD14863}v30000*	VDRC, 30000

Table 2.1: Drosophila strains used in Chapter 2.

GAL4 driver	% BS paralysis w/ UAS-kcc-RNAi-V	% BS paralysis w/ UAS-kcc-RNAi-B
5-HT	0	
43	2	
4G	44	
221	2	
477	11	
078Y	8	
104Y	0	
109(2)80	1	
201Y	0	100
A307	100	LETHAL
Act5C	LETHAL	LETHAL
Akh		0
alrm	22	23
c061	0	
c17	0	
c21	0	
c232	7	
c346	0	
c507	20	LETHAL
c632a	3	
c739	0	
c772	0	100
Cha [1]	100	LETHAL
Cha [2]	100	LETHAL
CQ2 [1]	0	
CQ2 [2]	0	
D42	97	
DJ761	0	
$elav^{C155}$	LETHAL	LETHAL
exex	56	
Gad1	0	
gcm		0
Gli	18	100
GMR		0
Gr66a	0	
He		0
L(3)31-1	100	
Lsp2		0
MB247	0	100
moody	0	61

mz0709	40	71
Mz97	0	
nan	2	
nrv2	0	66
neur	10	
ninaE	0	0
NP2222	31	100
OK107	0	96
OK6	0	LETHAL
Orco	0	
pain	0	
Pdf	0	
ppk [1]	1	
ppk [2]	0	
ppk	0	
R1	0	
R7	0	
Rdl	0	
repo	70	87
sca	42	
SG18	0	
Sgs3		0
TH	0	
tim		0

Table 2.2: Results of entire candidate GAL4 screen for BS paralysis caused by driving UAS-kcc-RNAi-V and UAS-kcc-RNAi-B.

Chapter 3
Genetic Screen for Enhancers of *para*^{bss1} Seizure-Induced Paralysis Identifies *charlatan* as a Seizure-Enhancer

Introduction

Intractable epilepsy is a debilitating disease affecting a large number of people. One million people in the USA are crippled by this disorder, where seizures are immutable by any of the available anti-epileptic drugs (AEDs) and surgery to resect epileptic foci is often impossible. For example, Dravet syndrome (also known as severe myoclonic epilepsy of infancy), is a rather uncommon but destructive intractable epilepsy (Guerrini, 2012). Dravet syndrome, an autosomal dominant disorder, is linked to lesions in the voltage-gated Na^+ channel gene SCN1A (Claes et al., 2001; Wang et al., 2012). Generalized tonic-clonic seizures are trademarks of children under one year old with Dravet syndrome, eventually leading to mental disabilities. Convulsive status epilepticus and sudden unexplained death in epilepsy (SUDEP) are prevalent. Dravet syndrome seizures are entirely resistant to tested combinations of AEDs at safe dosages.

In this chapter, I present a screen for mutations which may further exacerbate the already severe phenotypes of a *Drosophila* model of intractable epilepsy: the bang-sensitive (BS) mutant $para^{bss1}$. $para^{bss1}$ is a gain-of-function semi-dominant allele of the only *Drosophila* gene encoding voltage-gated Na^+ channels. The $para^{bss1}$ allele is a single change in a highly conserved nucleotide, with neuronal hyperexcitability likely due to a persistent Na^+ current after channel activation (Parker, Padilla, et al., 2011). $para^{bss1}$ exhibits the most severe seizure phenotypes of all the BS mutants. It has the lowest seizure-induction threshold and longest duration of post-seizure paralysis, and it is also the most difficult to suppress by AED or mutation (Kuebler & Tanouye, 2000; Parker, Howlett, et al., 2011; Pavlidis & Tanouye, 1995; Song & Tanouye, 2006). Still, just like most epileptic seizures, $para^{bss1}$ seizures are self-limiting, ending without the aid of any exogenous factors.

I hypothesized that there exists endogenous seizure-termination mechanisms conserved across phyla. Mainly because: 1- Seizure-disorders are prevalent, and seizures can be induced in most nervous systems given a sufficient stimulus. Meaning, animal nervous systems are "expecting" a degree of seizure-occurrence given that they evolved beneficial inhibitory mechanisms that might fail in some circumstances. 2- A mutation in an acid-sensing ion channel, ASIC1a, causes prolonged seizures, but does not significantly impact seizure threshold (Lv et al., 2011; Rho, 2009; Ziemann et al., 2008). Therefore, at least one example of a gene affecting aspects of seizures other than seizure-induction threshold already exists. 3- No genetic screen aimed at identifying genes important for seizure-termination had been performed to my knowledge. Identifying potential novel therapeutic targets through such a screen seemed highly probable. For these reasons, I performed a screen using the $para^{bss1}$ genetic background and chromosomal deficiencies—which remove ~5-30 genes—in heterozygous form for their effect on duration of seizure-induced paralysis. $para^{bss1}$ has the longest

duration of seizure-induced paralysis, and so, significant changes in duration of paralysis due to a genetic interaction was best measured in this sensitized background. Duration of paralysis of BS mutants is inversely proportional to seizure threshold (Parker, Howlett, et al., 2011). Thus, pinpointing genetic lesions which prolong seizure-induced paralysis might simultaneously reveal perturbed genes important for seizure-termination. Five chromosomal deficiencies consistently increased BS paralysis time. The transcription factor *charlatan* (*chn*) was identified as the causative seizure-enhancer within one of the deficiencies which increases BS paralysis duration of $para^{bss1}$.

Materials and Methods

Fly strains

Drosophila strains were reared on standard cornmeal-molasses agar media at room temperature (22-25°C). The *paralyzed*, *para*, gene is located at position 1-53.5 on the genomic map and it encodes *Drosophila*'s only predicted and identified voltage-gated Na^+ channel (Loughney, Kreber, & Ganetzky, 1989; Ramaswami & Tanouye, 1989). $para^{bss1}$, the allele used here, is the most seizure-sensitive of *Drosophila* mutants with the most difficult seizure-sensitivity to suppress by drug and by mutation (Ganetzky & Wu, 1982; Parker, Padilla, et al., 2011). $para^{bss1}$ is a gain-of-function mutation due to a substitution (L1699F) of a very conserved residue located in the third membrane-spanning segment (S3b) of homology domain IV (Parker, Padilla, et al., 2011). The *chn* RNAi stock was obtained from the Vienna Drosophila RNAi Center. All other stocks were obtained from the Bloomington Drosophila Stock Center. The $elav\text{-}GAL4^{C155},para^{bss1}$ recombinant was generated using standard *Drosophila* genetic crossing schemes and appropriate balancer stocks, followed by screening for red-eyed seizure-sensitive flies ($para^{bss1}$ is in a w^- background).

Behavioral assays

A screen was carried-out to detect novel seizure-enhancers based on changes in $para^{bss1}$ seizure-induced paralysis. The screen examined 150 stocks, each of which carried a different Df(2) or Df(3) chromosomal deletion with corresponding balancers in a $para^{bss1}/Y$ background. For Df(2) deletions: virgin female $para^{bss1};+;+$ flies were crossed to *+/Y;Df(2)/CyO;+* males. Male progeny of the genotype $para^{bss1}/Y;Df(2)/+;+$ were tested for enhancement of BS paralysis compared to their sibling controls $(para^{bss1}/Y;CyO/+;+)$. CO_2 was used to anesthetize flies before collection and tested the following day. For testing, 3-6 flies were placed in a food vial and stimulated mechanically with a VWR vortex mixer at maximum speed for 10 s. For analysis, recovery time was measured for each fly from the end of the vortex stimulation until it resumed an upright standing position or leaped onto the vial wall and started climbing. Mean Recovery Time (MRT) was the average time taken for flies exhibiting BS behavior to recover. Pools

of flies were combined (in total, n > 100 for each genotype). Normalized Mean Recovery Time (nMRT) is the MRT of the experimental flies divided by MRT of their control siblings. Only those flies that displayed BS paralysis were used for recovery time analysis. 50% recovery time, the time at which half of a BS fly population has recovered from paralysis, was used for initial identification of enhancers of BS-induced paralysis duration. 15-20 flies in a vial were used with 50% recovery time assays.

Electrophysiology

In vivo recording of seizure-like neuronal activity and seizure threshold determination in adult flies was performed as described previously (Kuebler & Tanouye, 2000; Lee & Wu, 2002). Flies 2-3 d post-eclosion were mounted in wax as described in Chapter 2, Materials and Methods. Stimulating, recording, and ground metal electrodes were made of uninsulated tungsten. Seizure-like activity was evoked by high-frequency stimulus (HFS) (0.5 ms pulses at 200 Hz for 300 ms) and detected by dorsal longitudinal muscle (DLM) recording. During the course of each experiment, the giant fiber (GF) circuit was monitored continuously as a proxy for holobrain function. For each genotype tested, n ≥ 10 males. Comparisons of paralytic recovery time and seizure threshold were Student's *t*-test. Error values were standard error of the mean, and statistical significance was as indicated.

Results

Screening for *para*^{bss1} enhancers with chromosomal deficiencies

para^{bss1} displays BS paralytic phenotypes akin to other BS mutants, although more extreme (see Chapter 1, Table 1.1). Any population of *para*^{bss1} flies is 100% BS if flies are not in a refractory state. Their average HFS voltage threshold, 3.2 ± 0.6 V HFS, is also the lowest amongst the bang-sensitives (Kuebler, Zhang, Ren, & Tanouye, 2001). Behavioral seizures are tonic-clonic-like, with up to seven bouts observed in some flies (see Chapter 1, Figure 1.2*D*, and (Parker, Padilla, et al., 2011). After the final ictal event, *para*^{bss1} flies remain paralyzed for an average of ~4 minutes, which is much longer than the duration of seizure-induced paralysis of any other BS mutant.

In spite of the intensity of *para*^{bss1} seizure phenotypes, I examined the ability of chromosomal deficiencies to lengthen the duration of *para*^{bss1} seizure-induced paralysis. Age and genetic background are known components influencing the duration of *para*^{bss1} seizure-induced paralysis, but no mapped genetic lesion specifically affecting this behavior has been reported (Parker, Padilla, et al., 2011). Stretches of the *para*^{bss1} second or third chromosomes were made haploid using chromosomal deficiencies, and modification of paralysis phenotypes were timed and compared to sibling controls without deficiencies. Specifically, *para*^{bss1}*/Y;(;)Df(2or3)/*+ flies, and their *para*^{bss1}*/Y;(;)Balancer/*+ sibling controls, were administered "bangs"

and the duration of their seizure-induced paralysis was recorded. I tested 150 stocks containing deficiencies in this manner (Table 3.1). Several deficiency chromosomes consistently showed increased recovery times for *para^{bss1}* males, and the five most potent deficiencies are listed in Table 3.2. *para^{bss1}/Y;Df(2R)Exel7135/+* males had a mean recovery time (MRT) of 363 s, compared to 234 s for *para^{bss1}/Y;CyO/+* balancer-possessing controls yielding a normalized mean recovery time (nMRT) of 1.55. Here I further explored Df(2R)Exel7135 for its ability to modify *para^{bss1}* seizure-induced paralysis. In the next section I researched the causative gene(s) within the deletion and examined effect on another major measure of *Drosophila* seizure-susceptibility, the seizure-induction threshold.

Reduced expression of *charlatan (chn)* contained in the Df(2R)Exel7135 chromosomal segment enhances *para^{bss1}* BS paralysis, but not seizure threshold

The Df(2R)Exel7135 deficiency is a deletion spanning from 51E2 to 51E11 on chromosome 2R and contains approximately 22 genes. Deletion analysis further limited this segment to 51E2 to 51E7 based on observations that the *para^{bss1}/Y* recovery time is not enhanced by the heterozygous Df(2R)BSC346/+ (51E7-52C2); but is enhanced by Df(2R)BSC651/+ (51C5-51E2) (Figure 3.1). It was found that *para^{bss1}* BS enhancement in the segment is accounted for by reduced expression of the *charlatan (chn)* gene. The gene is broken by the 51E2 breakpoints of Df(2R)Exel7135 and Df(2R)BSC651, and is the only apparent gene affected by both rearrangements. Further identification of *chn* as an enhancer of *para^{bss1}/Y* is by *UAS-chn-RNAi*. Flies of the genotype *elav-GAL4^{C155},para^{bss1}/Y;UAS-chn-RNAi/+* show increased BS recovery times with an MRT of 261.9 ± 17.1 s, compared to 105.6 ± 9.4 s for their *elav-GAL4^{C155},para^{bss1}/Y;+/+* sibling controls for an nMRT of 2.48 ($p<0.001$).

The *chn* gene encodes an NRSF/REST-like transcriptional repressor of neuronal-specific genes (Escudero, Caminero, Schulze, Bellen, & Modolell, 2005; Tsuda et al., 2006; Yamasaki, Lim, Niwa, Hayashi, & Tsuda, 2011). It has not been previously identified in seizure-susceptibility or electrical excitability. Surprisingly, the enhancement of *para^{bss1}* by *chn* was limited to BS paralysis recovery time phenotype, that is, an increase in the severity of this phenotype; there was no apparent enhancement of the other major phenotype: threshold for evoked seizure. For example, flies of the genotype *elav-GAL4^{C155},para^{bss1}/Y;UAS-chn-RNAi/+* have a seizure threshold of 3.32 ± 0.47 V HFS, similar to the threshold of 3.87 ± 0.53 V HFS ($p = 0.46$) for their sibling controls. *chn* also lengthened the duration of synaptic failure following a seizure compared to controls (data not shown). These findings are consistent with the results of Df(2R)Exel7135 and all of the other enhancers identified in this screen: the enhancers increased BS paralysis time to recovery, but did not reduce %BS paralysis or HFS threshold in

electrophysiology tests; both parameters defining seizure-induction threshold in *Drosophila*.

Discussion

Intractable epilepsy is a disease with currently no prospects for effective cures in sight. People are clinically diagnosed with intractable epilepsy if their seizures do not respond to two or more AEDs. Five mechanisms are thought to be the main targets of AEDs and other anti-epileptic molecules: 1- Potentiation of GABAergic inhibition. 2- Dampening of glutamatergic excitation. 3- Voltage-gated Na^+ channel antagonism. 4- Ca^{2+} channel antagonism. 5- Blockade of cell-swelling (Hochman, 2012; Loscher & Schmidt, 2002; Sirven, Noe, Hoerth, & Drazkowski, 2012). However, there are limits on the prescribed dosages of AEDs because of the obvious detrimental side-effects on brain cognition. Indeed, the targets of most AEDs described above are fundamental components of nervous system activity. When patients with intractable epilepsy have no options for surgery, or when AEDs and lifestyle changes to avoid precipitants are ineffective, they are left helpless. It appears that a revolution in epilepsy therapeutics is required to ameliorate such horrible living conditions whilst minimizing brain toxicity. Identification of novel drug targets which do not impact physiological behavior upon manipulation is one hope for humans with intractable epilepsy.

Using $para^{bss1}$, a *Drosophila* model of intractable epilepsy, I examined the extent to which its intense seizure phenotypes can be further exacerbated by genetic mutation. $para^{bss1}$ is thought to model Dravet syndrome given the underlying shared disruption in the highly conserved voltage-gated Na^+ channel genes *para* and SCN1A in flies and humans, respectively (Oliva et al., 2012; Parker, Padilla, et al., 2011). $para^{bss1}$ seizures are resistant to AEDs and genetic suppressor mutations identified through suppression of other BS mutant seizure phenotypes (Kuebler et al., 2001; Song & Tanouye, 2006, 2008). The forward-genetics screen outlined in this chapter resulted in identification of a slew of chromosomal deletions which enhance $para^{bss1}$ seizures.

The *chn* zinc finger transcription factor-encoding gene was identified as one causative gene amongst several in a deficiency which lengthened seizure-induced paralysis. Chn has been shown to act in early developmental processes in the eye, follicle cells and notum: it inhibits Delta, and it is activated and repressed by Notch and Ebi/SMR/Su(H), respectively (Escudero et al., 2005; Tsuda et al., 2006). Reduction of Chn perturbs the development of the peripheral nervous system (PNS) in embryos and adults. *chn* is a homolog of NRSF/REST transcriptional repressors of neuronal-specific genes; genes with NRSE/RE-1 sequences. Suppression by Chn is thought to occur for many neuronal genes including *Delta* (*Dl*), *hairy* (*h*), *Dopamine receptor 2* (*DopR2*), *ether a go-go* (*eag*), *nicotinic Acetylcholine*

Receptor beta 64B (*nAcRβ-64B*), and *shaking B* (*shakB*). However, unlike mammalian NRSF/REST, Chn has been shown to enhance expression of some genes via 21 bp cis-regulatory DNA elements (Yamasaki et al., 2011). Chn is believed to be a dual suppressor/enhancer in at least all arthropods. Thus, one can only speculate about the many *chn* mechanisms enhancing seizure-induced paralysis. The finding exemplifies a type of seizure-enhancer which could exert its effects through alteration of the neuronal architecture producing the measured phenotype. Although these types of enhancers might not be ideal direct therapeutic targets, their identification can aid in epilepsy diagnoses, precautionary treatments and future investigations.

Depending on how well $para^{bss1}$ models Dravet and/or other intractable epilepsies, the findings shown here could be important for unraveling the complexity of these diseases. Although *chn* seizure-enhancement could be specific to $para^{bss1}$, it could also be a general enhancer of seizures since it lengthened seizure-induced paralysis of another BS mutant, eas^{PC80} (data not shown, and (Pavlidis, Ramaswami, & Tanouye, 1994). These findings demonstrate a potential novel approach to seizure-suppression. Follow-up and similar studies could unearth new strategies for epilepsy therapy. Endogenous mechanisms that are in place to stop seizures are likely only to be revealed upon disruption in an already seizure-susceptible background. The *Drosophila* models of epilepsy seem to be excellent ones given their evolutionary relevance and ability to rapidly identify genes impacting manifestation of seizure states.

Acknowledgments
This study was supported by awards from the McKnight Foundation and the NIH (NS31231) to Mark A. Tanouye. I am grateful to members of the Tanouye lab, past and present, for fruitful discussions throughout the project.

REFERENCES

Allen, M. J., Drummond, J. A., Sweetman, D. J., & Moffat, K. G. (2007). Analysis of two P-element enhancer-trap insertion lines that show expression in the giant fibre neuron of Drosophila melanogaster. *Genes Brain Behav, 6*(4), 347-358. doi: 10.1111/j.1601-183X.2006.00263.x

Allen, M. J., & Godenschwege, T. A. (2010). Electrophysiological recordings from the Drosophila giant fiber system (GFS). *Cold Spring Harb Protoc, 2010*(7), pdb prot5453. doi: 10.1101/pdb.prot5453

Allen, M. J., Godenschwege, T. A., Tanouye, M. A., & Phelan, P. (2006). Making an escape: development and function of the Drosophila giant fibre system. *Semin Cell Dev Biol, 17*(1), 31-41. doi: 10.1016/j.semcdb.2005.11.011

Baumgartner, S., Littleton, J. T., Broadie, K., Bhat, M. A., Harbecke, R., Lengyel, J. A., . . . Bellen, H. J. (1996). A Drosophila neurexin is required for septate junction and blood-nerve barrier formation and function. *Cell, 87*(6), 1059-1068.

Ben-Ari, Y., Gaiarsa, J. L., Tyzio, R., & Khazipov, R. (2007). GABA: a pioneer transmitter that excites immature neurons and generates primitive oscillations. *Physiol Rev, 87*(4), 1215-1284. doi: 10.1152/physrev.00017.2006

Ben-Ari, Y., Khalilov, I., Kahle, K. T., & Cherubini, E. (2012). The GABA excitatory/inhibitory shift in brain maturation and neurological disorders. *Neuroscientist, 18*(5), 467-486. doi: 10.1177/1073858412438697

Ben-Ari, Y., Woodin, M. A., Sernagor, E., Cancedda, L., Vinay, L., Rivera, C., . . . Cherubini, E. (2012). Refuting the challenges of the developmental shift of polarity of GABA actions: GABA more exciting than ever! *Front Cell Neurosci, 6*, 35. doi: 10.3389/fncel.2012.00035

Benarroch, E. E. (2013). Cation-chloride cotransporters in the nervous system: General features and clinical correlations. *Neurology, 80*(8), 756-763. doi: 10.1212/WNL.0b013e318283bb1c

Benesova, J., Rusnakova, V., Honsa, P., Pivonkova, H., Dzamba, D., Kubista, M., & Anderova, M. (2012). Distinct expression/function of potassium and chloride channels contributes to the diverse volume regulation in cortical astrocytes of GFAP/EGFP mice. *PLoS One, 7*(1), e29725. doi: 10.1371/journal.pone.0029725

Berg, A. T., & Scheffer, I. E. (2011). New concepts in classification of the epilepsies: entering the 21st century. *Epilepsia, 52*(6), 1058-1062. doi: 10.1111/j.1528-1167.2011.03101.x

Blaesse, P., Airaksinen, M. S., Rivera, C., & Kaila, K. (2009). Cation-chloride cotransporters and neuronal function. *Neuron, 61*(6), 820-838. doi: 10.1016/j.neuron.2009.03.003

Boettger, T., Rust, M. B., Maier, H., Seidenbecher, T., Schweizer, M., Keating, D. J., . . . Jentsch, T. J. (2003). Loss of K-Cl co-transporter KCC3 causes deafness, neurodegeneration and reduced seizure threshold. *EMBO J, 22*(20), 5422-5434. doi: 10.1093/emboj/cdg519

Brand, A. H., & Perrimon, N. (1993). Targeted gene expression as a means of altering cell fates and generating dominant phenotypes. *Development, 118*(2), 401-415.

Byun, N., & Delpire, E. (2007). Axonal and periaxonal swelling precede peripheral neurodegeneration in KCC3 knockout mice. *Neurobiol Dis, 28*(1), 39-51. doi: 10.1016/j.nbd.2007.06.014

Cancedda, L., Fiumelli, H., Chen, K., & Poo, M. M. (2007). Excitatory GABA action is essential for morphological maturation of cortical neurons in vivo. *J Neurosci, 27*(19), 5224-5235. doi: 10.1523/jneurosci.5169-06.2007

Carmignoto, G., & Haydon, P. G. (2012). Astrocyte calcium signaling and epilepsy. *Glia, 60*(8), 1227-1233. doi: 10.1002/glia.22318

Chiu, A. W., & Bardakjian, B. L. (2004). Control of state transitions in an in silico model of epilepsy using small perturbations. *IEEE Trans Biomed Eng, 51*(10), 1856-1859. doi: 10.1109/tbme.2004.831520

Claes, L., Del-Favero, J., Ceulemans, B., Lagae, L., Van Broeckhoven, C., & De Jonghe, P. (2001). De novo mutations in the sodium-channel gene SCN1A cause severe myoclonic epilepsy of infancy. *Am J Hum Genet, 68*(6), 1327-1332. doi: 10.1086/320609

Colmenero-Flores, J. M., Martinez, G., Gamba, G., Vazquez, N., Iglesias, D. J., Brumos, J., & Talon, M. (2007). Identification and functional characterization of cation-chloride cotransporters in plants. *Plant J, 50*(2), 278-292. doi: 10.1111/j.1365-313X.2007.03048.x

Coulter, D. A., & Eid, T. (2012). Astrocytic regulation of glutamate homeostasis in epilepsy. *Glia, 60*(8), 1215-1226. doi: 10.1002/glia.22341

Cruz-Rangel, S., Melo, Z., Vazquez, N., Meade, P., Bobadilla, N. A., Pasantes-Morales, H., . . . Mercado, A. (2011). Similar effects of all WNK3 variants on SLC12 cotransporters. *Am J Physiol Cell Physiol, 301*(3), C601-608. doi: 10.1152/ajpcell.00070.2011

Danjo, R., Kawasaki, F., & Ordway, R. W. (2011). A tripartite synapse model in Drosophila. *PLoS One, 6*(2), e17131. doi: 10.1371/journal.pone.0017131

DeSalvo, M. K., Mayer, N., Mayer, F., & Bainton, R. J. (2011). Physiologic and anatomic characterization of the brain surface glia barrier of Drosophila. *Glia, 59*(9), 1322-1340. doi: 10.1002/glia.21147

Dzhala, V. I., Talos, D. M., Sdrulla, D. A., Brumback, A. C., Mathews, G. C., Benke, T. A., . . . Staley, K. J. (2005). NKCC1 transporter facilitates seizures in the developing brain. *Nat Med, 11*(11), 1205-1213. doi: 10.1038/nm1301

Edwards, J. S., Swales, L. S., & Bate, M. (1993). The differentiation between neuroglia and connective tissue sheath in insect ganglia revisited: the neural lamella and perineurial sheath cells are absent in a mesodermless mutant of Drosophila. *J Comp Neurol, 333*(2), 301-308. doi: 10.1002/cne.903330214

Edwards, T. N., Nuschke, A. C., Nern, A., & Meinertzhagen, I. A. (2012). Organization and metamorphosis of glia in the Drosophila visual system. *J Comp Neurol, 520*(10), 2067-2085. doi: 10.1002/cne.23071

Escudero, L. M., Caminero, E., Schulze, K. L., Bellen, H. J., & Modolell, J. (2005). Charlatan, a Zn-finger transcription factor, establishes a novel level of regulation of the proneural achaete/scute genes of Drosophila. *Development, 132*(6), 1211-1222. doi: 10.1242/dev.01691

Featherstone, David E. (2011). Glial solute carrier transporters in drosophila and mice. *Glia, 59*(9), 1351-1363. doi: 10.1002/glia.21085

Feng, Y., Ueda, A., & Wu, C. F. (2004). A modified minimal hemolymph-like solution, HL3.1, for physiological recordings at the neuromuscular junctions of normal and mutant Drosophila larvae. *J Neurogenet, 18*(2), 377-402. doi: 10.1080/01677060490894522

Filippov, V., Aimanova, K., & Gill, S. S. (2003). Expression of an Aedes aegypti cation-chloride cotransporter and its Drosophila homologues. *Insect Mol Biol, 12*(4), 319-331.

Fiumelli, H., Briner, A., Puskarjov, M., Blaesse, P., Belem, B. J., Dayer, A. G., . . . Vutskits, L. (2013). An ion transport-independent role for the cation-chloride cotransporter KCC2 in dendritic spinogenesis in vivo. *Cereb Cortex, 23*(2), 378-388. doi: 10.1093/cercor/bhs027

Gagnon, K. B., Adragna, N. C., Fyffe, R. E., & Lauf, P. K. (2007). Characterization of glial cell K-Cl cotransport. *Cell Physiol Biochem, 20*(1-4), 121-130. doi: 10.1159/000104160

Gagnon, K. B., & Delpire, E. (2013). Physiology of SLC12 Transporters: Lessons from Inherited Human Genetic Mutations and Genetically-Engineered Mouse Knockouts. *Am J Physiol Cell Physiol*. doi: 10.1152/ajpcell.00350.2012

Galanopoulou, A. S. (2010). Mutations affecting GABAergic signaling in seizures and epilepsy. *Pflugers Arch, 460*(2), 505-523. doi: 10.1007/s00424-010-0816-2

Gallentine, W. B., & Mikati, M. A. (2012). Genetic generalized epilepsies. *J Clin Neurophysiol, 29*(5), 408-419. doi: 10.1097/WNP.0b013e31826bd92a

Gamba, G., Saltzberg, S. N., Lombardi, M., Miyanoshita, A., Lytton, J., Hediger, M. A., . . . Hebert, S. C. (1993). Primary structure and functional expression of a cDNA encoding the thiazide-sensitive, electroneutral sodium-chloride cotransporter. *Proc Natl Acad Sci U S A, 90*(7), 2749-2753.

Ganetzky, B., & Wu, C. F. (1982). Drosophila mutants with opposing effects on nerve excitability: genetic and spatial interactions in repetitive firing. *J Neurophysiol, 47*(3), 501-514.
Gauvain, G., Chamma, I., Chevy, Q., Cabezas, C., Irinopoulou, T., Bodrug, N., . . . Poncer, J. C. (2011). The neuronal K-Cl cotransporter KCC2 influences postsynaptic AMPA receptor content and lateral diffusion in dendritic spines. *Proc Natl Acad Sci U S A, 108*(37), 15474-15479. doi: 10.1073/pnas.1107893108
Guerrini, R. (2012). Dravet syndrome: the main issues. *Eur J Paediatr Neurol, 16 Suppl 1*, S1-4. doi: 10.1016/j.ejpn.2012.04.006
Halassa, M. M., Fellin, T., & Haydon, P. G. (2007). The tripartite synapse: roles for gliotransmission in health and disease. *Trends Mol Med, 13*(2), 54-63. doi: 10.1016/j.molmed.2006.12.005
Hartenstein, V. (2011). Morphological diversity and development of glia in Drosophila. *Glia, 59*(9), 1237-1252. doi: 10.1002/glia.21162
Hebert, S. C., Mount, D. B., & Gamba, G. (2004). Molecular physiology of cation-coupled Cl- cotransport: the SLC12 family. *Pflugers Arch, 447*(5), 580-593. doi: 10.1007/s00424-003-1066-3
Hekmat-Scafe, D. S., Lundy, M. Y., Ranga, R., & Tanouye, M. A. (2006). Mutations in the K+/Cl- cotransporter gene kazachoc (kcc) increase seizure susceptibility in Drosophila. *J Neurosci, 26*(35), 8943-8954. doi: 10.1523/JNEUROSCI.4998-05.2006
Hekmat-Scafe, D. S., Mercado, A., Fajilan, A. A., Lee, A. W., Hsu, R., Mount, D. B., & Tanouye, M. A. (2010). Seizure sensitivity is ameliorated by targeted expression of K+-Cl- cotransporter function in the mushroom body of the Drosophila brain. *Genetics, 184*(1), 171-183. doi: 10.1534/genetics.109.109074
Hochman, D. W. (2012). The extracellular space and epileptic activity in the adult brain: explaining the antiepileptic effects of furosemide and bumetanide. *Epilepsia, 53 Suppl 1*, 18-25. doi: 10.1111/j.1528-1167.2012.03471.x
Horn, Z., Ringstedt, T., Blaesse, P., Kaila, K., & Herlenius, E. (2010). Premature expression of KCC2 in embryonic mice perturbs neural development by an ion transport-independent mechanism. *Eur J Neurosci, 31*(12), 2142-2155. doi: 10.1111/j.1460-9568.2010.07258.x
Jackson, G. (2011). Classification of the epilepsies 2011. *Epilepsia, 52*(6), 1203-1204; discussion 1205-1209. doi: 10.1111/j.1528-1167.2011.03093.x
Jayakumar, A. R., & Norenberg, M. D. (2010). The Na-K-Cl Co-transporter in astrocyte swelling. *Metab Brain Dis, 25*(1), 31-38. doi: 10.1007/s11011-010-9180-3
Jayakumar, A. R., Panickar, K. S., Curtis, K. M., Tong, X. Y., Moriyama, M., & Norenberg, M. D. (2011). Na-K-Cl cotransporter-1 in the mechanism

of cell swelling in cultured astrocytes after fluid percussion injury. *J Neurochem, 117*(3), 437-448. doi: 10.1111/j.1471-4159.2011.07211.x

Juang, J. L., & Carlson, S. D. (1994). Analog of vertebrate anionic sites in blood-brain interface of larval Drosophila. *Cell Tissue Res, 277*(1), 87-95.

Kahle, K. T., Rinehart, J., & Lifton, R. P. (2010). Phosphoregulation of the Na-K-2Cl and K-Cl cotransporters by the WNK kinases. *Biochim Biophys Acta, 1802*(12), 1150-1158. doi: 10.1016/j.bbadis.2010.07.009

Kahle, K. T., Staley, K. J., Nahed, B. V., Gamba, G., Hebert, S. C., Lifton, R. P., & Mount, D. B. (2008). Roles of the cation-chloride cotransporters in neurological disease. *Nat Clin Pract Neurol, 4*(9), 490-503. doi: 10.1038/ncpneuro0883

Kovacs, R., Heinemann, U., & Steinhauser, C. (2012). Mechanisms underlying blood-brain barrier dysfunction in brain pathology and epileptogenesis: role of astroglia. *Epilepsia, 53 Suppl 6*, 53-59. doi: 10.1111/j.1528-1167.2012.03703.x

Kuebler, D., & Tanouye, M. A. (2000). Modifications of seizure susceptibility in Drosophila. *J Neurophysiol, 83*(2), 998-1009.

Kuebler, D., Zhang, H., Ren, X., & Tanouye, M. A. (2001). Genetic suppression of seizure susceptibility in Drosophila. *J Neurophysiol, 86*(3), 1211-1225.

Le Van Quyen, M., Soss, J., Navarro, V., Robertson, R., Chavez, M., Baulac, M., & Martinerie, J. (2005). Preictal state identification by synchronization changes in long-term intracranial EEG recordings. *Clin Neurophysiol, 116*(3), 559-568. doi: 10.1016/j.clinph.2004.10.014

Lee, J., & Wu, C. F. (2002). Electroconvulsive seizure behavior in Drosophila: analysis of the physiological repertoire underlying a stereotyped action pattern in bang-sensitive mutants. *J Neurosci, 22*(24), 11065-11079.

Leiserson, W. M., & Keshishian, H. (2011). Maintenance and regulation of extracellular volume and the ion environment in Drosophila larval nerves. *Glia, 59*(9), 1312-1321. doi: 10.1002/glia.21132

Leiserson, William M., Forbush, Biff, & Keshishian, Haig. (2011). Drosophila glia use a conserved cotransporter mechanism to regulate extracellular volume. *Glia, 59*(2), 320-332. doi: 10.1002/glia.21103

Li, H., Khirug, S., Cai, C., Ludwig, A., Blaesse, P., Kolikova, J., . . . Rivera, C. (2007). KCC2 interacts with the dendritic cytoskeleton to promote spine development. *Neuron, 56*(6), 1019-1033. doi: 10.1016/j.neuron.2007.10.039

Loscher, W., Puskarjov, M., & Kaila, K. (2012). Cation-chloride cotransporters NKCC1 and KCC2 as potential targets for novel

antiepileptic and antiepileptogenic treatments. *Neuropharmacology*. doi: 10.1016/j.neuropharm.2012.05.045
Loscher, W., & Schmidt, D. (2002). New horizons in the development of antiepileptic drugs. *Epilepsy Res, 50*(1-2), 3-16.
Loughney, K., Kreber, R., & Ganetzky, B. (1989). Molecular analysis of the para locus, a sodium channel gene in Drosophila. *Cell, 58*(6), 1143-1154.
Lowenstein, D. H. (2008). Pathways to discovery in epilepsy research: rethinking the quest for cures. *Epilepsia, 49*(1), 1-7. doi: 10.1111/j.1528-1167.2007.01309.x
Lucas, O., Hilaire, C., Delpire, E., & Scamps, F. (2012). KCC3-dependent chloride extrusion in adult sensory neurons. *Mol Cell Neurosci, 50*(3-4), 211-220. doi: 10.1016/j.mcn.2012.05.005
Lv, R. J., He, J. S., Fu, Y. H., Zhang, Y. Q., Shao, X. Q., Wu, L. W., . . . Liu, H. (2011). ASIC1a polymorphism is associated with temporal lobe epilepsy. *Epilepsy Res, 96*(1-2), 74-80. doi: 10.1016/j.eplepsyres.2011.05.002
Macaulay, N., & Zeuthen, T. (2012). Glial K(+) clearance and cell swelling: key roles for cotransporters and pumps. *Neurochem Res, 37*(11), 2299-2309. doi: 10.1007/s11064-012-0731-3
Marchi, N., Angelov, L., Masaryk, T., Fazio, V., Granata, T., Hernandez, N., . . . Janigro, D. (2007). Seizure-promoting effect of blood-brain barrier disruption. *Epilepsia, 48*(4), 732-742. doi: 10.1111/j.1528-1167.2007.00988.x
Margineanu, D. G. (2010). Epileptic hypersynchrony revisited. *Neuroreport, 21*(15), 963-967. doi: 10.1097/WNR.0b013e32833ed111
McGuire, S. E., Le, P. T., Osborn, A. J., Matsumoto, K., & Davis, R. L. (2003). Spatiotemporal rescue of memory dysfunction in Drosophila. *Science, 302*(5651), 1765-1768. doi: 10.1126/science.1089035
Melom, J. E., & Littleton, J. T. (2013). Mutation of a NCKX eliminates glial microdomain calcium oscillations and enhances seizure susceptibility. *J Neurosci, 33*(3), 1169-1178. doi: 10.1523/JNEUROSCI.3920-12.2013
Navarro, V., Le Van Quyen, M., Clemenceau, S., Adam, C., Petitmengin, C., Dubeau, F., . . . Baulac, M. (2011). [Seizure prediction: from myth to reality]. *Rev Neurol (Paris), 167*(3), 205-215. doi: 10.1016/j.neurol.2010.07.027
Nusslein-Volhard, C., & Wieschaus, E. (1980). Mutations affecting segment number and polarity in Drosophila. *Nature, 287*(5785), 795-801.
Oland, L. A., & Tolbert, L. P. (2011). Roles of glial cells in neural circuit formation: insights from research in insects. *Glia, 59*(9), 1273-1295. doi: 10.1002/glia.21096
Oliva, M., Berkovic, S. F., & Petrou, S. (2012). Sodium channels and the neurobiology of epilepsy. *Epilepsia, 53*(11), 1849-1859. doi: 10.1111/j.1528-1167.2012.03631.x

Oshima, K., & Fehon, R. G. (2011). Analysis of protein dynamics within the septate junction reveals a highly stable core protein complex that does not include the basolateral polarity protein Discs large. *J Cell Sci, 124*(Pt 16), 2861-2871. doi: 10.1242/jcs.087700

Park, J. H., & Saier, M. H., Jr. (1996). Phylogenetic, structural and functional characteristics of the Na-K-Cl cotransporter family. *J Membr Biol, 149*(3), 161-168.

Parker, L., Howlett, I. C., Rusan, Z. M., & Tanouye, M. A. (2011). Seizure and epilepsy: studies of seizure disorders in Drosophila. *Int Rev Neurobiol, 99*, 1-21. doi: 10.1016/b978-0-12-387003-2.00001-x

Parker, L., Padilla, M., Du, Y., Dong, K., & Tanouye, M. A. (2011). Drosophila as a model for epilepsy: bss is a gain-of-function mutation in the para sodium channel gene that leads to seizures. *Genetics, 187*(2), 523-534. doi: 10.1534/genetics.110.123299

Pasantes-Morales, H., & Tuz, K. (2006). Volume changes in neurons: hyperexcitability and neuronal death. *Contrib Nephrol, 152*, 221-240. doi: 10.1159/000096326

Pavlidis, P., Ramaswami, M., & Tanouye, M. A. (1994). The Drosophila easily shocked gene: a mutation in a phospholipid synthetic pathway causes seizure, neuronal failure, and paralysis. *Cell, 79*(1), 23-33.

Pavlidis, P., & Tanouye, M. A. (1995). Seizures and failures in the giant fiber pathway of Drosophila bang-sensitive paralytic mutants. *J Neurosci, 15*(8), 5810-5819.

Pereanu, W., Shy, D., & Hartenstein, V. (2005). Morphogenesis and proliferation of the larval brain glia in Drosophila. *Dev Biol, 283*(1), 191-203. doi: 10.1016/j.ydbio.2005.04.024

Phelan, P., Nakagawa, M., Wilkin, M. B., Moffat, K. G., O'Kane, C. J., Davies, J. A., & Bacon, J. P. (1996). Mutations in shaking-B prevent electrical synapse formation in the Drosophila giant fiber system. *J Neurosci, 16*(3), 1101-1113.

Ramaswami, M., & Tanouye, M. A. (1989). Two sodium-channel genes in Drosophila: implications for channel diversity. *Proc Natl Acad Sci U S A, 86*(6), 2079-2082.

Raol, Y. H., & Brooks-Kayal, A. R. (2012). Experimental models of seizures and epilepsies. *Prog Mol Biol Transl Sci, 105*, 57-82. doi: 10.1016/b978-0-12-394596-9.00003-2

Rho, J. M. (2009). Arresting a seizure by dropping a little Acid. *Epilepsy Curr, 9*(2), 55-56. doi: 10.1111/j.1535-7511.2008.01291.x

Ringel, F., & Plesnila, N. (2008). Expression and functional role of potassium-chloride cotransporters (KCC) in astrocytes and C6 glioma cells. *Neurosci Lett, 442*(3), 219-223. doi: 10.1016/j.neulet.2008.07.017

Rivera, C., Voipio, J., & Kaila, K. (2005). Two developmental switches in GABAergic signalling: the K+-Cl- cotransporter KCC2 and carbonic

anhydrase CAVII. *J Physiol, 562*(Pt 1), 27-36. doi: 10.1113/jphysiol.2004.077495
Roy, S., Ernst, J., Kharchenko, P. V., Kheradpour, P., Negre, N., Eaton, M. L., . . . Kellis, M. (2010). Identification of functional elements and regulatory circuits by Drosophila modENCODE. *Science, 330*(6012), 1787-1797. doi: 10.1126/science.1198374
Russo, E., Gitto, R., Citraro, R., Chimirri, A., & De Sarro, G. (2012). New AMPA antagonists in epilepsy. *Expert Opin Investig Drugs, 21*(9), 1371-1389. doi: 10.1517/13543784.2012.705277
Schmidt, D. (2010). Effect of antiepileptic drugs on the postictal state. A critical overview. *Epilepsy Behav, 19*(2), 176-181. doi: 10.1016/j.yebeh.2010.06.019
Schmidt, D., & Noachtar, S. (2010). Outlook: the postictal state--future directions for research. *Epilepsy Behav, 19*(2), 191-192. doi: 10.1016/j.yebeh.2010.06.015
Seiffert, E., Dreier, J. P., Ivens, S., Bechmann, I., Tomkins, O., Heinemann, U., & Friedman, A. (2004). Lasting blood-brain barrier disruption induces epileptic focus in the rat somatosensory cortex. *J Neurosci, 24*(36), 7829-7836. doi: 10.1523/JNEUROSCI.1751-04.2004
Shekarabi, M., Moldrich, R. X., Rasheed, S., Salin-Cantegrel, A., Laganiere, J., Rochefort, D., . . . Rouleau, G. A. (2012). Loss of neuronal potassium/chloride cotransporter 3 (KCC3) is responsible for the degenerative phenotype in a conditional mouse model of hereditary motor and sensory neuropathy associated with agenesis of the corpus callosum. *J Neurosci, 32*(11), 3865-3876. doi: 10.1523/jneurosci.3679-11.2012
Shekarabi, M., Salin-Cantegrel, A., Laganiere, J., Gaudet, R., Dion, P., & Rouleau, G. A. (2011). Cellular expression of the K+-Cl- cotransporter KCC3 in the central nervous system of mouse. *Brain Res, 1374*, 15-26. doi: 10.1016/j.brainres.2010.12.010
Sirven, J. I., Noe, K., Hoerth, M., & Drazkowski, J. (2012). Antiepileptic drugs 2012: recent advances and trends. *Mayo Clin Proc, 87*(9), 879-889. doi: 10.1016/j.mayocp.2012.05.019
Song, J., & Tanouye, M. A. (2006). Seizure suppression by shakB2, a gap junction mutation in Drosophila. *J Neurophysiol, 95*(2), 627-635. doi: 10.1152/jn.01059.2004
Song, J., & Tanouye, M. A. (2008). From bench to drug: human seizure modeling using Drosophila. *Prog Neurobiol, 84*(2), 182-191. doi: 10.1016/j.pneurobio.2007.10.006
Stamoulis, C., & Chang, B. S. (2012). Space-time adaptive processing for improved estimation of preictal seizure activity. *Conf Proc IEEE Eng Med Biol Soc, 2012*, 6157-6160. doi: 10.1109/embc.2012.6347399

Steinhauser, C., Seifert, G., & Bedner, P. (2012). Astrocyte dysfunction in temporal lobe epilepsy: K+ channels and gap junction coupling. *Glia, 60*(8), 1192-1202. doi: 10.1002/glia.22313

Stork, T., Bernardos, R., & Freeman, M. R. (2012). Analysis of glial cell development and function in Drosophila. *Cold Spring Harb Protoc, 2012*(1), 1-17. doi: 10.1101/pdb.top067587

Sun, Q., Tian, E., Turner, R. J., & Ten Hagen, K. G. (2010). Developmental and functional studies of the SLC12 gene family members from Drosophila melanogaster. *Am J Physiol Cell Physiol, 298*(1), C26-37. doi: 10.1152/ajpcell.00376.2009

Sun, Y. T., Lin, T. S., Tzeng, S. F., Delpire, E., & Shen, M. R. (2010). Deficiency of electroneutral K+-Cl- cotransporter 3 causes a disruption in impulse propagation along peripheral nerves. *Glia, 58*(13), 1544-1552. doi: 10.1002/glia.21028

Surges, R., & Sander, J. W. (2012). Sudden unexpected death in epilepsy: mechanisms, prevalence, and prevention. *Curr Opin Neurol, 25*(2), 201-207. doi: 10.1097/WCO.0b013e3283506714

Tanis, J. E., Bellemer, A., Moresco, J. J., Forbush, B., & Koelle, M. R. (2009). The potassium chloride cotransporter KCC-2 coordinates development of inhibitory neurotransmission and synapse structure in Caenorhabditis elegans. *J Neurosci, 29*(32), 9943-9954. doi: 10.1523/jneurosci.1989-09.2009

Thom, M., Blumcke, I., & Aronica, E. (2012). Long-term epilepsy-associated tumors. *Brain Pathol, 22*(3), 350-379. doi: 10.1111/j.1750-3639.2012.00582.x

Timofeev, I., Bazhenov, M., Seigneur, J., & Sejnowski, T. (2012). Neuronal Synchronization and Thalamocortical Rhythms in Sleep, Wake and Epilepsy. In J. L. Noebels, M. Avoli, M. A. Rogawski, R. W. Olsen & A. V. Delgado-Escueta (Eds.), *Jasper's Basic Mechanisms of the Epilepsies*. Bethesda MD: Michael A Rogawski, Antonio V Delgado-Escueta, Jeffrey L Noebels, Massimo Avoli and Richard W Olsen.

Trinka, E., Hofler, J., & Zerbs, A. (2012). Causes of status epilepticus. *Epilepsia, 53 Suppl 4*, 127-138. doi: 10.1111/j.1528-1167.2012.03622.x

Tsuda, L., Kaido, M., Lim, Y. M., Kato, K., Aigaki, T., & Hayashi, S. (2006). An NRSF/REST-like repressor downstream of Ebi/SMRTER/Su(H) regulates eye development in Drosophila. *EMBO J, 25*(13), 3191-3202. doi: 10.1038/sj.emboj.7601179

Wang, J. W., Shi, X. Y., Kurahashi, H., Hwang, S. K., Ishii, A., Higurashi, N., . . . Hirose, S. (2012). Prevalence of SCN1A mutations in children with suspected Dravet syndrome and intractable childhood epilepsy. *Epilepsy Res, 102*(3), 195-200. doi: 10.1016/j.eplepsyres.2012.06.006

Widdess-Walsh, P., & Devinsky, O. (2010). Historical perspectives and definitions of the postictal state. *Epilepsy Behav, 19*(2), 96-99. doi: 10.1016/j.yebeh.2010.06.037

Wu, J. S., & Luo, L. (2006). A protocol for dissecting Drosophila melanogaster brains for live imaging or immunostaining. *Nat Protoc, 1*(4), 2110-2115. doi: 10.1038/nprot.2006.336

Xu, J. C., Lytle, C., Zhu, T. T., Payne, J. A., Benz, E., Jr., & Forbush, B., 3rd. (1994). Molecular cloning and functional expression of the bumetanide-sensitive Na-K-Cl cotransporter. *Proc Natl Acad Sci U S A, 91*(6), 2201-2205.

Yamasaki, Y., Lim, Y. M., Niwa, N., Hayashi, S., & Tsuda, L. (2011). Robust specification of sensory neurons by dual functions of charlatan, a Drosophila NRSF/REST-like repressor of extramacrochaetae and hairy. *Genes Cells, 16*(8), 896-909. doi: 10.1111/j.1365-2443.2011.01537.x

Zdebik, A. A. (2011). Beyond ion transport: KCC2 makes cells walk and talk. *J Physiol, 589*(Pt 24), 5903. doi: 10.1113/jphysiol.2011.221754

Zhang, R. W., Wei, H. P., Xia, Y. M., & Du, J. L. (2010). Development of light response and GABAergic excitation-to-inhibition switch in zebrafish retinal ganglion cells. *J Physiol, 588*(Pt 14), 2557-2569. doi: 10.1113/jphysiol.2010.187088

Ziemann, A. E., Schnizler, M. K., Albert, G. W., Severson, M. A., Howard, M. A., 3rd, Welsh, M. J., & Wemmie, J. A. (2008). Seizure termination by acidosis depends on ASIC1a. *Nat Neurosci, 11*(7), 816-822. doi: 10.1038/nn.2132

Chapter 3 Figures and Tables

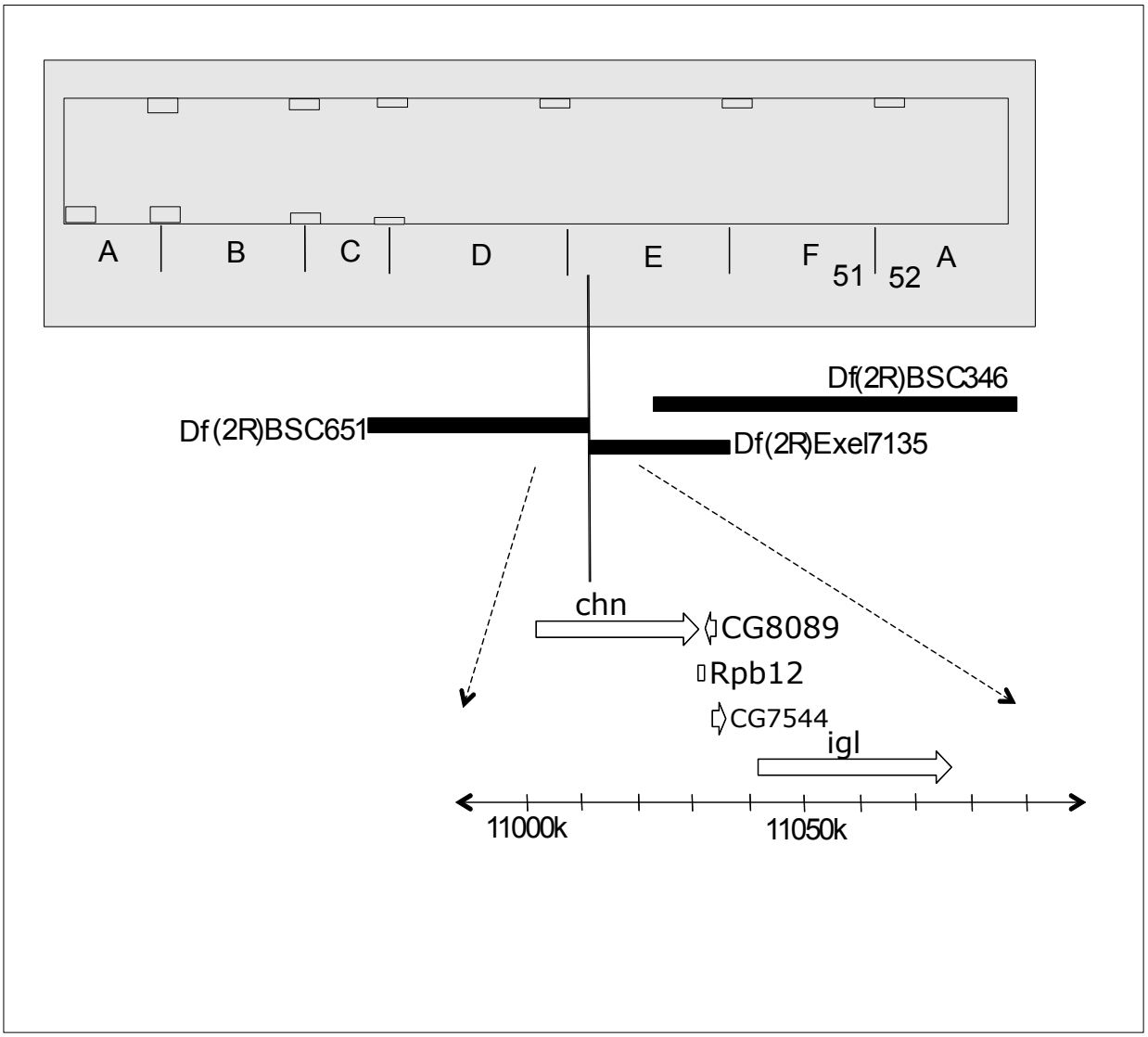

Figure 3.1: Chromosomal segment deleted in *Df(2R)Exel7135*. The upper panel of the figure depicts region 51 of the polytene chromosome. The *chn* gene is disrupted by the distal breakpoint of *Df(2R)BSC651* and the proximal breakpoint of *Df(2R)Exel7135*; both rearrangements enhance BS paralytic recovery time in *para*^{bss1} hemizygotes. The BS paralytic recovery time phenotype is not enhanced by the *Df(2R)BSC346*.

Bloomington Stock#	Chromosome	Df MRT (s)	Control MRT (s)	nMRT
7532	2	73	94	0.78
7533	2	155	152	1.02
7534	2	172	210	0.82
7535	2	114	120	0.95
7536	2	95	115	0.83
7537	2	97	127	0.76
7538	2	215	85	2.53
7539	2	160	177	0.90
7540	2	90	82	1.10
7541	2	171	191	0.90
7543	2	73	126	0.58
7544	2	132	129	1.02
7545	2	131	159	0.82
7546	2	205	190	1.08
7547	2	85	116	0.73
7548	2	90	106	0.85
7549	2	131	132	0.99
7551	2	143	126	1.13
7553	2	217	118	1.84
7554	2	128	108	1.19
7556	2	216	129	1.67
7557	2	186	216	0.86
7558	2	306	135	2.27
7559	2	284	215	1.32
7561	2	172	215	0.80
7748	2	97	138	0.70
7749	2	77	123	0.63
7750	2	96	121	0.79
7858	2	163	184	0.89
7859	2	232	102	2.27
7860	2	144	128	1.13
7862	2	119	157	0.76
7863	2	143	221	0.65
7864	2	131	139	0.94
7867	2	103	105	0.98
7869	2	120	157	0.76
7870	2	146	204	0.72
7871	2	145	190	0.76
7872	2	198	136	1.46
7873	2	142	214	0.66

7875	2	162	194	0.84
7876	2	106	111	0.95
7877	2	118	156	0.76
7879	2	264	164	1.61
7880	2	161	174	0.93
7881	2	99	115	0.86
7882	2	99	99	1.00
7883	2	111	101	1.10
7886	2	152	193	0.79
7887	2	114	99	1.15
7888	2	204	149	1.37
7890	2	118	120	0.98
7891	2	73	123	0.59
7893	2	144	161	0.89
7894	2	98	142	0.69
7895	2	88	106	0.83
7898	2	127	124	1.02
7900	2	109	175	0.62
7901	2	203	160	1.27
7902	2	104	147	0.71
7903	2	139	147	0.95
7906	2	192	239	0.80
7908	2	239	133	1.80
7909	2	241	217	1.11
7916	2	116	122	0.95
7998	2	107	113	0.95
2492	3	116	129	0.90
6962	3	107	109	0.98
7562	3	108	120	0.90
7562	3	149	160	0.93
7570	3	189	198	0.95
7570	3	91	98	0.93
7571	3	182	99	1.84
7623	3	256	248	1.03
7623	3	319	306	1.04
7737	3	109	116	0.94
7929	3	156	116	1.34
7983	3	190	175	1.09
8047	3	140	136	1.03
8047	3	126	88	1.43
8048	3	122	135	0.90
8048	3	107	82	1.30

8053	3	164	135	1.21
8059	3	159	160	0.99
8060	3	32	78	0.41
8061	3	101	59	1.71
8065	3	116	102	1.14
8065	3	137	90	1.52
8066	3	120	95	1.26
8068	3	56	75	0.75
8069	3	74	67	1.10
8070	3	163	178	0.92
8070	3	79	64	1.23
8072	3	110	107	1.03
8073	3	106	61	1.74
8073	3	99	58	1.71
8074	3	152	146	1.04
8074	3	128	97	1.32
8075	3	155	140	1.11
8080	3	110	114	0.96
8081	3	200	213	0.94
8082	3	92	121	0.76
8082	3	119	130	0.92
8088	3	104	127	0.82
8096	3	178	175	1.02
8096	3	89	76	1.17
8097	3	117	99	1.18
8097	3	136	105	1.30
8099	3	157	145	1.08
8100	3	150	127	1.18
8101	3	145	113	1.28
8104	3	114	88	1.30
8682	3	96	77	1.25
8962	3	115	88	1.31
8962	3	73	56	1.30
8967	3	101	82	1.23
8974	3	170	98	1.73
9080	3	74	80	0.93
9084	3	116	96	1.21
9090	3	107	143	0.75
9207	3	95	103	0.92
9355	3	92	81	1.14
9481	3	76	75	1.01
9486	3	170	161	1.06

9629	3	223	226	0.99
9693	3	221	229	0.97
9693	3	154	148	1.04
9700	3	162	154	1.05
9701	3	185	172	1.08
9701	3	149	100	1.49
23668	3	108	111	0.97
23668	3	107	94	1.14
24137	3	103	78	1.32
24139	3	119	79	1.51
24140	3	124	112	1.11
24143	3	83	79	1.05
24392	3	170	87	1.95
24410	3	169	162	1.04
24410	3	146	97	1.51
24413	3	190	134	1.42
24415	3	124	91	1.36
24915	3	160	102	1.57
24941	3	115	113	1.02
24941	3	152	116	1.31
24952	3	184	173	1.06
24968	3	192	197	0.97
24990	3	125	89	1.40
25001	3	123	144	0.85
25014	3	119	132	0.90
25019	3	150	162	0.93

Table 3.1 Complete list of stocks with chromosomal deficiencies and the effect of these deficiencies on *para^{bss1}*/Y MRT compared to sibling controls. Values of the length of time that hemizygous *para^{bss1}/Y* males remained paralyzed are depicted as mean recovery time (MRT). To minimize the effects of genetic background, experimental males of the general genotype: *para^{bss1}/Y;Df/+* were compared directly to sibling control brothers arising from the same cross (genotype: *para^{bss1}/Y;Balancer/+*). The ratio of MRT for experimental males with that of their control siblings is listed as normalized mean recovery time (nMRT).

Deficiency	Deleted Interval	Experimental (Df) MRT (s)	Control (Balancer) MRT (s)	nMRT
Df(2R)Exel7135	51E2-51E11	363	234	1.55
Df(2R)Exel6078	58B1-58D1	306	135	2.27
Df(2R)Exel7094	44A4-44B3	232	102	2.27
Df(2R)Exel6071	57B3-57B16	217	118	1.84
Df(2R)Exel6056	44A4-44C2	215	85	2.53

Table 3.2: Chromosomal deletions that were most effective at enhancing the behavioral bang-sensitive (BS) paralytic phenotype of *para^{bss1}/+* flies. Values of the length of time that hemizygous *para^{bss1}/Y* males remained paralyzed are depicted as mean recovery time (MRT). To minimize the effects of genetic background, experimental males of the general genotype: *para^{bss1}/Y;Df/+* were compared directly to sibling control brothers arising from the same cross (genotype: *para^{bss1}/Y;Balancer/+*). The ratio of MRT for experimental males with that of their control siblings is listed as normalized mean recovery time (nMRT).